The role of TNF receptor type 2 on myeloid cells in sepsis - functional analysis

DISSERTATION ZUR ERLANGUNG DES DOKTORGRADES
DER NATURWISSENSCHAFTEN (DR. RER. NAT.)
DER NATURWISSENSCHAFTLICHEN FAKULTÄT III
– BIOLOGIE UND VORKLINISCHE MEDIZIN –
DER UNIVERSITÄT REGENSBURG

vorgelegt von

Johannes Polz

aus Pfaffenhofen an der Ilm

Juli 2010

Die vorliegende Arbeit entstand im Zeitraum von September 2007 bis Juli 2010 am Institut für Immunologie des Klinikums der Universität Regensburg unter der Anleitung von Frau Prof. Dr. Daniela N. Männel.

Prüfungsausschuss:
Herr Prof. Dr. Stephan Schneuwly (Vorsitz)
Frau Prof. Dr. Daniela N. Männel
Herr PD Dr. Thomas Langmann
Herr Prof. Dr. Richard Warth

Das Promotionsgesuch wurde eingereicht am: 28.06.2010

Die Arbeit wurde angeleitet von: Frau Prof. Dr. Daniela N. Männel

Unterschrift:

“In digging for potatoes, it is not so important that
you dig like hell as you dig where the potatoes are!”

Carly Hertley
(President of Hartley´s Potato Chips)

Für meine Eltern

Abstract

Das Krankheitsbild der Sepsis geht im Zusammenhang mit Sekundärinfektionen häufig mit hoher Morbidität und Mortalität einher und ist daher ein wichtiges Themengebiet der angewandten biomedizinischen Forschung. Dr. Theo Sterns hat 2005 in seiner Doktorarbeit beschrieben, dass die Abwesenheit von TNF-Rezeptor Typ-2 (TNFR2) im Mausmodell für Sepsis, der CLP-induzierten Peritonitis, einen Schutz vor einer folgenden Zweitinfektion bewirkt. Ziel dieser Arbeit war es, diesen *in vivo* Befund auf myeloide Zellen zu übertragen, um nachvollziehen zu können, ob in diesem zellulären System TNFR2-vermittelte Mechanismen einen Einfluss auf die Pathogenese der Sepsis haben.

Es stellte sich heraus, dass $CD11b^{+}$ $CD11c^{-}$ Zellen aus der Milz nach Restimulation mit LPS und IFN-γ erst dann in der Lage sind, Stickoxid (NO) zu produzieren, wenn die Maus mit einer CLP vorbehandelt wurde, und, dass die Zellen aus $TNFR2^{-/-}$ Tieren bedeutend weniger NO produzieren. Das NO-Produktionsdefizit zeigte sich auch in weiteren myeloiden Zellen sogar aus naiven $TNFR2^{-/-}$ Tieren, wie z.B. in peritonealen Exsudatzellen (PEC) und Dendritischen Zellen, welche *in vitro* aus knochenmarkständigen Vorläuferzellen generiert wurden (BMDC).

Am Modell der BMDC wurde das Fehlen von TNFR2 detailliert untersucht. Es zeigte sich, dass BMDC von $TNFR2^{-/-}$ Mäusen eine reduzierte IL-6-Produktion nach Restimulation mit LPS und IFN-γ aufweisen. Die Zellausbeute und Proliferation von $TNFR2^{-/-}$ BMDC ist jedoch bei gleicher Sterblichkeitsrate reduziert. In Zusammenhang mit erhöhten Proliferationsraten bei $TNFR1^{-/-}$ BMDC, welche von der Arbeitsgruppe um Lutz auch als „unsterblich“ beschrieben wurden, ist dies ein starkes Indiz für ein TNFR2-vermitteltes Proliferationssignal. BMDC von $TNFR2^{-/-}$ Tieren zeigten in der späten Phase der Differenzierung zu BMDC einen höheren Anteil an Zellen, welche die Aktivierungsmarker MHCII, CD80 und CD86 trugen. Der Anteil der myeloiden Suppressorzellen (MDSC) hingegen war während der ganzen Differenzierung erniedrigt. Dies ist ein Indiz dafür, dass in $TNFR2^{-/-}$ Zellsystemen die T-Zell-Antwort verbessert abläuft, da einerseits die Antigen präsentierenden Zellen eine bessere Antigenpräsentation aufweisen und zusätzlich eine reduzierte Suppressivität vorherrscht. TNFR2 scheint somit eine suppressive Funktion für T-Zellen zu vermitteln.

Da löslicher TNFR2 große Mengen an löslichem TNF biologisch inaktiveren kann, wurde die Frage geklärt, ob die beschriebenen Effekte auf intrinsischen TNFR2-Signalen beruhen, oder ob sie über veränderte TNF-Konzentrationen TNFR2 vermittelt sind. BMDC aus Knochenmark-chimären Wildtyp Mäusen, welche mit $TNFR2^{-/-}$ Knochenmark rekonstituiert wurden, zeigten weiterhin reduzierte NO-Produktion und einen erhöhten Anteil an Aktivierungsmarkern. BMDC-Kulturen, welche zu Beginn der Differenzierung aus 50% Wildtyp und 50% $TNFR2^{-/-}$ Knochenmarkszellen zusammengesetzt wurden, gewährleisteten identische Konzentrationen

an löslichem TNF und löslichem TNFR2 für beide Populationen. Die TNFR2$^{-/-}$ BMDC aus diesen Kulturen wiesen alle Phänotypen auf, die auch für TNFR2$^{-/-}$ Reinkulturen gezeigt wurden: reduzierte NO und IL-6 Produktion, sowie ein erhöhter Anteil an Aktivierungsmarkern bei einem erniedrigten Prozentsatz an MDSC. Dies ist ein starkes Indiz dafür, dass das Fehlen intrinsischer Signale in TNFR2$^{-/-}$ BMDC für diese Befunde verantwortlich ist und Umgebungseffekte über lösliches TNF während der Kultur eine untergeordnete Rolle spielen. Epigenetische Modifikationen in TNFR2$^{-/-}$ Systemen, welche womöglich bereits sehr früh in der Ontogenese über das Fehlen intrinsischer TNFR2- oder auch über verstärkte TNFR1- Signale induziert werden, können in diesen Modellen letztendlich als Ursache für die erwähnten Phänotypen nicht ausgeschlossen werden. Um eine Klärung dieser Frage zu ermöglichen, wurden monoklonale Antikörper gegen TNFR2 generiert, um mittels möglicherweise blockierender Antikörper den TNFR2$^{-/-}$ Phänotyp *in vitro* nachahmen zu können und somit einen endgültigen Beweis für das Fehlen intrinsischer TNFR2-Signale zu erbringen. Es konnte jedoch weder agonistische noch antagonistische Funktionalität in einem speziell entwickelten zelluläreren Assay basierend auf Fusionsproteinen aus den Extrazellulardomänen von TNFR1 und TNFR2 und der Intrazellulardomäne von humanem Fas nachgewiesen werden.

Index of content

Index of figures

Index of formulas

Index of tables

Abbreviation	Description
A	Adenine
A	Austria
AF647	Alexa Fluor® 647
Akt	Serine-threonine kinase
AP	Activating protein
AP	Alcaline phosphatase
APC	Allophycocyanin
APC	Antigen presenting cells
APS	Ammoniumperoxodisulfate
Arg1	Arginase 1
BM	Bone marrow
BMDC	Bone marrow-derived dendritic cells
Bp	Basepair
BrdU	Bromodeoxyuridine
BSA	Bovine serum albumin
C	Cytosine
C/EPT	CCAAT binding enhancer binding proteins
cAMP	Cyclic adenosine monophosphate
CARS	Compensated anti-inflammatory response syndrome
CAT-2B	Cationic amino acid transporter 2B
CD	Cluster of differentiation
cDNA	Complementary DANN
CFA	Complete Freund’s adjuvans
sGC	Soluble guanylate cyclase
CHO	Chinese hamster ovary cell
cIAP	Cellular inhibitor of apoptosis protein
CLP	Cecal ligation puncture
cm²	Square centimeter
COX	Cyclo-oxygenase
CP	Crossing point
CRD	Cystein-rich domains
CREP	cAMP response element-binding protein
D	Day
DC	Dendritic cells

DD	Death domain
ddH_2O	H_2O bidest
DMSO	Dimethylsulfoxide
DANN	Deoxyribonucleic acid
DS-2	Drosophila schneider cell
E	Efficiency
e.g.	For example, latin: "exempli gratia"
Ed	Extracellular domain
EDTA	Ethylenediaminetetraacetic acid
ELISA	Enzyme-linked immunosorbent assay
ERK	Extracellular signal-regulated kinases
FACS	Fluorescence-activated cell sorting
FADD	Function associated death domain
FAS	FasR, CD95
FCS	Fetal calf serum
FITC	Fluorescein isothiocyanate
FLT3	FMS-like tyrosine kinase 3
FoxP3	Forkhead box P3
FW	Forward
G	Gram
G	Guanine
G-CSF	Granulocyte-colony stimulating factor
GER	Germany
GM-CFU	Granulocyte / macrophage colony-forming units
GM-CSF	Granulocyte / macrophage colony-stimulating factor
GMP	Guanosine monophosphate
GR1	Granulocyte-differentiation antigen
H	Hour
HAT	hypoxanthine aminopterin thymidine
HEPES	4-(2-hydroxyethyl)-1-piperazineethanesulfonic acid
HK	House keeping gene
HRP	Horseradish peroxidase
HSC	Hematopoietic stem cells
HAT	Hypoxanthine Thymidine
i.e.	That is, latin "id est"

i.p.	Intraperitoneal
i.v.	Intravenous
IAP1	Inhibitors of apoptosis inducing proteins
ICAM-1	Intercellular adhesion molecule-1
id	Intracellular domain
IFA	Incomplete Freund's adjuvans
IFN-γ	Interferon- γ
Ig	Immunoglobulin
IKKα	IκB kinase α
IKKβ	IκB kinase β
IL-1ra	IL-1 receptor antagonist
IMC	Immature myeloid cells
iNOS	Inducible NO-synthases
Int	Intermediate
IP	Feron-inducible protein
JAK	Janus kinase
JNK	c-Jun N-terminal kinases
Kb	Kilobase
kDa	Kilodalton
L	Liter
L-929^{m}	Murine aneuploid fibrosarcoma cell line
LPS	Lipopolysaccharide
Ly6C	Lymphocyte antigen 6 C
Ly6G	Lymphocyte antigen 6 G
M	Molar
m/v	Mass / volume
mA	Milliampere
mAB	Monoclonal antibody
Max	Maximal
M-CFU	Macrophage colony-forming units
MCP	Monocyte chemotactic protein
MDC (CCL22)	Macrophage-derived chemokine
MDSC	Myeloid–derived suppressor cells
Mg	Milligram
MHC	Major histocompatibility complex

Min	Minute
MIP	Mitogen-activated protein
mL	Milliliter
mM	Millimolar
MO	Monocytic morphology
MOG	Myelin oligodendrocyte glycoprotein
mRNA	Messenger ribonucleic acid
MTT	3-(4,5-Dimethylthiazol-2-yl)-2,5-diphenyltetrazolium bromide
MV	Mean value
NF-κB	Nuclear factor kappa-light-chain-enhancer of activated B cells
Ng	Nanogram
NIK	NF-κB inducing kinase
NK cels	Natural killer cells
Nm	Nanometer
NO	Nitric oxide
OD	Optical density
PBS	Phosphate buffered saline
PCR	Polymerase chain reaction
PE	Phycoerythrin
PEC	Peritoneal exudate cells
PEG	Polyethylene glycol
PerCP	Peridinin chlorophyll protein complex
PGE	Prostaglandin E
PGI	Prostacyclin
pH	p[H] value
PI3K	Phosphatidylinositol 3-kinases
PLADs	Pre-ligand assembly domains
PMN	Polymorphonuclear cells
POX	Peroxidase
pre-TNF	Transmembrane form of TNF, stored in the golgi apparatus
PVDF	Polyvinylidene fluoride
RIP	Receptor-interacting protein
RNA	Ribonucleic acid
ROS	Reactive oxygen species

RPMI	Roswell Park Memorial Institute
RT	Room temperature
RV	Reverse
S	Second
S	Soluble
SCF	Stem cell factor
SD	Standard deviation
SDS	Sodiumdodecylsulfate
SIRS	Systemic inflammatory response syndrome
SODD	Silencer of death domain
SP2/0-Ag14	Myeloma cell line
STAT	Signal transducers and activators of transcription protein
T	Thymidine
TACE	TNFα converting enzyme
TARC (CCL17)	Thymus and activation regulated chemokine
TBS	Tris buffered saline
TBS-T	TBS supplemented with 0.5 % (v/v) Triton-X 100
TEMED	Tetramethylethylenediamine
TG	Target gene
TGF-ß	Tumor growth factor ß
T_H1	Type 1 helper T cell
T_H2	Type 2 helper T cell
TLR	Toll-like receptor
T_m	Melting temperature
TNF	Tumor necrosis factor
TNFR1	Tumor necrosis factor receptor type 1
TNFR2	Tumor necrosis factor receptor type 2
TRADD	TNF receptor associated death domain
TRAF	TNFR-associated factor
Treg	Regulatory T cell
Tween 20	Polyoxyethylene (20) sorbitan monolaurate
U	Enzyme activity unit
USA	United States of America
V	Volt
v/v	Volume / volume

VCAM-1	Vascular cell adhesion molecule
VEGF	Vascular endothelial growth factor
WB	Western Blot
Wirbel (TNFR1/2 -/-)	Mouse fibroblast TNFR1/2 double knockout
Wt	Wildtype
X6310 (X63Ag8-653) GM-CSF	Myeloma cell line
°C	Degree celsius
µg	Microgram
µL	Microliter
µm	Micrometer
µM	Micromolar
18s	Rribosomal RNA subunit 18s
Λ	Wavelength

1 Introduction

1.1 Preamble

Fundamental research on the effects of tumor necrosis factor (TNF) and tumor necrosis factor receptor type 2 (TNFR2) performed in this research group was the basis of this thesis. Dr. Theo Sterns reported that TNFR2 deficient mice were protected from a secondary infection during the phase of sepsis that is usually characterized as sepsis-induced immunosuppression (Sterns, Pollak et al. 2005).

1.2 The TNF / TNF receptor superfamily

The TNF / TNF receptor superfamily consists of 19 ligands and 29 receptors. The signals generated within this group of molecules take part in the regulation of immune response, haematopoiesis, and morphogenesis but are also implicated in tumorigenesis, transplant rejection, septic shock, viral replication, bone resorption, rheumatoid arthritis, and diabetes. In addition to specific functional effects on the target cells, members of the TNF / TNF receptor superfamily deliver general signals such as signals for proliferation, survival, differentiation, or apoptosis (Aggarwal 2003).

The ligands and the receptors of the TNF / TNF receptor superfamily are membrane-bound and soluble and mostly restricted to cells and tissues of the immune system. Ligands often are pluri-specific as they can interact with more than one receptor. Interestingly, redundancy within the different effects caused by the different ligand-receptor pairs has not been found so far indicating very unique and focused functions. Ligands of the TNF superfamily are biologically active type 2 transmembrane proteins with intracellular N-termini that trigger the respective receptors as self-assembling, non-covalent bound trimers (Peschon, Slack et al. 1998). The ligands of the TNF superfamily show a structural homology of 20 – 30%. The homologue sequences are essential for the assembly of the trimeric structure. The non-homologue areas guarantee specific receptor recognition and activation (Loetscher, Stueber et al. 1993; Fesik 2000). Various ligands are biologically active in both the membrane-bound and the proteolytically cleaved soluble form (Idriss and Naismith 2000).

Receptors of the TNF receptor superfamily are type 1 transmembrane proteins featuring cystein-rich domains (CRD). Highly conservated cystein residues within the protein generate intrachain disulfide bridges that are responsible for the typical pseudo-repeats of these

receptors (Smith, Farrah et al. 1994). The number of CRD within the receptors of the TNF receptor superfamily varies from 1 to 6 (Hehlgans and Pfeffer 2005).

1.2.1 Structure of TNF

Tumor necrosis factor (TNF) is a member of the cytokine family. Cytokines comprise numerous small molecules that are mainly secreted by cells of the immune system and act as messengers. They are proteins, peptides, or glycoproteins and are extensively used in cellular communication. Cytokines regulate differentiation, proliferation, and apoptosis of cells and influence the cytokine production of the target cells in many cases (Burke, Naylor et al. 1993).

TNF is one of the most prominent members of the TNF / TNF receptor superfamily and was one of the main research targets in this study. The molecule was described first in 1975 as an endotoxin-induced glycoprotein with antitumor effects on transplanted sarcomas in mice as it caused haemorrhagic necrosis (Carswell, Old et al. 1975).

Many TNF-related and TNF receptor-related molecules were discovered since the initial description of TNF and its receptors as the first cloned members of this familiy in both human and mouse (Loetscher, Pan et al. 1990; Lewis, Tartaglia et al. 1991).

TNF is a type 2 membrane protein that stays membrane-bound as a pre-protein and is cleaved off by metalloproteinases to be released from the producer cells as mature soluble TNF (Gearing, Beckett et al. 1994; Black 2002). The receptor binding site of TNF is formed by the groove between two adjoining ligand chains and, hence, TNF trimers exhibit three receptor binding sites. Trimerization of soluble TNF is necessary for efficient activation of TNF receptors. Membrane-associated as well as soluble forms of TNF are biologically active. Mouse TNF is glycosylated and shows 80% sequence homology compared to human TNF. TNF does not undergo posttranscriptional modification (Pennica, Hayflick et al. 1985).

TNF is expressed at the transcriptional level with an unusually long and uncommon leader sequence in multiple cell types like macrophages, monocytes, T and B cells, granulocytes, and even mast cells (Echtenacher, Mannel et al. 1996). During inflammation those cells initially produce a transmembrane form of TNF (pre-TNF) of 26 kDa stored in the Golgi apparatus (Shurety, Merino-Trigo et al. 2000) or at the cell membrane. As a consequence of long-lasting stimulation, metalloproteinases cleave the extracellular domain of TNF, releasing a soluble TNF homotrimer of three mature 17 kDa TNF molecules (Black, Rauch et al. 1997; Moss, Jin et al. 1997). The most prominent member of these metalloproteinases is the membrane-bound TNFα converting enzyme (TACE).

1.2.2 Functions of TNF

Both 26 kDa pre-TNF and the 17 kDa soluble TNF homotrimer provide biological activity via two identified membrane TNF receptors, tumor necrosis factor receptor type 1 (TNFR1) of an apparent molceluar weight of 50 kDa and tumor necrosis factor receptor type 2 (TNFR2) of about 75 kDa (Smith, Davis et al. 1990). Many of the proinflammatory properties of TNF can be explained by their effects on vascular endothelium and endothelial leukocyte interactions. When exposed to TNF, endothelial cells support the inflammatory response by expressing different adhesion molecules such as E-selectin, intercellular adhesion molecule-1 (ICAM-1), and vascular cell adhesion molecule-1 (VCAM-1) as well as chemokines like interleukin-8 (IL-8), monocyte chemotactic protein-1 (MCP-1), and interferon-inducible protein 10 (IP-10). The binding to adhesion molecules enables leukocytes to invade the tissue by crossing the vascular endothelium. Chemokines guide the migration to the center of inflammation independent of antigen recognition (Pober, Bevilacqua et al. 1986; Munro, Pober et al. 1989; Rollins, Yoshimura et al. 1990). The TNF-mediated expression of adhesion molecules and chemokines is regulated in distinct temporal, spatial, and anatomical patterns (Messadi, Pober et al. 1987; Petzelbauer, Pober et al. 1994; Bradley and Pober 1996). Additionally, TNF is able to cause vasodilation via inducing the expression of cyclo-oxygenase 2 (COX2) and the associated production of the vasodilator prostacyclin 2 (PGI2) (Mark, Trickler et al. 2001). This explains “rubor” (erythema) and “calor” (heat), two of the four classical signs of inflammation. “Tumor” (swelling), the third indicator in this row, results among others from TNF-mediated increased vascular permeability and subsequent trans-endothelial passage of fluid and macromolecules that create edema. TNF increases the risk of intravascular thrombosis as it induces the expression of pro-coagulant proteins like tissue factor and down-regulates anti-coagulant proteins such as thrombomodulin (Bevilacqua, Pober et al. 1986). One of the most prominent roles of TNF in normal inflammation consists in the orchestration of the host defense to bacterial, viral, and parasitic infections. Nevertheless, exact control of TNF is essential as unregulated exposure to TNF can be harmful to the organism.

1.2.3 Regulation of TNF receptors

Expression of TNFR1 and TNFR2 can be observed in most cell lines and in normal and diseased tissues (Al-Lamki, Wang et al. 2001). TNFR2 is mainly expressed on hematopoietic cells and, in contrast to TNFR1, highly regulated (Hehlgans and Pfeffer 2005). The extracellular ligand binding domains of the two TNF receptors are structurally similar and contain cystein-rich subdomains. The intracellular portions of the two receptors exhibit no sequence homology and

do not signal via intrinsic enzyme activity. Signal transduction is generated through the acquisition of cytosolic proteins to specific protein-protein interaction domains (Ledgerwood, Pober et al. 1999). The ability of TNFR1 and TNFR2 to signal via both identical and unrelated proteins depicts the common and independent function of both receptors. Membrane-bound TNF is able to activate both TNFRs whereas soluble TNF activates TNFR1 more efficiently than TNFR2 (Grell 1995).

1.2.3.1 Signaling of TNFR1

TNFR1 is a 50 – 55 kDa type I transmembrane protein. In resting cells it is predominantly stored in the Golgi apparatus from where it can be carried over onto the cell surface. The relevance of the intracellular storage of TNFR1 is only vaguely understood. The most probable hypothesis describes the possibility of increasing cell membrane TNFR1 density very fast and without new protein synthesis. This would lead to enhanced susceptibility of the cell to TNF (Bradley, Thiru et al. 1995). TNFR1, expressed on the surface, is trimerized in the membrane through pre-ligand assembly domains (PLADs) located at the distal end of the cystein-rich domain (Bennett, Macdonald et al. 1998). Silencer of death domain (SODD) prevents constitutive signaling as it is associated to the cytoplasmatic domains of non-stimulated TNFR1 (Lanford, Lan et al. 1999). After binding of TNF to TNFR1 receptor the resulting receptor-ligand complex is internalized (Schutze, Machleidt et al. 1999) and the death domain containing signal transduction adapter molecule TNF receptor associated death domain (TRADD) is recruited. From that point, two possible signaling pathways can be activated either inducing apoptosis or proinflammatory gene expression.

In the case of apoptosis additional death domain-containing proteins, i.e. FADD and also the procaspases 8 and 10, are recruited to the TNFR1-TRADD complex. The successful activation leads to DNA degradation and cell death (Hsu, Xiong et al. 1995; Ashkenazi and Dixit 1998). TNFR1-bound TRADD can also recruit cellular inhibitor of apoptosis protein (cIAP) (Rothe, Pan et al. 1995) and receptor-interacting protein (RIP) (Kelliher, Grimm et al. 1998). Those molecules enable TNFR-associated factor 2 (TRAF2) to join the TNFR1-signaling complex (Liu, Hsu et al. 1996). This complex formation results in the activation of different kinases, e.g. NIK (NF-κB inducing kinase), IKKα and β (IκB kinase α and β), mitogen-activated protein (MAP) kinases, c-Jun N-terminal (JNK) kinase, and p38 kinase (Liu, Hsu et al. 1996; Eder 1997; Kelliher, Grimm et al. 1998; Mercurio and Manning 1999). The activation of these kinases further mediates the activation of transcription factors and, thus, induces the expression of proinflammatory and antiapoptotic genes. For the induction of apoptosis the internalization of

the TNF-TNFR1 complex is required whereas the activation of the nuclear factor kappa-light-chain-enhancer of activated B cells (NF-κB) pathway can be seen after ligand binding even if the internalization of TNFR1 is prevented (Schutze, Machleidt et al. 1999).

1.2.3.2 Signaling of TNFR2

TNFR2 is a 75 – 80 kDa membrane-bound protein with immanent structural similarities to TNFR1 in the extracellular domains mainly consisting of cysteine-rich repeats (Beutler and van Huffel 1994). The intracellular domains of TNFR1 and TNFR2 exhibit no homology. Consequently, the functions of both receptors are different. Due to a missing death domain, the main function of TNFR2 is the recruitment of TRAF2 and the activation of the NF-κB pathway. The cellular effects can be manifold: cytokines are produced as well as intracellular regulatory proteins with potential anti-apoptotic features such as TRAF1 and TRAF2 and the inhibitors of apoptosis inducing proteins (c-IAP1 and c-IAP2) (Wang, Mayo et al. 1998). Furthermore, alternative intracellular signaling architectures are known to employ activation of p38 kinase and N-terminal JNK kinase (Liu, Hsu et al. 1996; Kelliher, Grimm et al. 1998). In contrast to TNFR1, which is found on almost all tissues and cells, the expression of TNFR2 seems to be more restricted and precisely regulated especially in lymphoid tissues and cells (Grell, Douni et al. 1995). As TNFR2 has no death domain, direct induction of apoptosis is not possible and, therefore, induction of anti-apoptotic processes via NF-κB can be assumed. Nevertheless, enhanced apoptosis was reported when TNFR1 and TNFR2 were triggered together with TNF. TNFR1 and TNFR2 have similar affinities to their ligand TNF at room temperature, but TNF-TNFR2 complexes are formed only transiently (Grell, Wajant et al. 1998).
TNFR2 is required for antigen-mediated T cell differentiation and survival (Kim, Priatel et al. 2006) and induces the expression of intracellular adhesion molecule (ICAM-1), E-selectin, and MCP-1/JE on endothelial cells (Chandrasekharan, Siemionow et al. 2007). Furthermore, TNFR2 influences the migration of intestinal epithelial cells as well as Langerhans cells (Takayama, Yokozeki et al. 1999; Corredor, Yan et al. 2003) and is known to induce proliferation in various types of cells and angiogenesis (Theiss, Simmons et al. 2005).

1.2.4 Reverse signaling of TNFR2 via membrane-bound TNF

Reverse signaling, employing the intracellular domains of the whole membrane-bound TNF as signaling domains and TNF receptors as possible ligands, has been discussed by many authors. It has been shown that CD3-mediated activation of transcription of interferon-γ (IFN-γ)

and IL-4 can be influenced in a costimulatory way when T cells were incubated with anti-TNF antibodies (Ferran, Dautry et al. 1994). Reverse signaling in human monocytes and macrophages was suggested to generate resistance to lipopolysaccharide (LPS) (Eissner, Kirchner et al. 2000). E-selectin expression in activated human CD4 T cells has been reported to depend on reverse signaling via membrane-bound TNF (Harashima, Horiuchi et al. 2001).
When the membrane-bound form of TNF is highly expressed on tumor cells it can promote NF-κB activation through reverse signaling and supporting tumor cell survival. In contrast, there is also evidence that membrane-bound TNF, when acting as a ligand, inhibits NF-κB signaling and, thus, induces tumor cell death (Zhang, Yan et al. 2008).
Currently, it is widely accepted that TNF, being a factor that strongly regulates growth, differentiation, and death of both hematopoietic and non-hematopoietic cell types, is one of the key players in pathophysiology. By directing its two transmembrane receptors to deliver signals of cellular proliferation, differentiation, or apoptosis, TNF seems not only to orchestrate acute responses to infection and immunological injury, but also to act as a balancing factor required for the re-establishment of physiological homeostasis and immune regulation. The level, timing, and duration of TNF activity are of critical regulatory significance.

1.2.5 TNF inhibitor function of soluble TNFR2

Both TNFR1 and TNFR2 can be proteolytically cleaved and released from the cell membrane. The soluble forms of those receptors remain biologically active as they can still bind TNF (Bazzoni and Beutler 1995). The soluble forms of TNFRs represent biological markers for inflammatory processes as they are very efficient in neutralizing soluble TNF (Wallach, Engelmann et al. 1991). Increased levels of TNFRs can be found in cancer, rheumatoid arthritis, lupus erythematodes, HIV, and sepsis (Aderka, Englemann et al. 1991; Cope, Aderka et al. 1992; Aderka, Wysenbeek et al. 1993; Schroder, Stuber et al. 1995; Hober, Benyoucef et al. 1996). In the mouse model of cecal ligation puncture (CLP), which causes septic peritonitis, high serum levels of soluble TNFR2 can be detected. The occurrence of soluble TNFR2 in this experimental setup is about 100 times higher than that of soluble TNFR1 (Villa, Sartor et al. 1995). This might be explained by the induced expression of TNFR2 during inflammation. Interestingly, high levels of soluble TNFR2 can also be found in the urine of naïve mice (Eva Pfeifer, personal communication).

1.2.6 Anti-TNF therapy

The overproduction of TNF can be causal, maybe as intermediate mediator, for a number of autoimmune diseases like rheumatoid arthritis, ankylosing spondylitis, and psoriasis (Sacca, Cuff et al. 1998; Bradley 2008). There are several ways to abrogate the harmful influence of excessive levels of TNF. On the one hand there are neutralizing anti-TNF antibodies like Infliximab and Adalimumab. On the other hand recombinant fusion proteins consisting of human TNFR2 and the Fc portion of human IgG1 (Etanercept) bind and deactivate TNF. Both strategies reduce the concentrations of biologically active TNF and, consequently, alleviate the disease patterns caused by chronic TNFR-signaling (Feldmann and Maini 2001; Victor, Gottlieb et al. 2003). However, 25% to 38% of rheumatoid arthritis patients treated with Eternacept do not respond to the medication compared to 21% to 42% of non-responders treated with Infliximab. This is not due to general unresponsiveness to anti-TNF therapy as it can be overcome by the administration of Infliximab to patients that do not respond to Eternacept, and reciprocally (Alonso-Ruiz, Pijoan et al. 2008).

1.2.7 Affinity of human and mouse TNF for mouse TNF receptors

Similar to the human system, soluble mouse TNF preferentially binds to mouse TNFR1 while membrane-bound mouse TNF is capable of efficient binding to both mouse TNFR1 and mouse TNFR2 (Grell, Douni et al. 1995; Papadakis and Targan 2000). Human TNF is only able to activate mouse TNFR1 but not mouse TNFR2 while mouse TNF triggers both human TNFR1 and human TNFR2 (Tartaglia, Weber et al. 1991).

1.2.8 TNFR2$^{-/-}$ systems

Cellular TNFR2$^{-/-}$ systems, both *in vivo* and *in vitro*, are characterized by impaired TNF-signaling. In such case, intrinsic TNFR2-signaling is abrogated and at the same time soluble bioactive TNF concentrations are not diminished via soluble TNFR2. Furthermore, reverse signaling can be excluded as the ligand for membrane-bound TNF, namely the soluble or membrane-bound TNFR2, is missing. However, reverse signaling via TNFR1 might occur. Nevertheless, not only TNFR2-related functions are impaired. Higher levels of soluble TNF might lead to higher TNFR1-signaling. This has to be taken into consideration when data generated from TNFR2$^{-/-}$ mice or cells are to be interpreted. Figure 1 illustrates the possible interactions of TNF receptors with TNF in the mice used for this thesis.

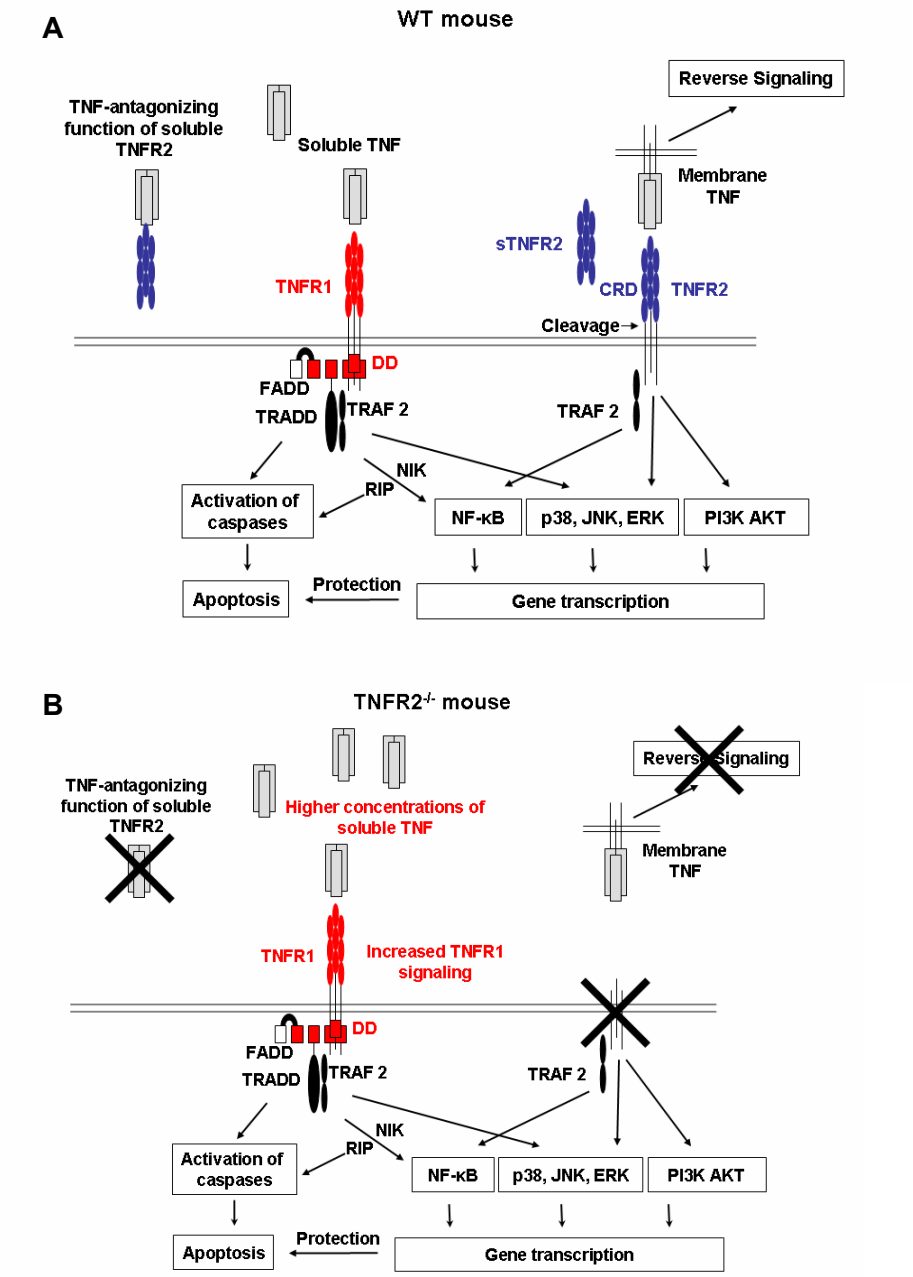

Figure 1: The TNF / TNFR system in cellular systems of wt and TNFR2$^{-/-}$ mice

(A) In C57BL/6 wt mice and cell cultures TNF can signal via TNFR1 and TNFR2. Additionally, reverse signaling via TNFR2 as ligand and membrane-bound TNF as receptor is possible and TNFR2 might act as a regulator for soluble and biologically active TNF. (B) If TNFR2 is missing, TNFR2 intrinsic signaling and reverse signaling via TNFR2 as ligand and membrane-bound TNF as receptor are prevented. Higher concentrations of soluble TNF might trigger TNFR1 as the modulatory function of soluble TNFR2 is missing.

1.2.9 Phenotype of TNFR2 knockout mice (TNFR2$^{-/-}$)

The use of knockout mice is the best choice to investigate the functional role of the respective protein *in vivo* and *in vitro*. In this work TNFR2$^{-/-}$ mice were used. These mice were generated by Dr. Mark Moore (Deltagen). TNFR2$^{-/-}$ mice exhibit several phenotypic characteristics. Sterns et al. found that TNFR2$^{-/-}$ mice are protected from a secondary infection in a phase of sepsis that is usually characterized as sepsis-induced immunosuppression. Further, TNFR2$^{-/-}$ mice show decreased numbers of regulatory T cells (Treg) after CLP (Chen, Baumel et al. 2007), they are fully protected from experimental cerebral malaria (Lucas, Juillard et al. 1997), and they cannot be protected from lethal septic peritonitis by prior LPS treatment (Echtenacher and Mannel 2002). Mice without functional TNFR2 show exacerbated myelin oligodendrocyte glycoprotein (MOG_{35-55})-induced experimental autoimmune encephalomyelitis (Suvannavejh, Lee et al. 2000), and are more susceptible to dextran sodium sulfate-induced colitis (Stillie and Stadnyk 2009). Furthermore, it has been reported that TNFR2 is involved in the development of proteinuria in severe glomerulonephritis (Vielhauer, Stavrakis et al. 2005) and that TNFR2$^{-/-}$ mice are protected from the pathology of glomerulonephritis induced by antibodies against the glomerular basement membrane.

1.2.10 Anti-mouse TNFR2 monoclonal antibodies (mAB)

Usually, knock-out ($^{-/-}$) mice allow to analyze the function of the respective missing protein by studying the effects of its lack. In the case of TNFR2, however, there is one ligand, two receptors, and, in addition, the possibility of reverse signaling. In TNFR2$^{-/-}$ mice not only forward and reverses signaling via TNFR2 are abrogated as TNFR1-signaling could also be strongly influenced by changes in the available concentrations of soluble TNF. In order to exclude side effects of TNFR1-signaling in TNFR2$^{-/-}$ mice, the observed effects should be reproduced in cells of wildtype mice treated with antagonistic reagents that specifically block the TNFR2. *Vice versa*, in cells of wildtype mice treated with selective agonistic substances, the distinct role of TNFR2 could be examined. Functional agonistic or antagonistic anti-mouse TNFR2 antibodies are the means of choice for selective activation or blockade of TNFR2. In order to facilitate the application of such antibodies *in vivo* over longer periods of time without the induction of an immune reaction against these substances, mouse anti-mouse antibodies are ideally suited. Unfortunately, neither agonistic nor antagonistic anti-mouse TNFR2 are available nor other reagents that selectively activate or block TNFR2.

1.3 Sepsis and immunoparalysis

The term sepsis originally defined a disease state based on a bacterial infection that spreads all over the organism via the blood and develops systemic impacts. Sepsis is a serious medical condition that is characterized by a whole-body inflammatory state and the presence of a known or suspected infection (Ayres 1985; Balk and Bone 1989). Sepsis is increasingly considered as a common cause of morbidity and mortality, particularly in elderly, immunocompromised, and critically ill patients (Manship, McMillin et al. 1984).

The characteristic mechanisms and processes caused by sepsis are subdivided in a biphasic model: the initial phase is characterized by a hyper-inflammatory state followed by a hypo-inflammatory state as the second phase (Hoflich and Volk 2002). The hyper-inflammatory phase is also called “systemic inflammatory response syndrome” (SIRS) and results from a strong reaction of the immune system to infections, traumata, pancreatitis, inflammation of tissue and organs, burns, or intensive surgical intervention (Balk and Parrillo 1992). SIRS comprises the interactions of bacterial components such as toll-like receptor (TLR) ligands and endogenous mediators of the immune system with their specific targets or receptors. This phase is characterized by the release of pro-inflammatory cytokines like TNF, IL-1β, IFN-γ, granulocyte colony-stimulating factor (G-CSF), IL-6, and IL-12 (Goldie, Fearon et al. 1995). This cytokine profile resembles a type 1 helper T cell (T_H1) immune response. Additionally, acute phase proteins are released from the liver. Furthermore, granulocytes and monocytes are activated and exhibit high metabolic activity. These cells emigrate from the bone marrow and migrate into the infected and inflamed tissue. As part of the innate immune system these cells initiate and increase the expression of multiple pro-inflammatory mediators and cytokines. Together, these reactions cause fever, hypotension, vasodilation, an increase of vascular permeability, and, finally, organ dysfunction and multi-organ failure.

Overt nitric oxide (NO) production by the inducible form of NO-synthases (iNOS) is assumed to play an important role in early sepsis-related vasoregulative failure. In response to inflammatory stimuli, NO levels increase rapidly within minutes to hours (Vincent 2001). This leads to hypotension (Rees 1995; Rosselet, Feihl et al. 1998; Scott, Mehta et al. 2002) and refractoriness to the vasopressor catecholamines (Gray, Schott et al. 1991). Animals treated with selective iNOS-inhibitors or transgenic mice deficient in iNOS showed less hypotension and increased microvascular reactivity under septic conditions (MacMicking, Nathan et al. 1995; Wei, Charles et al. 1995; Hollenberg 2002).

In response to the overwhelming cytokine storm and pro-inflammatory effects caused by SIRS, the organism reacts with a backlash called “compensatory anti-inflammatory response syndrome” (CARS) (Bone, Grodzin et al. 1997). This counter-regulation is meant to restore the

homeostasis and is mediated by both the innate and the adaptive immune system (Guillou 1993). In particular, T cells orchestrate the regulatory effects as they change their specific cytokine profile. The initial T_H1-typical cytokine profile changes into a type 2 helper T cell (T_H2) type expressing high amounts of IL-4, IL-5, IL-10, and IL-13 (Di Santo, Meazza et al. 1997). Additionally, very potent pro-inflammatory acting cells like lymphocytes and dendritic cells are eliminated by apoptosis (Ding, Chung et al. 2004). Furthermore, high concentrations of molecules antagonizing the proinflammatory cytokines are produced. The biological activity of TNF, one of the most potent inflammatory cytokines during sepsis, is reduced by the expression of high amounts of soluble TNFR2 (Goldie, Fearon et al. 1995; Mannel and Echtenacher 2000). This anti-inflammatory response rapidly develops during sepsis and aims to dampen the initial pro-inflammatory event. It seems to predominate in some patients and to induce a state of "immunoparalysis". In this case the immune system is not able to react to a second infection in an adequate way leading to organ failure and death.

It has been shown that monocytes of septic patients with immune suppression express lower amounts of major histocompatibility complex II (MHCII) (Docke, Randow et al. 1997) Furthermore, the endotoxin-induced TNF expression was reduced. These two phenomena could be restored by *ex vivo* treatment of peripheral blood mononuclear cells with IFN-γ. The *in vivo* treatment of a small number of immunosuppressed septic patients with IFN-γ supported these findings. Additionally, the clearance of infections was ameliorated and the mortality was slightly reduced by IFN-γ treatment.

In this work CLP was used to induce septic peritonitis in mice, as it is a clinically relevant and widely used animal model for sepsis (Buras, Holzmann et al. 2005; Deitch 2005; Rittirsch, Hoesel et al. 2007). The CLP surgery is performed so that ligation distal to the ileocecal valve and needle puncture of the ligated cecum cause leakage of fecal contents into the peritoneum, with subsequent development of polymicrobial bacteremia and sepsis (Rittirsch, Huber-Lang et al. 2009). Various species of bacteria become detectable in the blood followed by progressive SIRS, septic shock, and multiorgan injury (Alexander, Sheppard et al. 1991; Yasuda, Leelahavanichkul et al. 2008). Mice treated with CLP generally develop severe hypotension but no apparent hyperdynamic phase (Ganopolsky and Castellino 2004). The cytokine profile induced by CLP is comparable with the one observed in human sepsis. Anti-TNF treatment in sepsis does not lead to better prognosis neither in mice and nor in humans (Echtenacher, Falk et al. 1990; Eskandari, Bolgos et al. 1992; Remick, Newcomb et al. 2000; Miyaji, Hu et al. 2003; Yasuda, Yuen et al. 2006). Furthermore, CLP-induced sepsis leads to increased lymphocyte apoptosis resembling the immunosuppression in the later phase of human sepsis (Ayala and Chaudry 1996; Hotchkiss, Tinsley et al. 2003). CLP-induced shock differs clearly from LPS-

induced sepsis and is more closely related to human sepsis. The clinical features and drug responses caused by CLP are more similar to the human etiopathology than the LPS model. Nevertheless, some key features of humans sepsis like kidney and lung injury cannot be induced by CLP. The CLP model is illustrated in Figure 2.

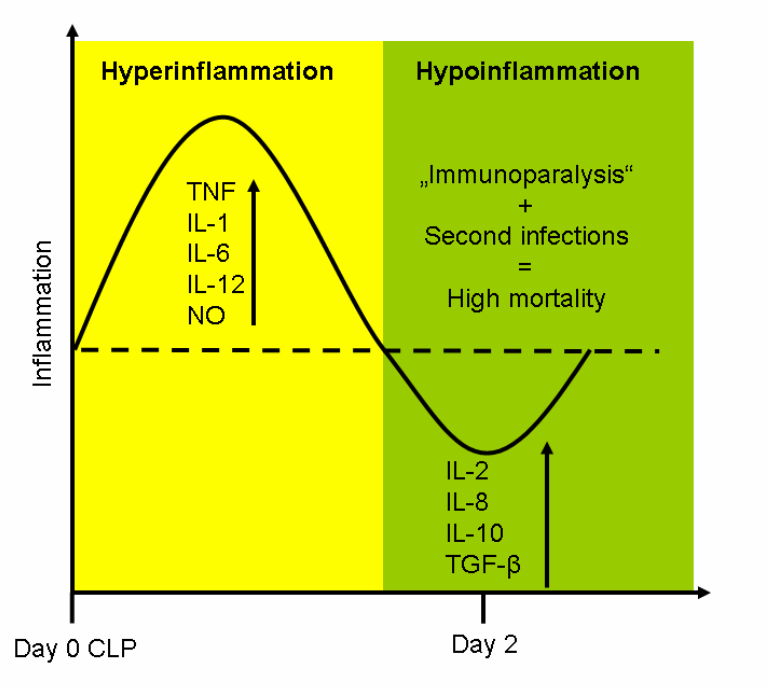

Figure 2: Inflammatory state after CLP

1.4 Myeloid cells

Hematopoietic stem cells (HSCs) are multipotent stem cells located in the bone marrow. These cells can differentiate into three different lineages: the myeloid lineage, the lymphoid lineage, and the erythroid-megakaryocyte lineage. The myeloid lineage comprises monocytes and macrophages, granulocytes, and polymorphonuclear cells - neutrophils, basophiles, and eosinophils. Different from this, T and B cells constitute the lymphoid lineage whereas erythrocytes and platelets derived from megakaryocytes form the erythroid-megakaryocyte lineage (Katsura 2002).

Myeloid cells are characterized by the expression of cluster of differentiation 11b (CD11b), one subunit of the CD11b / CD18 heterodimer (Arnaout, Gupta et al. 1988). CD11b is an integrin cell surface receptor, strongly regulated depending on the differentiation status, and tissue specific. The CD11b / CD18 heterodimer is expressed exclusively on the surface of mature monocytes, macrophages, neutrophils, and natural killer cells (Todd, Nadler et al. 1981).

1.4.1 Macrophages

1.4.1.1 Historical background

Macrophages are cells that functionally react early in the host defense as part of the innate immune system. In the year 1905 Ilya Mechnikov revealed the importance of phagocytes for the development and homeostasis of the immune system as well as for the host defense from infections. These processes were termed “innate immune reactions”. Parallel to this, Paul Ehrlich started to work on a phenomenon which is today known as “adaptive immunity”. Both researchers were awarded the Nobel Prize in physiology and medicine in the year 1908. Macrophages link innate and adaptive immunity and remain an important area of immunological research (Nathan 2008).

1.4.1.2 Monocyte-derived macrophages

Monocytes circulate in the peripheral blood and have the capacity to differentiate into tissue-resident macrophages as well as into more specialized cells like dendritic cells and osteoclasts. Monocytes are generated in the bone marrow and represent a direct descendant from a common myeloid progenitor that is shared with neutrophils. After circulating for several days these peripheral blood monocytes enter tissues and replenish the tissue macrophage populations (Volkman and Gowans 1965). The monocyte development in the bone marrow starting from the hematopoietic stem cell comprises the stages of granulocyte / macrophage colony-forming units (GM-CFU), macrophage colony-forming units (M-CFU), monoblasts, pro-monocytes, and finally lymphocyte antigen 6 C^+ ($Ly6C^+$) “inflammatory” monocytes which are released into the peripheral blood. Inflammatory monocytes are the source of macrophages, dendritic cells, and osteoclasts in tissues. This is illustrated in Figure 3. Macrophages can be subdivided into different populations depending on the tissue they migrate to and on their function. For instance, osteoclasts are found in bone, microglia cells in the central nervous system, alveolar macrophages in the lung, kupfer cells in the liver, histiocytes in connective tissue, and white-pulp-, red-pulp-, marginal-zone-, and metallophilic-macrophages in the spleen (Mosser and Edwards 2008). The specific roles of these macrophages are the maintenance of homeostasis and the immune reaction in the respective organs. Furthermore, they immigrate and initiate immune reactions at the place of the infection.

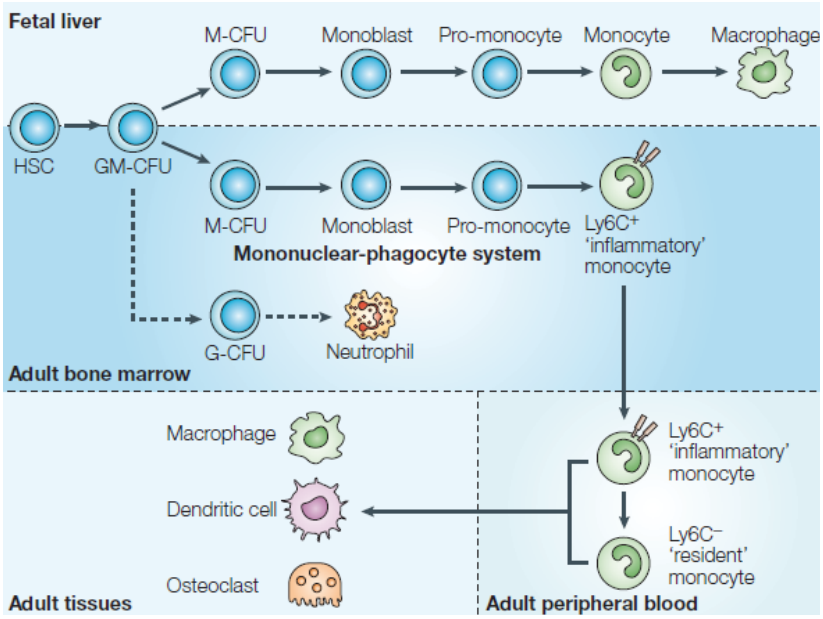

Figure 3: Monocyte differentiation and macrophage development
(Gordon and Taylor 2005)

In the human system macrophages can be generated by *in vitro* culture of peripheral blood monocytes with M-CSF for 4 days (Lutter, Ugocsai et al. 2008). Mouse macrophages cannot be generated in an adequate amount as the yield of peripheral blood monocytes is limited. Mouse macrophages used in this work were either isolated from the spleen (spleen macrophages) or as a main part of peritoneal exudate cells 18 hours after phosphate buffered saline (PBS) injection into the peritoneal cavities.

Additionally, bone marrow-derived dendritic cells (BMDC) were used as another source of myeloid cells (Lutz, Kukutsch et al. 1999). Bone marrow cells were grown in granulocyte / macrophage colony-stimulating factor (GM-CSF)-supplemented medium for 10 days. This led to the differentiation of the cells into $CD11c^+$ dendritic cells. Nevertheless, almost all of these cells kept the CD11b marker for myeloid cells (Nikolic, de Bruijn et al. 2003).

1.4.2 Biological relevance of macrophages

Macrophages are part of the mononuclear phagocyte family and exhibit broad phenotypic heterogeneity as a consequence of varying cellular differentiation, widespread tissue distribution, and different reactivity to many endogenous and exogenous stimuli. Constitutive and induced migration into the tissues is one characteristic attribute of macrophages. Additionally, interactions with altered host cells, modified molecules, and exogenous agents contribute to the differentiation of macrophages. Macrophages are resident phagocytic cells in

lymphoid and nonlymphoid tissues and believed to be involved in steady-state tissue homeostasis via clearance of apoptotic cells and the production of growth factors. Macrophages are equipped with a broad range of pathogen-recognition receptors that make them efficient at phagocytosis and induce production of inflammatory cytokines (Gordon 2002). These mediators are recognized by a multitude of both plasma-membrane associated and intracellular receptors. Consequently, the respective substances are taken up by phagocytosis or endocytosis, are processed, and presented on MHCII molecules. In addition, intracellular signaling occurs and gene expression patterns are activated or repressed. This leads to altered adhesion and migration and causes the secretion of various cytokines and cellular mediators as well as the activation of effector functions. Ligands on pathogenic host cells are recognized by a range of scavenger-type receptors resulting in the specific induction or suppression of macrophage inflammatory responses, depending on mechanisms not fully understood (Fadok, Bratton et al. 1998; Gordon 2003). The recognition of foreign ligands is mediated either indirectly by a multitude of receptors that use opsonins like antibodies, complement, collectins, and LPS-binding protein or in a direct way employing TLR and lectins for the recognition of carbohydrates, proteins, lipids, and nucleic acids. One of the most prominent intracellular signaling molecules that is activated after recognition of these substances is NF-κB (Gordon 2003).

Macrophage activation can be divided into innate and humoral as well as classical and alternative ways. Both pairs of definitions for macrophage activation are somewhat overlapping.

The innate activation of macrophages is induced by microbial stimuli such as TLR ligands or β-glucans and induces the upregulation of costimulatory molecules, the generation of low molecular weight metabolites like NO and reactive oxygen species (ROS), and the expression and release of cytokines like IFN-α/β, TNF, IL-6, and IL-12.

Humoral activation of macrophages is mediated by the activation of Fc- or complement-receptors and mainly results in cytolytic processes.

The classical activation of macrophages requires two distinct signals. The priming stimulus is IFN-γ from T cells. Consequently, the T cell milieu and activation state strongly interfere and regulate macrophage activation. The second signal is TNF either exogenously-derived or produced by the macrophage itself as a consequence of the contact with microbial triggers like TLR ligands (Mosser 2003). This induces the upregulation of MHCII and costimulatory molecules like CD80 and CD86, and, consequently, leads to an improved antigen presentation and CD4 T cell activation (Mosser and Zhang 2008). Furthermore, classically activated macrophages can be characterized by the production of NO, oxydative burst as well as the

expression of IL-1, IL-6, IL-12, and TNF. The effects result in microbicidal activity and cellular immunity, but can cause tissue damage as well.
Alternative activation requires IL-4, IL-10, or IL-13 as extracellular signals. These cytokines are generally considered to originate from T_H2 T cell reactions. This also leads to upregulation of MHCII expression and improves endocytosis as well as antigen presentation, interestingly with minor effects on CD4 T cell activation and proliferation. Additionally, the expression of intracellular Arginase 1 (Arg1), selective chemokines such as macrophage-derived chemokine (MDC, CCL22), thymus and activation regulated chemokine (TARC, CCL17), and mannose receptor is increased. The characteristic cytokines produced by alternatively activated macrophages are IL-10 and IL-1 receptor antagonist (IL-1ra). Alternatively activated macrophages are thought to be crucial for humoral immunity, allergic and anti-parasite responses as well as repair mechanisms (Gordon 2003).
During the very early stages of mammalien ontogeny developmental embryonic macrophages are produced in the yolk sac (Cline and Moore 1972; Enzan 1986). They are necessary for the clearance of apoptotioc cells and, thus, play a crucial role in organogenesis.

1.4.3 Interleukin 6

The pro-inflammatory cytokine IL-6 plays an important role in immunity and links the innate with the adaptive immune system. IL-6 is a pleiotropic cytokine produced by many types of cells such as macrophages, T cells, fibroblasts, and endothelial cells. The expression of IL-6 is induced by stimuli such as bacteria, viruses, and other cytokines such as IL-1 and TNF. IL-6 promotes growth, differentiation and expansion of B cells as well as the production and secretion of immunoglobulins. It induces the differentiation and activation of macrophages and T cells and initiates the production and release of acute phase proteins (Kishimoto 2006).

1.4.4 Regulation of the iNOS expression and NO signaling

The level of iNOS-derived NO is mostly regulated at the transcriptional level. Depending on the stimulation and cell type, different signaling pathways are activated to express transcription factors that are required to induce iNOS mRNA expression, i.e. activators such as activating protein 1 (AP-1), protein kinase C, janus kinase (JAK), tyrosine kinase, MAP kinase, and raf-1 protein kinase or inhibitors such as protein tyrosine phosphatase and phosphoinositide-3-kinase. Both the proximal and distal region of the iNOS promoter features binding sites for transcription factors NF-κB and Jun / Fos heterodimers as well as CCAAT binding enhancer

binding proteins (C/EBT), cyclic adenosine monophosphate (cAMP) response element-binding protein (CREB), and the signal transducers and activators of transcription protein (STAT) family (Aktan 2004). The signaling effect of NO occurs by the nitrosation of heme-iron present in the enzyme soluble guanylate cyclase (sGC). sGC is a heterodimeric enzyme that converts guanosine triphosphate to cyclic guanosine monophosphate (GMP) which mediates the signaling.

1.4.5 Different types of myeloid cells used in this study

Different types and sources of myeloid cells were used in this work, especially peritoneal exudate cells (PEC), $CD11b^+$ spleen cells, and bone marrow-derived dendritic cells (BMDC).

1.4.5.1 Peritoneal exudate cells (PEC)

PEC were used as the source of myeloid cells representing primary macrophages. PEC migrate into the peritoneal cavity after injection of PBS and can easily be isolated via peritoneal lavage. Up to 90% of the PEC are macrophages.

1.4.5.2 $CD11b^+$ splenocytes

About 5% of the spleen cells in healthy mice are $CD11b^+$ myeloid cells. The cells can easily be isolated from the spleen of either naïve or experimentally treated mice.

1.4.5.3 Bone marrow-derived dendritic cells (BMDC)

The generation of BMDC is an advanced culture method for generating large quantities of relatively pure myeloid cells from mouse bone marrow (Lutz, Kukutsch et al. 1999). The cells are grown in a GM-CSF-containing medium and differentiate into $CD11b^+$ $CD11c^+$ myeloid cells with dendritic phenotype within 10 days.

1.4.6 Myeloid-derived suppressor cells (MDSC)

More than 20 years ago myeloid cells with suppressive properties were described in cancer patients (Buessow, Paul et al. 1984; Young, Newby et al. 1987). There is strong evidence that myeloid cells with suppressive activity contribute to the negative regulation of the immune

system in cancer and other diseases. Those cells were termed myeloid–derived suppressor cells (MDSC). They are part of the myeloid lineage and can be characterized by an immature state and a specific capacity to suppress T cell functions. Additionally, MDSC contribute to the regulation of the innate immunity as they are able to modulate the cytokine production of macrophages (Sinha, Clements et al. 2007).

MDSC are a subpopulation of cells called “immature myeloid cells” (IMC) that comprise myeloid progenitor cells as well as immature forms of myeloid cells. IMC originate from the bone marrow. In healthy organisms they differentiate very quickly into mature granulocytes, macrophages, and dendritic cells. In pathologic conditions like cancer, infectious diseases, sepsis, trauma, and autoimmune diseases the differentiation of IMC is partially blocked leading to increased MDSC numbers and higher activation. Activated MDSC are characterized by the expression of the immunosuppressive factors iNOS and Arg1. iNOS requires L-arginine as substrate and catalyzes the generation of NO and ROS (Gabrilovich and Nagaraj 2009) and Arg1 depletes l-arginine. The granulocyte-differentiation epitope (GR1) is expressed early in the myeloid development in the bone marrow and can be detected using the RB6-8C5 antibody (Fleming, Fleming et al. 1993). The epitope recognized by this antibody is part of both Ly6C and Ly6G. These proteins are members of the Ly6 family which are phospatidylinositol-anchored cell surface glycoproteins with a molecular weight between 12 and 20 kDa (Gumley, McKenzie et al. 1995). IMC are $CD11b^+$ $GR1^+$ and can be subdivided into polymorphonuclear $CD11b^+ Ly6C^{int} Ly6G^+$ granulocytic cells ($Ly6C^{int} Ly6G^+$ / PMN-MDSC) and MDSC with monocytic morphology (MO-MDSC / MDSC) characterized by the markers $CD11b^+ Ly6C^+ Ly6G^-$. PMN-MDSC produce high amount of ROS but almost no NO. Contrary to this, MDSC are induced by inflammation and provide low production of ROS but high amounts of NO (Movahedi, Guilliams et al. 2008; Youn, Nagaraj et al. 2008). Especially MDSC are very potent in suppressing both CD4 and CD8 T cell proliferation (Zhu, Bando et al. 2007).

MDSC have to be expanded and activated, in order to fully develop efficient suppressive properties. Granulocyte/macrophage colony-stimulating factor (GM-CSF) is a very potent cytokine for the MDSC development as it interacts very early with expansion, maturation, and differentiation of early hematopoietic progenitors (Barreda, Hanington et al. 2004). During inflammation high concentrations of GM-CSF are produced and released from activated T cells, natural killer (NK) cells, dendritic cells (DC), and, interestingly, various tumors. GM-CSF may lead to expansion, redistribution, and functional changes of $CD11b^+$ $GR1^+$ cells and may force the development of functional MDSC (Ribechini, Greifenberg et al. 2010). Consequently, one way to generate MDSC *in vitro* is the incubation of mouse bone marrow cells with GM-CSF. It has been shown that low GM-CSF conditions are sufficient to generated immature DC and

MDSC between day 8 and 10 of the BMDC culture whereas this can be reached within 4 days under high GM-CSF concentrations. Such MDSC generated *in vitro* from mouse bone marrow cells efficiently suppress both CD4 and CD8 T cell proliferation and other effector mechanisms (Rossner, Voigtlander et al. 2005). Besides GM-CSF, several other mediators and pathological conditions like vascular endothelial growth factor (VEGF), prostaglandin E2, interferon-γ (IFN-γ), tumors, infections, graft versus host disease, chronic inflammation, and autoimmunity are known to be involved in increased MDSC generation (Ribechini, Greifenberg et al. 2010). It has also been shown that MDSC numbers are drastically increased in polymicrobial sepsis (Delano, Scumpia et al. 2007). MDSC were found in bone marrow, spleen, and lymph nodes. This effect can be mimicked by the administration of a combination of LPS and IFN-γ resulting in activation and development of splenic MDSC along with a partial blockade of DC development (Greifenberg, Ribechini et al. 2009). Figure 4 illustrates the origin of MDSC.

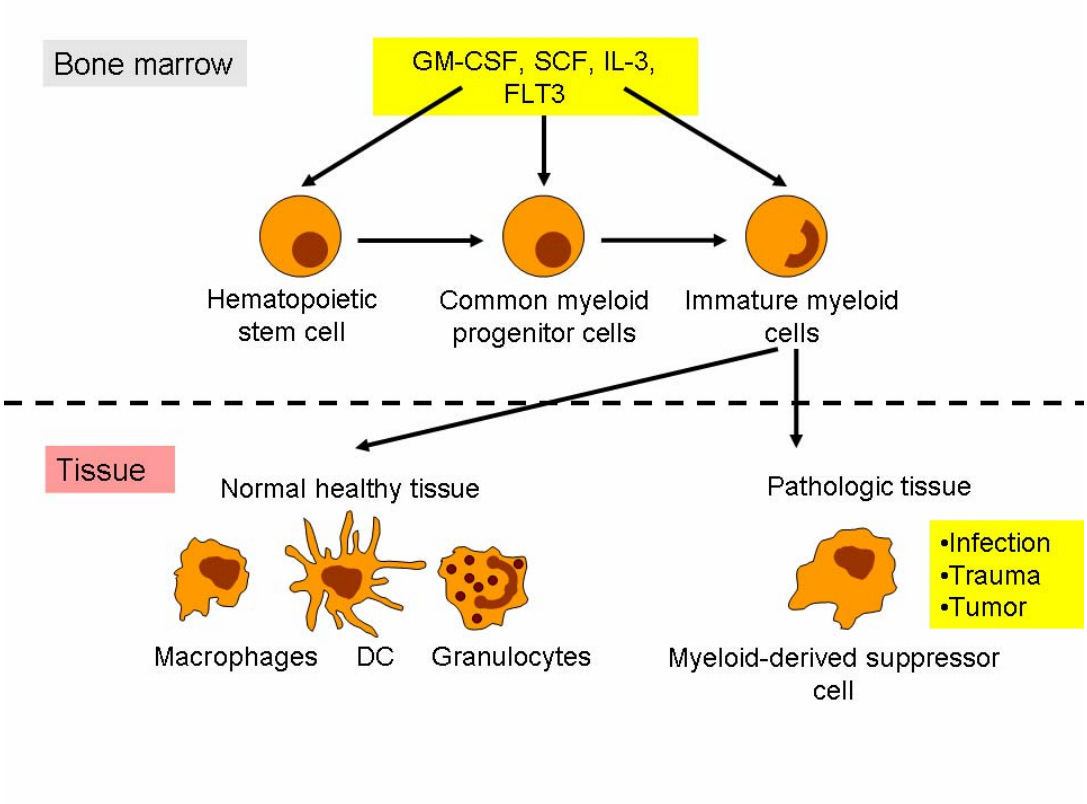

Figure 4: MDSC development

Myelopoiesis in the bone marrow is orchestrated by several cytokines including GM-CSF, stem-cell factor (SCF), IL-3, and FMS-related tyrosine kinase 3 (FLT3). Hematopoietic stem cells differentiate into common myeloid progenitor cells and, afterwards, into immature myeloid cells. In healthy conditions these cells migrate to peripheral organs and differentiate into macrophages, DC, or granulocytes. In pathological conditions such as provided by infection, trauma, or tumor normal differentiation is abrogated and MDSC arise from immature myeloid cells (Gabrilovich and Nagaraj 2009).

The majority of studies concerning MDSC reveal that the immunosuppressive effects require cell-cell contact. This indicates that the suppressive effects function either via cell-surface receptors, through the release of short-lived mediators or by changes in the micro-environment of the target cells (Gabrilovich and Nagaraj 2009). One of the most prominent mechanisms of T cell suppression constitutes the depletion of the non-essential amoni acid L-arginine. L-arginine serves as a substrate for two enzymes, Arg1 and iNOS. Arg1 converts L-arginine to urea and L-ornithine whereas iNOS generates NO and L-citrulline (Bronte and Zanovello 2005). Adequate L-arginine availability is crucial for proper T cell function. It is depleted by Arg1 from the microenvironment whereby T cell proliferation is suppressed. This is mediated by several mechanisms. CD3 ζ-chain expression is reduced leading to a reduction of costimulatory signals (Rodriguez, Zea et al. 2002). Furthermore, upregulation of cell cycle regulators cyclin D3 and cyclin-dependend kinase 4 is impaired (Rodriguez, Quiceno et al. 2007). iNOS contributes to the depletion of L-arginine as it is required as substrate for the generation of NO. NO inhibits JAK3 and STAT5 function in T cells and reduces the MHCII expression on antigen presenting cells (APC) whereby the T cell functions are constricted (Bingisser, Tilbrook et al. 1998; Harari and Liao 2004). Additionally, NO is known to directly induce apoptosis in T cells (Rivoltini, Carrabba et al. 2002). Recently, data from tumor models revealed that the suppressive activity of PMN-MDSC is based on Arg1 expression whereas the suppressive effects in MO-MDSC are based on STAT1 and iNOS expression (Movahedi, Guilliams et al. 2008).

Another suppressive MDSC mechanism is the production of ROS, especially in tumor-bearing organisms. ROS production in MDSC can be initiated by treating the cells with factors expressed from tumors, i.e. tumor growth factor β (TGF-β), IL-3, IL-6, IL-10, platelet-derived growth factor and GM-CSF (Sauer, Wartenberg et al. 2001; Youn, Nagaraj et al. 2008).

Peroxynitrite emerges from the chemical reaction of NO with superoxide anions and is one of the most powerful oxidants generated in organisms. It induces the nitrosylation and nitration of the amino acids cystein, methionine, tryptophane, and tyrosine in T cells and, thus, deactivates T cell receptors and costimulatory molecules (Vickers, MacMillan-Crow et al. 1999).

The capability of MDSC to support the *de novo* generation of forkhead box $P3^+$ ($FoxP3^+$) Treg *in vivo* has been shown (Huang, Pan et al. 2006). The different ways of MDSC generation, induction, activation, and their suppressive interactions and mechanisms are described in Figure 5.

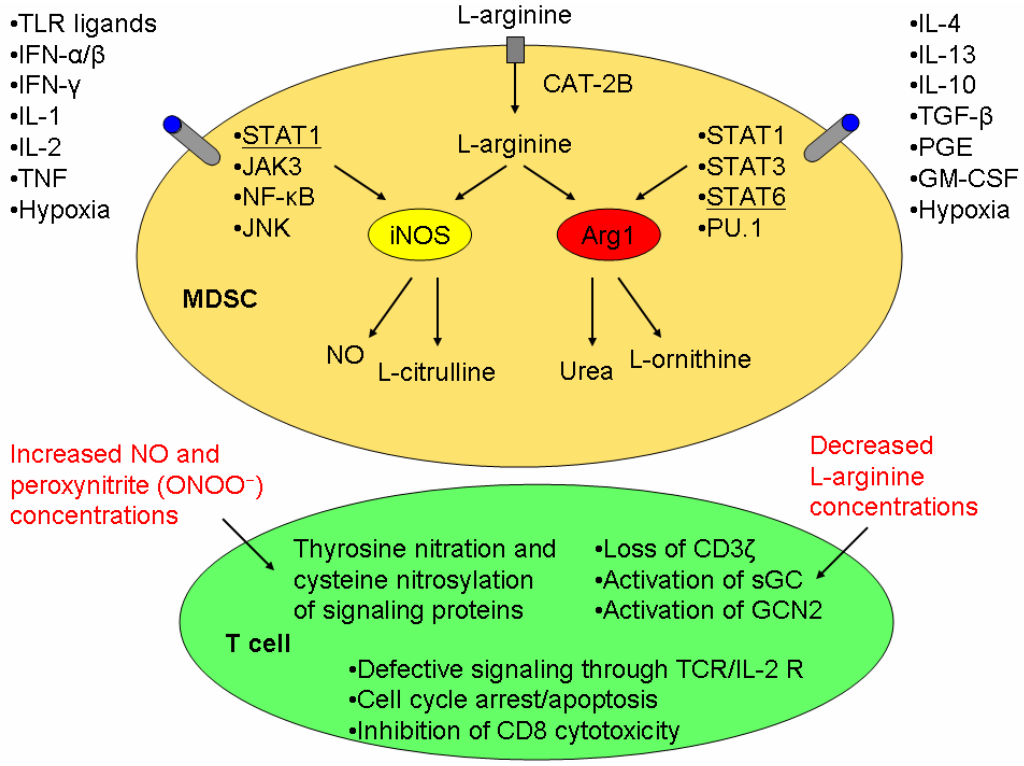

Figure 5: Activation and suppressive mechanisms of MDSC

The cationic amino acid transporter 2B (CAT-2B) transfers L-arginine into the cytoplasma of MDSC. iNOS is expressed in MDSC after stimulation with various mediators like TLR ligands, IFN-γ, or TNF, via the transcriptional control of STAT1 or NF-κB. iNOS utilizes L-arginine as substrate to generate NO. NO can react with superoxide anions to form peroxinitrite. Other cytokines like TGF-β, IL-4, and GM-CSF activate STAT6 and other transcription factors and increase the expression of Arg1. Arg1 depletes L-arginine. Reduced L-arginine concentrations lead to the loss of ζ-chain integrity in T cells and disable proper T cell activation. Peroxinitrite is responsible for the nitration and nitrosylation especially of cystein residues and causes impaired function of signaling proteins in T cells. NO causes defective TCR signaling, cell cycle arrest, and apoptosis and is responsible for the inhibition of CD8 cytotoxicity (Sica and Bronte 2007).

1.5 Aim of the thesis

The aim of this work was to investigate the role of TNFR2 on myeloid cells, in particular under septic conditions caused by CLP. Dr. Theo Sterns reported that TNFR2 deficient mice were protected from a secondary infection during the phase of sepsis that is usually characterized as sepsis-induced immunosuppression (Sterns, Pollak et al. 2005). One hypothesis of this work was that MDSC in TNFR2$^{-/-}$ mice are more frequent or more active compared to MDSC in C57BL/6 wildtype mice and, thus, are responsible for the protection of TNFR2$^{-/-}$ mice from immunoparalysis. Another hypothesis was that missing direct cellular TNFR2-signaling in

myeloid cells causes the beneficial course of disease in CLP-treated TNFR2$^{-/-}$ mice after secondary infection compared to wildtype mice. Therefore, it was examined how myeloid cells influence the impact of CLP in mice and whether this cellular phenotype could be responsible for the protection of TNFR2$^{-/-}$ mice from a secondary infection in sepsis. This included the investigation of the general functions of TNFR2$^{-/-}$ myeloid cells and macrophages with a special focus on myeloid-derived suppressor cells.

Furthermore, it should be clarified whether the cellular phenotypes that were found in septic TNFR2$^{-/-}$ mice are due to the lack of direct TNFR2-signaling or due to possible side effects caused by the absence of TNFR2. The latter consist of missing reverse signaling via membrane-bound TNF and soluble TNFR2 as well as of higher soluble TNF concentrations leading to increased and continuous TNFR1-signaling as a consequence of the lack of soluble TNF being trapped by soluble TNFR2. In this context the question arose whether TNFR2$^{-/-}$ mice are TNF tolerant as they might be continuously exposed to higher levels of soluble TNF and whether this might cause epigenetic modifications. For the exploration of these issues different types of myeloid cells from naïve and CLP-treated mice were analyzed in terms of numbers, frequency, activation, MDSC phenotype, Arg1 and iNOS mRNA expression, and production of NO as well as the production profile of cytokines and soluble TNFR2. By the use of mixed C57Bl/6 wt and TNFR2$^{-/-}$ cultures and bone marrow chimeric mice it should be examined whether missing TNFR2-signaling or altered TNFR1 stimulation is responsible for the phenotypes seen in TNFR2$^{-/-}$ myeloid cells.

Another attempt of this thesis was to directly activate or block the TNFR2 *in vivo* and *in vitro*. Therefore, monoclonal mouse anti-mouse TNFR2 antibodies were to be generated and tested for TNFR2-specific agonistic and antagonistic properties. Specific activation of TNFR2 could identify effects caused by TNFR2-signaling whereas specific TNFR2 blockade would transform wildtype cells into a TNFR2$^{-/-}$ status. With such tools, effects seen in TNFR2$^{-/-}$ cellular systems could be mimicked in wildtype cells treated with antagonistic TNFR2 mAB.

2 Materials and methods

2.1 Materials

2.1.1 Instrumentation

Item	Manufacturer	City (Country)
Blaubrand® hemocytometer	Brand GmbH + Co KG	Wertheim (GER)
Cell Safe, Incubator	Integra Bioscience GmbH	Fernwald (GER)
Centrifuge Shandon Cytospin 4	ThermoScientific GmbH	Karlsruhe (GER)
Circular shaker GFL-3015	Omnilab GmbH	Mettmenstetten (GER)
Eppendorf 5417R centrifuge	Eppendorf AG	Hamburg (GER)
Eppendorf 5418R centrifuge	Eppendorf AG	Hamburg (GER)
Eppendorf 5810R centrifuge	Eppendorf AG	Hamburg (GER)
Eppendorf BioPhotometer	Eppendorf AG	Hamburg (GER)
Film developing device Optimax Typ TR	MS Laborgeräte GmbH	Heidelberg (GER)
Gel documentation device GeneGenius	Syngene	Cambridge (UK)
Gel drying device model 483	Bio-Rad Laboratories GmbH	München (GER)
Gel electrophoresis device	Bio-Rad Laboratories GmbH	München (GER)
Heat incubator	WTB Binder GmbH	Tuttlingen (GER)
HiTrap™ protein G HP columns	GE Healthcare GmbH	München (GER)
iQ5 real-time PCR cycler	Bio-Rad Laboratories GmbH	München (GER)
Laminar flow HB2448	Thermo Fisher Scientific GmbH	Bonn (GER)
LSRII, Flow cytometer	BD Biosciences GmbH	Heidelberg (GER)
MACS® MultiStand	Miltenyi Biotec GmbH	Bergisch Gladbach (GER)
Magnetic stirrer MR2002	Heidolph GmbH & Co. KG	Schwabach (GER)
Microplatereader Emax	Molecular Devices	München (GER)
Microscope Diaplan	Olympus GmbH	Hamburg (GER)
Microscope Olympus CK2	Olympus GmbH	Hamburg (GER)
MidiMACS™ Separator	Miltenyi Biotec GmbH	Bergisch Gladbach (GER)
Mini PROTEAN electrophoresis system	Bio-Rad Laboratories GmbH	München (GER)
MiniMACS™ Separator	Miltenyi Biotec GmbH	Bergisch Gladbach (GER)
MS2 IKA® vortexer	IKA®	Staufen (GER)
Nitrogen tank	German Cryo GmbH	Jüchen (GER)
PCR device MyCycler	Bio-Rad Laboratories GmbH	München (GER)

pH-Meter Inolab	WTW	Weilheim (GER)
Pipetting unit accujet pro	Brand GmbH	Wertheim (GER)
Power supply unit PowerPac 300	Bio-Rad Laboratories GmbH	München (GER)
Power supply unit PowerPack P25	Biometra GmbH	Göttingen (GER)
Protein isolation device Econo System	Bio-Rad Laboratories GmbH	München (GER)
Sartorius L2200S	Sartorius AG	Göttingen (GER)
Sartorius R16OP balance	Sartorius AG	Göttingen (GER)
Thermo-block Bio TDB-100	Biometra GmbH	Göttingen (GER)
Thermo-shaker TS-100	Biometra GmbH	Göttingen (GER)
Water-bath TW12	Julabo GmbH	Seelbach (GER)
Western blot device fastblot B34	Biometra GmbH	Göttingen (GER)

2.1.2 Consumables

Item	**Manufacturer**	**City (Country)**
Amersham Hyperfilm ECL	GE Healthcare GmbH	München (GER)
Biosphere filter tips (10 µL, 20 µL, 100 µL, 1mL)	Sarstedt AG & Co	Nümbrecht (GER)
Biosphere filter tips nuclease-free (10 µL, 20 µL, 100 µL, 1mL)	Sarstedt AG & Co	Nümbrecht (GER)
Cannulas BD Plastipak	BD Biosciences GmbH	Heidelberg (GER)
Cell culture flasks (25 cm², 75 cm², 175 cm²)	BD Biosciences GmbH	Heidelberg (GER)
Cell scraper (25 cm)	Sarstedt AG & Co	Nümbrecht (GER)
Cellstrainer (40 µM)	BD Biosciences GmbH	Heidelberg (GER)
Centrifugation tubes (15 mL, 50 mL)	BD Biosciences GmbH	Heidelberg (GER)
Cover slides for hemocytometer	Engelbrecht GmbH	Edermünde (GER)
Cryogenic tubes	Nalge Nunc GmbH	Langenselbold (GER)
Dialysis membrane type 20	Biomol GmbH	Hamburg (GER)
Eppendorf cup (1.5 / 2 mL)	Eppendorf AG	Hamburg (GER)
Eppendorf UVette® cuvettes	Eppendorf AG	Hamburg (GER)
FACS tubes BD Falcon	BD Biosciences GmbH	Heidelberg (GER)
Glas columns for protein purification (Ni-NTA)	Bio-Rad Laboratories GmbH	München (GER)

MACS® Cell Separation Columns 25 LS/MS	Miltenyi Biotec GmbH	Bergisch Gladbach (GER)
Microtiter plate micro well	Nalge Nunc GmbH	Langenselbold (GER)
Multiwell cell culture plates (6, 12, 24, 48, 96)	BD Biosciences GmbH	Heidelberg (GER)
Paper filter for cytospin	Labonard	Mönchengladbach (GER)
Parafilm® M	American National Can Group	Chicago (USA)
Petri dishes	Sarstedt AG & Co	Nümbrecht (GER)
Polystyrene tubes	BD Biosciences GmbH	Heidelberg (GER)
PVDF transfer membran immobilon	Millipore GmbH	Schwalbach (GER)
Reaction vessels (15 mL, 50 mL)	Greiner GmbH	Frickenhausen (GER)
Sample slide (sliced, matt-edge)	Engelbrecht GmbH	Edermünde (GER)
Serological pipettes (5mL, 10mL, 25mL)	Sarstedt AG & Co	Nümbrecht (GER)
Sterile filter 0.2 µm	Sartorius AG	Göttingen (GER)
Sterile filter bottletop 75 mm	Nalge Nunc GmbH	Langenselbold (GER)
Suture clip (7.5 x 1.75 mm)	Tierärztebedarf J. Lehnecke GmbH	Schortens (GER)
Syringes (1mL, 2mL, 5mL, 10mL)	BD Biosciences GmbH	Heidelberg (GER)
Whatman paper	A. Hartenstein	Würzburg (GER)
96 well PCR plate (semi-skirted)	PEQLAB Biotechnologie GMBH	Erlangen (G)
Microseal ‘B’ film	Bio-Rad Laboratories GmbH	München (GER)

2.1.3 Chemicals and reagents

Item	**Manufacturer**	**City (Country)**
Acrylamide / bisacrylamide rotiphorese gel 30	Roth gmbH & Co. KG	Karlsruhe (GER)
Agarose, elecrophoresis grade	Bio&Sell e.K.	Nürnberg (GER)
Ampicilline	Roche Diagnostics GmbH	Penzberg (GER)

BD OptEIA Substrat Reagent A and B	BD Biosciencess GmbH	Heidelberg (GER)
Carboxyfluorescein succinimidyl ester	Invitrogen GmbH	Karlsruhe (GER)
Chelating Sepharose Fast Flow	GE Healthcare GmbH	München (GER)
Cytofix / Cytoperm	BD Biosciencess GmbH	Heidelberg (GER)
DNA standard (100 bp and 1 kb Ladder)	New England Biolabs GmbH	Frankfurt / Main (GER)
dNTP-Mix (10 mM)	Promega GmbH	Mannheim (GER)
Ethylenediaminetetraacetic acid	Promega GmbH	Mannheim (GER)
Fetale bovine serum	PAN Biotech GmbH	Aidenbach (GER)
Gentamycine	PAN Biotech GmbH	Aidenbach (GER)
Go-Taq	Promega GmbH	Mannheim (GER)
HAT-supplement	PAN Biotech GmbH	Aidenbach (GER)
HT-supplement	PAN Biotech GmbH	Aidenbach (GER)
Hygromycine	PAA Laboratories GmbH	Pasching (A)
Insect Xpress™	Lonza GmbH	Wuppertal (GER)
Kanamycine	PAN Biotech GmbH	Aidenbach (GER)
Ketaminehydrochloride 5%	WDT eG Garbsen	Garbsen (GER)
LPS (*S. abortus equi*)	Prof. M. Freudenberg	Max-Planck-Institute of Immunology (GER)
M-MLV RT 5 x reaction buffer	Promega GmbH	Mannheim (GER)
Neomycin (G418)	PAN Biotech GmbH	Aidenbach (GER)
NOWA Solution A and B	MoBiTec GmbH	Göttingen (GER)
Nucelase-free water	Promega GmbH	Mannheim (GER)
Oligo-dT Primer	Promega GmbH	Mannheim (GER)
Penicillin/ Streptomycin	Invitrogen GmbH	Karlsruhe (GER)
Perm / Wash (10 x)	BD Biosciencess GmbH	Heidelberg (GER)
Phosphat buffered salines	PAA Laboratories GmbH	Pasching (A)
Polyethylenglycol 1500	Roche Diagnostics GmbH	Penzberg (GER)
Precision Plus Protein All Blue Standard	Bio-Rad Laboratories GmbH	München (GER)
Recombinant mouse IFNγ	Peprotech GmbH	Hamburg (GER)
Recombinant mouse TNF	Peprotech GmbH	Hamburg (GER)
RNaseZap®	Ambion GmbH	Kassel (GER)
RPMI 1640 PAA	PAN Biotech GmbH	Aidenbach (GER)
Skimmed milk powder	Granovita GmbH	Lüneburg (GER)

TMB substrate reagent set	BD Biosciencess GmbH	Heidelberg (GER)
TNC-mTNF	Prof. H. Wajant	University of Würzburg (GER)
Triton X-100	Serva Feinbiochemica GmbH	Heidelberg (GER)
Xylazinehydrochloride 2%	WDT eG Garbsen	Garbsen (GER)

The solvents or chemicals not mentioned here were purchased either from Merck KGaA (Darmstadt, Germany) or Sigma-Aldrich GmbH (Taufkirchen, Germany).

2.1.4 Antibodies

Antibodies for ELISA / Western blot

Item	Modification	Manifacturer	City (Country)
Donkey anti-human IgG (H+L) HRP	HRP	Dianova GmbH	Hamburg (GER)
Goat anti-mouse IgG (whole molecule) POX	POX	Sigma Aldrich GmbH	Taufkirchen (GER)
Goat anti-mouse IgG (γ-chain specific) AP	AP	Sigma Aldrich GmbH	Taufkirchen (GER)
Mouse anti-Penta-His mAB	None	Qiagen GmbH	München (GER)
Mouse anti-V5 mAB	None	Invitrogen GmbH	Karslruhe (GER)
Mouse anti-V5 mAB HRP	HRP	Invitrogen GmbH	Karslruhe (GER)

Antibodies for FACS and MACS

Item	Clone	Modification	Manifacturer	City (Country)
7-AAD viability staining solution		7-AAD	BioLegend	San Diego / California (USA)
Alexa Fluor® 647 Annexin V		AF647	BioLegend	San Diego / California (USA)
anti-APC isolation micro beads			Miltenyi Biotec GmbH	Bergisch Gladbach (GER)
anti-BrdU		FITC	BD Biosciencess	Heidelberg (GER)
anti-mouse B220	RA3-6B2	PerCP	BD Biosciencess	Heidelberg (GER)
anti-mouse CD11b	M1/70	APC	eBioscience	San Diego / California (USA)

anti-mouse CD11b	M1/70	FITC	BD Biosciences	Heidelberg (GER)
anti-mouse CD11b	M1/70	PE	eBioscience	San Diego / California (USA)
anti-mouse CD11b isolation micro beads			Miltenyi Biotec GmbH	Bergisch Gladbach (GER)
anti-mouse CD11c	N418	Biotin	eBioscience	San Diego / California (USA)
anti-mouse CD11c	N418	PE	eBioscience	San Diego / California (USA)
anti-mouse CD11c	N418	AF700	eBioscience	San Diego / California (USA)
anti-mouse CD11c isolation micro beads			Miltenyi Biotec GmbH	Bergisch Gladbach (GER)
anti-mouse CD19	6D5	PE	BD Biosciences	Heidelberg (GER)
anti-mouse CD4	L3T4	Pacific blue	eBioscience	San Diego / California (USA)
anti-mouse CD4	L3T4	PE	eBioscience	San Diego / California (USA)
anti-mouse CD4	L3T4	PerCP	eBioscience	San Diego / California (USA)
anti-mouse CD4 isolation micro beads			Miltenyi Biotec GmbH	Bergisch Gladbach (GER)
anti-mouse CD45.1	A20	Biotin	BD Biosciences	Heidelberg (GER)
anti-mouse CD45.1	A20	PE	BD Biosciences	Heidelberg (GER)
anti-mouse CD45.1	A20	APC AF750	BD Biosciences	Heidelberg (GER)
anti-mouse CD45.2	104	Biotin	BD Biosciences	Heidelberg (GER)
anti-mouse CD45.2	104	FITC	BD Biosciences	Heidelberg (GER)
anti-mouse CD45.2	104	PerCP-Cy5.5	BD Biosciences	Heidelberg (GER)
anti-mouse CD80	60-10A1	Biotin	BD Biosciences	Heidelberg (GER)
anti-mouse CD86	GL-1	Biotin	BD Biosciences	Heidelberg (GER)
anti-mouse CD86	GL-1	FITC	eBioscience	San Diego / California (USA)
anti-mouse CD86	GL-1	Pacific blue	BioLegend	San Diego / California (USA)
anti-mouse CD8α	53-6.7	AF647	BD Biosciences	Heidelberg (GER)

anti-mouse CD8α	53-6.7	PE	BD Biosciences	Heidelberg (GER)
anti-mouse Fcγ-Rezeptor II/III	2.4G2		Own production	
anti-mouse Ly6C	AL-2	Biotin	BD Biosciences	Heidelberg (GER)
anti-mouse Ly6C	AL-2	FITC	BD Biosciences	Heidelberg (GER)
anti-mouse Ly6G	1A8	PE	BD Biosciences	Heidelberg (GER)
anti-mouse Ly6G	1A8	V450	BD Biosciences	Heidelberg (GER)
anti-mouse MHCII	M5/114.1 5.2	APC	Miltenyi Biotec GmbH	Bergisch Gladbach (GER)
anti-mouse MHCII	M5/114.1 5.2	AF700	Miltenyi Biotec GmbH	Bergisch Gladbach (GER)
anti-mouse MHCII	M5/114.1 5.2	FITC	eBioscience	San Diego / California (USA)
anti-mouse TNFR1	55R-286	AF647	AbD Serotec	Düsseldorf (GER)
anti-mouse TNFR2	TR75-89	PE	AbD Serotec	Düsseldorf (GER)
anti-mouse TNFR2	TR75-89	AF647	AbD Serotec	Düsseldorf (GER)
Rabbit anti-mouse Ig FITC		FITC	DakoCytomation GmbH	Hamburg (GER)
Straptavidine secondary conjugate		Pacific orange	Invitrogen GmbH	Karlsruhe (GER)

2.1.5 ELISA Kits

Item	**Manufacturer**	**City (Country)**
Mouse IL-6 DuoSet ELISA development kit	R&D Systems GmbH	Wiesbaden (GER)
Mouse sTNF RII/TNFRSF1B DuoSet ELISA development kit	R&D Systems GmbH	Wiesbaden (GER)
Mouse TNF-alpha DuoSet ELISA development kit	R&D Systems GmbH	Wiesbaden (GER)

2.1.6 Buffers and solutions

Item	Composition
12.5% resolving gel	0.85 mL acrylamide / bisacrylamide rotiphorese gel 30, 1.5 mL 0.5 M Tris pH 6.8, 3.75 mL ddH_2O, 60 µL 10% SDS, 5 µL TEMED, 50 µL APS
4% collection gel	6.25 mL acrylamide / bisacrylamide rotiphorese gel 30, 3.75 mL 1.5 M Tris pH 8.8, 5 mL ddH_2O,150 µL 10% SDS, 10 µL TEMED, 100 µL APS
AP substrate buffer (pH 9.8)	9.8% diethanolamine, 24 mM $MgCl_2$
BD FACS™ Lysis Solution (10x)	BD Biosciences GmbH
Blocking buffer for TNFR2ed-huIgG ELISA	10% skimmed milk powder (w/v) in TBS
Blocking buffer for Western blot	5% skimmed milk powder (w/v) in TBS-T
Blotting buffer (10x)	2 M glycine, 250 mM Tris
Buffer for cell sort (Sort buffer)	PBS, 0.5% (w/v) BSA, 2 mM EDTA
Buffer for magnetic cell separation (MACS buffer)	PBS, 0.5% (w/v) BSA, 2 mM EDTA
Coomassie staining buffer	10% acetic acid, 40% ethanol, 0.2% comassie brilliant blue R250
Coomassie destaining buffer	10% acetic acid, 40% ethanol
Elution buffer for chelating sepharose protein purification	250 mM imidazole, 20 mM Na_2HPO_4, 0.5 M NaCl, pH 7.5
Elution buffer for IgG purification (protein G)	0.1 M Glycin (pH 3.1)
Erythrocyte lysis buffer	0.17 M NH_4Cl, 20 mM HEPES
FACS-Puffer	2% FCS in PBS
Freezing medium (2x)	20% DMSO, 80% FCS
Griess reagent A	1% sulfanilamide (w/v), 5% H_3PO_4
Griess reagent B	0.1% naphtyl-ethylenediamine dihydrochloride
Laemmli electro-mobility buffer (5x)	120 mM Tris Base, 0.95 M Glycin, 0.5% SDS
Laemmli loading buffer (4x)	0.5 M Tris, pH 6.8, 40% glycine, 0.04% β-mercaptoethanol, 4% SDS, 0.005% bromephenole-blue
Loading dye solution (6x)	0.25% bromephenole-blue, 0.25% xylencyanole, 30% glycerole

Neutralization buffer for IgG-purification (protein G)	1 M Tris-HCl (pH 11)
PBS (pH 7.3)	137 mM NaCl, 6.5 mM Na_2HPO_4 x H_2O, 1.5 mM KH_2PO_4, 2.7 mM KCl
PBS-T	0.05% Tween 20 in PBS
Permeabilization reagent	PBS, 1% BSA, 0.01% Triton-X 100
Reagent Diluent for R&D ELISA	1% BSA (w/v) in PBS-T
Reagent Diluent for TNFR2ed-huIgG ELISA	1% skimmed milk powder (w/v) in TBS
Reagent Diluent for Western blot	1% skimmed milk powder (w/v) in TBS-T
Standard for Griess reagent	10 mM $NaNO_2$
Stop solution for AP ELISA	2 M NaOH
Stop solution for HRP ELISA	2 N H_2SO_4
Substrate solution for AP ELISA	0.06% p-nitrophenylphosphate in AP substrate buffer
TAE-buffer	40 mM Tris-acetate, 1 mM EDTA
TBS-Puffer	8 g NaCl, 0.2 g KCl, 3 g Tris Base, H_2O bidest ad 1 l
TBS-T	0.05% Tween 20 in TBS
Tris-buffer for SDS-PAGE collection gel	1,5 M Tris-HCl (pH 8,8)
Tris-buffer for SDS-PAGE separation gel	0.5 M Tris-HCl (pH 6,8)
Trypan blue solution (pH 7.4)	0.16% (w/v) trypan blue, 150 mM NaCl
Wash buffer I for chelating sepharose protein purification	20 mM Na_2HPO_4, 0.5 M NaCl, pH 7.5
Wash buffer II for chelating sepharose protein purification	10 mM imidazole, 20 mM Na_2HPO_4, 0.5 M NaCl, pH 7.5

All buffers and solutions were prepared using ddH_2O.

2.1.7 Kits

Item	Manufacturer	City
BCA Protein Assay Reagent	Pierce / Thermo Fisher Scientific GmbH	Bonn (GER)
BD Pharmingen™ - FITC BrdU Flow Kit	BD Biosciences	Heidelberg (GER)

Diff-Quick Differential Staining Set	Dade Behring GmbH	Eschborn (GER)
DOTAP Liposomal Transfection Reagent	Roche Diagnostics GmbH	Penzberg (GER)
IsoGold Rapid Mouse-Monoclonal Isotyping Kit™	BioAssays	Ijamsville / Indiana (USA)
NucleoSpin® RNA II	MACHEREY NAGEL GmbH & Co. KG	Düren (GER)
Q SYBR Green Supermix	Bio-Rad Laboratories GmbH	München (GER)
Reverse Transcription System	Promega GmbH	Mannheim (GER)

2.1.8 Oligonucleotides

All used oligonucleotides were obtained from Metabion GmbH (Martinsried). Melting temperatures were either taken from the manufacturer's recommendations or calculated according to the equation shown in Formula 1. The oligonucleotides employed in cloning and polymerase chain reaction (PCR) are listed in Table 1and Table 2.

$$T_m\ [°C] = 4\ x\ (G + C) + 2\ x\ (A + T)$$

Formula 1: Calculation of the melting temperature of oligonucleotides

Table 1: Oligonucleotides for quantitative real-time PCR

Oligonucleotides for quantitative real-time PCR					
Target	**Name**	**Sequence (5' - 3')**	**Tm [°C]**	**Exon spanning**	**Amplicon lenght [bp]**
18s	18s FW	GTAACCCGTTGAACCCCATT	58	Yes	180
	18s RV	CCATCCAATCGGTAGTAGCG	60	Yes	
ARG1	ARG1 FW	AGTCTGGCAGTTGGAAGCAT	59.87	Yes	172
	ARG1 RV	CATCTGGGAACTTTCCTTTC	59.16	Yes	
IL-6	IL-6 FW	TGCAAGAGACTTCCATCCAG	58.96	Yes	203
	IL-6 RV	TGCCATTGCACAACTCTTTT	59.32	Yes	
iNOS	iNOS FW	GCTGTTCTCAGCCCAACAAT	60.26	Yes	214
	iNOS RV	TGCAAGTGAAATCCGATGTG	60.67	Yes	
β-Actin	β-Actin FW	TCACCCACACTGTGCCCATCTACGA	61	No	348
	β-Actin RV	GGATGCCACAGGATTCCATACCCA	59.1	No	

Table 2: Oligonucleotides for cloning

Cloning of TNFR2ed fusion protein in DesMTA (TNFR2ed-V5His)		
Target	**Name**	**Sequence (5' - 3')**
TNFR2	mp75ed MTA Bam H1 5'	CCCGGATCCGTGCCCGCCCAGGTTGTCTTG
TNFR2	mp75ed 3' Not1	TGGCGGCCGCCAGCCACCCTTGGTACTTTG

Cloning of TNFR2ed-hulgG fusion protein in DesMTA (TNFR2ed-hulgG)		
Target	**Name**	**Sequence (5' - 3')**
TNFR2	mp75ed MTA Spe 5'	CCCACTAGTGTGCCCGCCCAGGTTGTCTTG
TNFR2	hIg 3' Nos	CGCGGCGGCCATCATTTACCCGGAGACACG

Cloning of TNFR1ed-huFasid fusion protein in pQCXIP		
Target	**Name**	**Sequence (5' - 3')**
TNFR1	TNFR1 Bam huFas fusion 5'	GGGGGATCCATGGGTCTCCCCACCGTGCCTGG
TNFR1	TNFR1 EcoRV huFas fusion 3'	GGGGATATCCATTAAACTGATGAAGATAAAGG
huFas	5' EcoRV huFas	GGGGATATCAAGAGAAAGGAAGTACAGAAAAC
huFas	3' Xho huFas	GGGCTCGAGCTAGACCAAGCTTTGGATTTC

Cloning of TNFR2ed-huFasid fusion protein in pQCXIP		
Target	**Name**	**Sequence (5' - 3')**
TNFR2	TNFR2 Bam Fas fusion 5'	GGGGGATCCATGGCGCCCGCCGCCCTCTGGG
TNFR2	TNFR2 EcoRV Fas fusion 3'	GGGGATATCCTTGGCATCTCTTTGTAGGCAGG
huFas	5' EcoRV huFas	GGGGATATCAAGAGAAAGGAAGTACAGAAAAC
huFas	3' Xho huFas	GGGCTCGAGCTAGACCAAGCTTTGGATTTC

2.1.9 Plasmids

Table 3 lists the vectors used for the transfection or transduction of target cells. DesMTA was used to express and secrete TNFR2ed constructs for protein purification and isolation in DS-2 Drospohila Schneider cells. pQCXIP and pcDNA3 were employed to generate cell lines expressing membrane-bound TNFR2 constructs.

Table 3: Plasmids

Item	Manufacturer	City
pcDNA3.1	Invitrogen	Karslruhe (GER)
pQCXIP	Clontech, BD Biosciences	Heidelberg (GER)
pMT/Bip/V5-His (DesMTA)	Invitrogen	Karslruhe (GER)

Furthermore, a TNFR2 expression plasmid was used. In detail, mouse TNFR2 cDNA was inserted into the multiple cloning site of the plasmid pcDNA3.1 using BamH1 and XhoI restriction enzymes. All expression plasmids were verified by sequencing.

2.1.10 Cell culture media

Standard medium: cultivation of primary splenocytes, PEC and mammalian cell lines (CHO, L-929^{m} cells, SP2/0-Ag14, and Wirbel cells)

RPMI 1640, 10% (v/v) FCS, 50 µM β-mercaoptoethanol, 100 U/mL penicillin, 100 U/mL Streptomycin

BMDC Medium: generation of bone marrow-derived dendritic cells

RPMI 1640, 10% (v/v) fetal calf serum (FCS), 10% (v/v) GM-CSF supernatant, 50 µM β-mercaoptoethanol, 100 U/mL penicillin, 100 U/ml streptomycin

HAT-medium: selection of myeloma cells

RPMI 1640, 10% (v/v) FCS, 0.02% (v/v) hypoxanthine aminopterin thymidine (HAT) stock, 50 µM β-mercaoptoethanol, 100 U/mL penicillin, 100 U/ml streptomycin

HT-medium: selection of myeloma cells

RPMI 1640, 10% (v/v) FCS, 0.02% (v/v) hypoxanthine thymidine (HT) stock, 50 µM β-mercaptoethanol, 100 U/mL penicillin, 100 U/mL streptomycin

Medium for the cultivation of DS-2 Schneider cells

Insect Xpress^{TM}, 100 µg/mL kanamycine

2.1.11 Mouse strains

C57BL/6J wildtype mice (Jenvier, Le Genest, France)

C57BL/6J Ly5.1 (CD45.1, breeding at the University of Regensburg) (Shen, Saga et al. 1985)

C57BL/6J TNFR2$^{-/-}$ (breeding at the University of Regensburg) (Erickson, de Sauvage et al. 1994)

C57BL/6J OVA-transgenic (OTII) (breeding at the University of Regensburg) (Barnden, Allison et al. 1998)

2.1.12 Eukaryotic cell lines

The cell lines used within this work are listed in Table 4.

Table 4: Eukaryotic cell lines

Name	Description	ATCC®	Medium	Plasmide	Antibiotics
CHO	Chinese hamster ovary cell	CCL-61™	Standard medium		
CHO TNFR2	Chinese hamster ovary cell		Standard medium	pcDNA3.1	Neomycin (G418) (1.4 mg/mL)
DS-2	Drosophila Schneider cell	CRL-1963™	Insect XpressTM		
DS-2 TNFR2ed huIgG	Drosophila Schneider cell		Insect XpressTM	pMT/Bip/V5-His hygro	Hygromycine (300 µg/mL)
DS-2 TNFR2ed V5His	Drosophila Schneider cell		Insect XpressTM	pMT/Bip/V5-His hygro	Hygromycine (300 µg/mL)
L-929^{m}	Murine aneuploid fibrosarcoma cell line	CCL-1™	Standard medium		
SP2/0-Ag14	Myeloma cell	CRL-1581™	Standard medium		
Wirbel (TNFR1/2$^{-/-}$)	Mouse fibroblast TNFR1/2 double knockout		Standard medium		
Wirbel TNFR1ed huFasid	Mouse fibroblast TNFR1/2 double knockout		Standard medium	pQCXIP	Puromycine (1.4 µg/mL)
Wirbel TNFR2ed huFasid	Mouse fibroblast TNFR1/2 double knockout		Standard medium	pQCXIP	Puromycine (1.4 µg/mL)
X6310 (X63Ag8-653) GM-CSF	Myeloma cell		Standard medium		

2.1.13 Software and internet resources

This manuscript was prepared with Microsoft Office Word 2007. Graphs and diagrams were prepared using either Microsoft Office Excel 2007 or Graph Pad Prism version 5.01.
Quantitative real-time PCR raw data were obtained from IQ5^{TM}Optical System Software 2.0.
Flow cytometry data analyzes were done using BD FACSDiva software, BD CellQuest pro software or FlowJo software. The list of references was compiled using EndNote X3 software. Statistic analyzes were computed employing either Microsoft Office Excel 2007 or Graph Pad Prism version 5.01.
Furthermore, the listed internet references were utilized:

- Ensembl Genome Browser http://www.ensembl.org/index.html
- Pubmed http://www.ncbi.nlm.nih.gov/pubmed
- EMBL-EBI http://www.ebi.ac.uk/
- NCBI http://www.ncbi.nlm.nih.gov

2.2 Molecular biology

2.2.1 Working with DNA

2.2.1.1 Sequencing of plasmid DNA

Sequencing of deoxyribonucleic acid (DNA) vectors was performed by Geneart AG, Regensburg. 300 ng plasmid were diluted in 10 µL nuclease-free water containing 1 pmol of the primer used for the sequencing reaction and shipped to the company.

2.2.2 Working with RNA

Throughout the handling with cells, RNA, and cDNA contaminations with nucleases were avoided using RNaseZap® and nuclease free filter-tips.

2.2.2.1 RNA isololation

RNA was isolated using the NucleoSpin® RNA II isolation kit from MACHEREY NAGEL GmbH & Co. KG and the protocol “Total RNA purification from cultured cells and tissue with NucleoSpin® RNA II”.

Adherent cells were lysed directly after removing the medium by addition of 350 µL of RA1 buffer supplemented with 1% (v/v) 99% β-mercaptoethanol. Remaining non-adherent cells were centrifuged for 5 min with 12000 g at 4°C and the supernatant was discarded. The lysate of the adherent cells was transferred to the pelleted cells, in order to achieve total RNA recovery from the sample. The cell lysates were stored at -80°C until RNA extraction. RNA was eluated in 50 µL ddH_2O.

2.2.2.2 RNA concentration determination using a photometer

RNA samples were diluted 1 to 50, in order to reach RNA concentrations within the linear measuring range of the photometer. The optical density value (OD-value) corresponds to the absorbance of an optical element for a given wavelength λ per unit distance and is calculated by Formula 2 and explained in Table 5.

$$OD_\lambda = \frac{A_\lambda}{l} = -\frac{1}{l} * \log T = -\frac{1}{l} * \log \frac{I_0}{I}$$

Formula 2: Optical density

Table 5: Abbreviations and descriptions of Formula 2

Abbreviation	Description
l	Distance [cm] that light travels through the sample
A_λ	Absorbance at wavelength λ
T	Transmittance per unit
I_0	Intensity of the incident light beam
I	Intensity of the transmitted light beam

The maximum absorbance is 260 nm for nucleic acid and 280 nm for proteins. An $OD_{260\ nm}$ value of 1 is equivalent to an RNA concentration of 40 µg/mL. The ratio of $OD_{260\ nm}$ to $OD_{280\ nm}$ indicates if there are contaminations with. Therefore, the ratio $OD_{260\ nm}$ / $OD_{280\ nm}$ is used as an indicator for the quality of the nucleic acid and should be at 2.0 for RNA. Only RNA samples with an $OD_{260\ nm}$ / $OD_{280\ nm}$ ratio between 1.7 and 2 were used.

2.2.2.3 cDNA synthesis

RNA concentrations were adjusted to 1 µg / 12 µL. 12 µL were combined with 2 µL Oligo dT Primer (C1101, Promega). The tube was shortly vortexed and centrifuged followed by 5 min denaturation of the RNA at 70°C in the heat block. After this annealing of the primers to the

poly-A tails of mRNA was achieved by incubating the sample for 5 min on ice. 11 µL of the homogeneously mixed MMLV master mix described in Table 6 were added and the reverse transcription was performed at 42°C for 60 min.

Table 6: Master mix for reverse transcription reaction

MMLV Master mix	[µL]
M-MLV RT 5x Reaction Buffer	5
Nucleotide mix (10 mM)	1.25
M-MLV Reverse Transcriptase	1
Nuclease-free water	3.75
Total	11

After reverse transcription the reverse transcriptase enzyme was inactivated by 5 min incubation at 70°C. cDNA was stored at -20°C. In the case of very low RNA yields due to limited numbers of cells the volume of 3.75 µL RNAse / DNAse free H_2O was subtracted from the master mix. Instead of this, 15.75 µL of pure RNA were used as template for the reverse transcription reaction.

2.2.2.4 Quantitative real-time PCR

The quantitative polymerase chain reaction (qPCR) is a method to quantify a selected polynucleotide sequence by amplifying its initial concentration to a level at which an accurate detection can be made (Bustin 2000; Kubista, Andrade et al. 2006; Nolan, Hands et al. 2006). This level is called crossing point (CP) and it is defined as the number of PCR cycles that are necessary to detect the first reliable fluorescence signal from Sybr Green I added to the reaction. PCR amplifies the targeted nucleic acid in the sample and this amplification is considered to be exponentially in its most progressive phase. SYBR Green I is an asymmetrical cyanine dye used as a nucleic acid stain. The fluorescent dye SYBR Green I binds to the minor groove of the DNA double helix. In solution, the unbound dye exhibits very little fluorescence, however, fluorescence is greatly enhanced upon DNA-binding (Zipper, Brunner et al. 2004). The resulting DNA-dye-complex absorbs blue light (λmax = 488 nm) and emits green light (λmax = 522 nm). As SYBR Green I is not able to distinguish between target sequences and unspecific DNA amplification product or primer dimers, melting curve analysis were performed to control reliable PCR products. At the end of the 45 amplification cycles amplicons were melted for 1 min at 95°C following an annealing step for 1 min at 55°C. Melting curve analysis was performed by 0.5°C stepwise heating-up of the sample until 95°C. The fluorescence signal

decreases slowly until the melting temperature of the amplicon where a strong decline of the fluorescence signal can be detected. If more than one strong decline of fluorescence was detected, the results of this sample were seen as invalid.

2.2.2.4.1 Primer design

Primers were designed using the coding sequence of the target mRNA. They were to be between 18 and 23 base pairs long and should provide a specific melting temperature between 58°C and 61°C. All primers used were designed by exon-spanning of at least 4 base pairs. This avoids amplification of contaminating genomic DNA. In addition, the sequences of all primers were blasted against the whole mouse transcriptome. Primers were defined as valid when the homology with other mRNA transcripts was lower than 70%. The length of the respective amplicons was to be between 100 and 350 base pairs, in order to guarantee accurate and fast PCR results. Primers were purchased from Metabion GmbH (Martinsried). The parameters of the primer pairs are listed in Table 1.

2.2.2.4.2 Quantitative real-time PCR setup

cDNA (1 µg / 25 µL) was diluted 1 to 5 with nuclease-free water. 5 µL were transferred into real-time PCR 96-well plates. Master mix was prepared as a multiple of the reagent volumes shown in Table 7 with the primer pairs for the target and the housekeeper gene listed in Table 1.

Table 7: Master mix for quantitative real-time PCR

Master mix (1x)	V [µL]
Primer FW (100 µM)	0.1
Primer RV (100 µM)	0.1
Q SYBR Green Supermix	12.5
Nuclease-free water	7.3
Total	**20**

20 µL of the master mix were transferred to the 5 µL cDNA provided before. Each cDNA sample was assayed in at least two technical replicates.

2.2.2.4.3 Quantitative real-time PCR program

Quantitative real-time PCR was performed using the Bio-Rad iQ5 real-time PCR cycler. Single well factors collection was activated, in order to adjust the data interpretation software to the autofluorescence of every well. Table 8 illustrates the controlling and timing of the thermocycler.

Table 8: Protocol for quantitative real-time PCR

Cycle	Repeats	Step	Dwell T [mm.ss]	Setpoint [°C]	PCR / Melt Data Acquisition	ΔT [°C]	End T [°C]
Hot Start	1		4.00	95.0			
PCR	45	Melting	0.20	95.0			
		Amplification	1.00	59.0	Real Time		
Melting	1		1.00	95.0			
Annealing	1		1.00	55.0			
Melting Curve	81		0.30	55.0	Melting Curve	0.5	95.0
Cooling	1		0.30	5.0			

2.2.2.4.4 Data interpretation

Efficiency of the PCR reaction was determined in the up-front for every pair of primers and ranged between 1.95 and 2.0. The mRNA expression data were calculated assuming a PCR efficiency of 2 and either the delta CP method or the delta-delta CP method as described in Formula 3 and Table 9 (Pfaffl 2001).

$$\Delta CP = CP_{target\ gene} - CP_{reference\ gene}$$

$$\Delta\Delta CP = \Delta CP_{treated\ sample} - \Delta CP_{\ untreated\ sample}$$

$$TG\ mRNA\ expression_{relative\ to\ HK} = E^{\ -\Delta CP} = 2^{\ -\Delta CP}$$

$$TG\ mRNA\ expression_{relative\ to\ untreated\ sample} = E^{\ -\Delta\Delta CP} = 2^{\ -\Delta\Delta CP}$$

Formula 3: Quantitative real-time PCR data interpretation

Table 9: Abbreviations and descriptions of Formula 3

Abbreviation	Description
CP	Crossing point
TG	Target gene
HK	House keeping gene
E	Efficiency

2.2.3 Working with proteins

2.2.3.1 Expression of recombinant proteins in Drosophila DS-2 Cells

DS-2 cells were transfected with pMT/Bip/V5-His (DesMTA) vectors and grown until high cellular density was achieved. Following protein expression induction using 0.5 mM $CuSo_4$ recombinant proteins tagged with a leader sequence were expressed. The leader sequence provides the secretion of the recombinant proteins and is cleaved from the target protein during this process. Thus, recombinant proteins were easily purified from the supernatant without lysis of the cells. Supernatants were collected 4 – 5 days after induction.

2.2.3.2 Measuring of protein concentrations

Protein concentrations were determined using BCA Protein Assay Reagent (Pierce / Thermo Fisher Scientific GmbH) according to the manual of the manufacturer.

2.2.3.3 SDS-PAGE

Sodium dodecyl sulfate (SDS)-PAGE separates proteins according to their molecular weight using electrophoretic mobility (Laemmli 1970). In this work the Mini Protein Electrophoresis system (Bio-Rad Laboratories GmbH) was employed. First, a 12.5% resolving gel was cast and overlaid with butanol. After complete polymerization butanol was removed, 4% collection gel was filled into the rack, and the comb generating the slots for the samples was inserted. 15 µL of the samples were mixed with 5 µL 4 x Laemmli loading buffer and denaturized for 5 min at 95°C. After polymerization of the collection gel the system was inserted into the apparatus and the basins containing the anode and the cathode were filled with 1x Laemmli electro-mobility buffer. The cationic basin covered the loading area of the gel. The comb was removed and 20 µL of the samples as well as 10 µL of the standard were transferred into the single slots of the gel. The separation of the proteins occurred with 35 mA and 200 V. After runs were completed either staining of the proteins using coomassie or blotting of the proteins to polyvinylidene fluoride (PDVF) membranes (Western blot) was performed.

2.2.3.4 Coomassie staining

Protein detection in polyacrylamide gels or on PVDF membranes following Western blot analysis was performed using coomassie-blue. Gels or membranes were incubated in

coomassie staining buffer for 1 h and non-bound dye was removed by incubation in coomassie destaining buffer over-night. The heat and vaccum gel drying device was used to dry gels, PVDF membranes were air-dried.

2.2.3.5 Western blot

Proteins separated with SDS-PAGE were transferred to PVDF-membranes (Towbin, Staehelin et al. 1979). One PVDF-membrane and 6 slides of whatman papers were tailored to the size of the gels. Following short incubation in methanol, the membranes were washed in ddH_2O and transferred to 1 x blotting buffer. The whatman papers and the gel were also immersed in 1 x blotting buffer. Three whatman papers were placed on top of each other on the anode plate of the western blot device Fastblot B43 (Biometra GmbH) followed by the PVDF-membrane, the gel, and 3 more whatman papers. Great importance was payed to bubble-free assembling. The cathodic lid of the apparatus was closed and proteins were transferred for 1 h using 1.0 mA per cm^2 gel and 200 V. Following the protein transfer, the membranes were blocked at 4°C for 1 h or longer with blocking buffer. The purified antibodies used for the detection were diluted in 10 mL of reagent diluent and incubated with the membranes at RT on a shaker for 1 to 2 h. After 3 washes with 20 mL TBS-T for 5 min the membranes were incubated with a secondary peroxidase-coupled antibody diluted in 10 mL TBS containing 1% skimmed milk powder (w/v) for 30 min. Following another washing procedure as described before, the membranes were developed using NOWA A and B solution. Those two solutions were mixed in equal parts and pipetted over the membrane. Resulting chemiluminescence was detected and visualized by applying a film for an exposure time between 30 s and 5 min.

2.2.3.6 ELISA

The principle of the enzyme-linked immunosorbent assay (ELISA) method is the antibody-based antigen detection. The antigen was either directly coated to the surface of a microtiter plate or captured using a capture antibody according to the sandwich-ELISA principle. Coating with both antigen and capture antibody required buffers free of other proteins. Thereafter, the supernatants were discarded. A blocking step using buffers with high concentrations of proteins unspecific for the employed antibodies saturated all protein binding sites of the well and avoided unspecific binding of antibodies in the following procedures. The supernatants were discarded. The antigen containing sample like cell culture supernatants or serum was diluted and transferred to the microtiter plate where target proteins were retained by the capture antibody.

Following several washes, the primary antibody was diluted in reagent diluent containing blocking protein and pipetted to the microtiter plate where it bound to the antigen. The secondary antibodies were either unlabeled or labeled with biotin or directly conjugated with a detection enzyme like alkaline phosphatase (AP) or peroxidase (POX). If the secondary antibody was not labeled, a tertiary antibody labeled with AP or POX was to be used. If the secondary antibody was biotinylated, it was detected using streptavidine conjugates with either AP or POX. The detection was based on enzymatic activity due to the incubation with proper substrates. Educts of those reactions were measured either at 450 nm (POX) or 405 nm (AP). Absolute quantification was performed employing a standard row of known antigen concentrations.

2.2.3.6.1 ELISA for the detection of mouse serum IgG titers

For the determination of IgG titers in the serum of mice 200 ng TNFR2 huIgG expressed in DS-2 cells were coated in 100 µL PBS per well (96-well plate) at 4°C over night. As the mice were immunized with TNFR2ed V5His expressed from DS-2 cells, the detection of false-positive antibodies specific for V5His epitope could be avoided. The supernatants were discarded and a wash step of 3 washes with 300 µL TBS-T was performed. Now the wells were blocked using 300 µL blocking solution at RT for 1 h. Following another wash step, log2 dilutions of the serum were prepared in PBS on an extra plate in duplicates and 100 µL per well were transferred to the ELISA plate. As negative control serum of naïve TNFR2$^{-/-}$ mice was used and analyzed identically. After an incubation time of 2 h at RT supernatants were removed and plates were washed as described above. The detection antibody anti-mouse-IgG-AP (γ-chain-specific) was diluted 1 to 5000 in reagent diluent and 100 µL per well were transferred to the ELISA plate. After an incubation time of 90 min at RT the plates were subjected to another wash step. One tablet 4-nitrophenyl phosphate disodium salt hexahydrate was diluted in 20 mL AP substrate buffer and mixed properly. 100 µL of the reagent were loaded in each well of the ELISA plate. The reactions were stopped by the transfer of 50 µL 2M NaOH to each well when sufficient yellow coloration of several wells was reached. OD values were detected at 405 nm using ELISA reader Emax instrument (Molecular Devices, München).

2.2.3.6.2 ELISA for the detection of IgG from hybridoma supernatants

ELISA was used to detect hybridoma clones that produced specific antibodies against TNFR2. The method used is as described in 2.2.3.6.1 with few alterations. The supernatants of the

hybridoma clones were taken and directly loaded onto the ELISA plate after washing off the blocking solution. The serum of the mouse at the day of the splenectomy was diluted 1 to 5000 in PBS and served as positive control. Negative controls consisted of either pure medium or supernatants from hybridomas that were negatively tested for the respective antigen.

2.2.3.6.3 ELISA for the detection of TNF, TNFR2, and IL-6

Quantification of soluble forms of the receptor TNFR2 and the cytokines TNF and IL-6 in supernatants of cell cultures was performed using the respective ELISA Duo Sets from R&D Systems. Samples were used pure or diluted up to 1 to 25. The used ELISA kits are listed in 2.1.5. The detection limits were 31.25 pg/mL for TNF ELISA, 15.625 pg/mL for TNFR2 ELISA, and 16.625 pg/mL for IL-6 ELISA. For the detection of TNF and TNFR2 in non-stimulated BMDC cultures during the differentiation into DC the supernatants were used pure and the detection limits were changed. Supernatants of stimulated cells and the respective non-stimulated controls were diluted 1 to 5 for TNF ELISA, 1 to 10 for TNFR2 ELISA, and 1 to 25 for IL-6 ELISA. Consequently, the detection limits were 156.25 pg/mL for the TNF ELISA, 156.25 pg/mL for the TNFR2 ELISA, and 390.625 pg/mL for the IL-6 ELISA.

2.2.3.7 Detection of NO – Griess reagent

Griess reagent A and B were used to detect NO concentrations in the supernatants of cells. 100 µL of the supernatant were transferred to a 96-well plate. Standard for the Griess reagent was diluted 1 to 100 in medium to generate the highest standard concentration of 100 µg/mL followed by 7 log2 dilutions in medium. Medium was used as blank control. Standard and samples were measured in duplicates. Griess reagent A and B were equally mixed and 100 µL were transferred in each case to the 100 µL sample or standard. OD was measured at 540 nm employing ELISA reader Emax instrument (Molecular Devices, München). The detection limit of this method is 2 µM.

2.2.3.8 Biological assay for TNF detection – L-929^m cell kill

L-929^m cells can be used to detect very little amounts of biologically active and available soluble TNF as they die dose-dependent. 2 x 10^4 L-929^m cells were seeded in 100 µL medium per 96-well microtiter plate on day 0. On day 1 the supernatants were discarded. Soluble TNF standard was titrated in log2 dilutions and 100 µL were transferred to the cells in three technical replicates. Samples of unknown soluble TNF concentrations were loaded to the cells in the

same step and in three technical replicates. 100 µL 2 x actinomycin D containing medium (4 µg/mL) were added to the standards and samples. On day 2 the viability of the cells was detected via MTT-assay as described in 2.2.3.9.

2.2.3.9 Viability assay using MTT

MTT offers a method to detect the viability of cells as a value of mitochondrial activity. Mitochondrial reductase reduces yellow 3-(4,5-Dimethylthiazol-2-yl)-2,5-diphenyltetrazolium bromide to purple formazane proportionally to the mitochondrial activity. 2 x 10^4 cells of interest were seeded per well in 96-well microtiter plates and submitted to the respective biological test in 200 µL. On day 2 10 µL MTT stock solution (5 µg/mL) were added to every well and incubated for 4 h. By the addition of 70 µL of 20% SDS per well cells were lysed and formazane crystals were resolved within 24 h. OD values as an indicator for the viability of the cells were detected at 540 nm using ELISA reader Emax instrument (Molecular Devices, München). Biological assays were conducted with at least 2 technical replicates per sample.

2.2.3.10 Purification of V5His-tagged proteins

Proteins consisting of the extracellular domain (ed) of TNFR2 tagged with a V5His sequence for chromatographic purification (TNFR2ed-V5His) were expressed in DS-2 Schneider cells and purified using Chelating Sepharose Fast Flow (GE Healthcare GmbH). TNFR2ed-V5His expression in DS-2 cells was induced with 0.5 mM $CuSO_4$ for 4 days in cell culture flasks. The supernatant was taken and centrifuged at 4°C and 3220 g for 10 min. The supernatants free of debris were filtered using sterile filters (bottletop). 50 mL aliquots of the supernatant were mixed with 110 µL chelating sepharose in a 50 mL reaction tube and shaked over night at 4°C. Following another centrifugation step (10 min, 4 °C, 3220 g), the pelleted chelating sepharose was recovered using Pasteur pipettes. The pellets were pooled and placed into a chromatographic tube. After 3 washes with wash buffer I another 3 washes with wash buffer II were performed. Every single wash was conducted using twice the volume of the chelating sepharose in the tube. After that proteins were eluated several times using 1.5 mL elution buffer. The fractions were collected. The single fractions were analyzed for protein content using SDS page, western blot analysis (mouse anti Penta-His mAB, second AB goat anti-mouse IgG (whole molecule) POX), and coomassie staining. The fractions were dialyzed against PBS over night at 4°C and protein concentrations were determined according to 2.2.3.2.

Fractions were pooled. They were diluted to a concentration of 1 mg/mL and stored until use at -80°C.

2.2.3.11 Purification of human IgG-tagged proteins

Fusion proteins consisting of TNFR2ed and the Fc portion of human IgG-tagged for chromatographic purification (TNFR2ed-huIgG) were expressed in DS-2 Schneider cells and purified using HiTrap™ protein G HP columns (GE Healthcare GmbH). TNFR2ed-huIgG expression in DS-2 cells was induced with 0.5 mM $CuSO_4$ for 4 days in cell culture flasks. The supernatants were taken and centrifuged for 10 min at 4°C and 3220 g. The sterile and debris-free supernatants were purified by the Econo System from Bio-Rad. HiTrap™ Protein G HP Columns from GE Healthcare were equilibrated with PBS before the supernatants were loaded on the column with a flow rate of 0.8 mL / min without recirculation. Afterwards, the column was flushed with PBS until the $OD_{280\ nm}$ of the UV detector reached the blank value of PBS. The bound proteins were eluated using elution buffer and a flow rate of 0.5 mL / min. Fractions of 1 mL were collected and immediately neutralized using 20 - 40 µL neutralization buffer. The single fractions were analyzed for their protein content using SDS page, western blot analysis (Donkey anti-human IgG (H+L) horseradish peroxidase (HRP)), and coomassie staining. The fractions were dialyzed against PBS at 4°C over night and protein concentrations were determined according to 2.2.3.2. Fractions were pooled, diluted to a concentration of 1 mg/mL, and stored until use at -80°C.

2.2.3.12 Purification of IgG from hybridoma supernatants

The sterile and debris-free supernatant of the hybridoma clones were purified using the Econo System from Bio-Rad. HiTrap™ Protein G HP Columns from GE Healthcare were equilibrated with PBS before the supernatants were loaded to the column with a flow rate of 0.8 mL / min without recirculation. Afterwards, the column was flushed with PBS until the $OD_{280\ nm}$ of the UV detector reached the blank value of PBS. The bound proteins were eluated using elution buffer containing 0.1 M glycin (pH 3.1) and a flow rate of 0.5 mL / min. Fractions of 1 mL were collected and immediately neutralized using 20 - 40 µL neutralization buffer 1 M Tris-HCl (pH 11). 10 µL of the single eluates were analyzed for the antibody content using SDS page followed by coomassie staining. The eluates were pooled according to the size of their bands in high, medium, and low density antibody fractions. These pools were dialyzed against PBS at 4°C over night before protein concentrations were determined employing BCA Protein Assay

Reagent from Pierce / Thermo Fisher Scientific. After sterile-filtration using a 0.2 µM filter the antibodies were stored at 4°C.

2.3 Cell-biological methods

2.3.1 Cell culture conditions

The work with cell cultures was done using sterile reagents, pipettes, and vessels and employing the laminar flow sterile cabinet HERAsafe® KS (Thermo Fisher Scientific GmbH). Consumables, reagents, and cell lines are listed in 2.1.2, 2.1.3, and 2.1.6. The used cell lines and the specific medium are listed in 2.1.12. Mammalian cells were cultured at 37°C, 5% CO_2, and 95% humidity. Cells were split 2 or 3 times per week at a ration of 1 to 10. DS-2 Schneider cells were grown at 28°C without additional CO_2 supply.

2.3.2 Cryo preservation of cells – freezing and thawing

For longterm storage at -196°C 1 - 10 x 10^6 cells were pelleted and resuspended in 1 mL 1 x freezing medium. The suspension was transferred into cryotubes and subsequently gently deep-frozen. The cryotubes were carried over into the nitrogen tank (-196°C) for long-term storage after one week.

In order to thaw those cells the cryotubes were warmed up in the water bath (37°C) until the last ice crystals had disappeared. The cells were gently resuspended using a 1 mL pipette and transferred into a 15 mL reaction tube containing 14 mL cold medium. Following a centrifugation step (300 g, 7 min, 4°C), the supernatant was discarded and the pellet was resuspended in medium. The cells were transferred into cell culture flasks and cultured under the conditions described in 2.3.1.

2.3.3 Determination of cell numbers

Cells in single cell suspensions were counted using a Neubauer hemocytometer. In brief, cells were mixed with at least 50% (v/v) trypan blue and 10 µL of the mixture were placed in the space between the hemocytometer and the cover slip. Cell concentrations in the sample were calculated according to Formula 4 . The mean value of four independent areas containing 50 to 100 cells counted was calculated, in order to minimize the variance.

$$Concentration\ of\ cells = \frac{number\ of\ cells\ counted\ in\ one\ chamber}{volume\ of\ the\ chamber} \times dilution\ factor$$

Formula 4: Calculation of cell numbers using Neubauer hemocytometer

2.3.4 Stimulation of cells

Cells were stimulated by mixing the cells and the 2 x stimulation master mix in equal volumes. Double concentrated stimulation master mix was generated by mixing 1 µL of 1 mg/mL LPS (*S. abortus equi*), 20 µL of 20 µg/mL IFN-γ, and 4 mL medium resulting in 250 ng/mL LPS and 100 ng/mL IFN-γ. Cells were seeded in medium and the same volume of 2 x stimulation solution was added to reach final concentrations of 125 ng/mL LPS and 50 ng/mL IFN-γ. Unless otherwise indicated, 2.5 x 10^5 cells were stimulated in 1 mL final volume.

2.3.5 Generation of GM-CSF-containing supernatant

X6310 (X63Ag8-653) GM-CSF cells were used as a source of a supernatant containing recombinant mouse GM-CSF and employed for BMDC generation as described in 2.4.6. The cells were split two times per week and the medium was collected from cultures that were 2 to 3 days old. The supernatants were centrifuged (10 min, 3220 g, 4°C), filtered in order to guarantee sterility using a bottle top filter system, and stored at -20°C. The concentration of GM-CSF was determined to be 250 ng/mL (personal communication: Dr. Philip Groβ).

2.3.6 Stable transfection of eukaryotic cells using DOTAP

Dotap Liposomal Transfection Reagent was used for stable transfection of cells. Transfections were performed according to the protocol of the manufacturer.

2.3.7 Stable retroviral transduction of eukaryotic cells

Eukaryotic Wirbel cells deficient for both TNFR1 and TNFR2 were stably transduced with TNFR1ed-huFasid and TNFR2ed-huFasid constructs using retroviral vectors. The transfection was performed by PD Dr. W. Schneider according to the protocol employed previously (Schneider-Brachert, Tchikov et al. 2004).

2.3.8 Cytospin

For the generation of cytospin preparations 5 x 10^4 cells (PEC) were resuspended in 100 µL medium and centrifuged at 700 rpm for 5 min using Shandon Cytospin 4 (ThermoScientific GmbH) onto glass slides. Those were dried for 1 h at RT before they were differentially stained as described in 2.3.9.

2.3.9 Differential staining

Diff-Quick Differential Staining Set was used to stain cells (PEC) coated to glass slides and air dried (see 2.3.8). Object slides were submerged into fixation solution (6 times), staining solution I (8 times), staining solution II (2 times), and finally rinsed employing ddH_2O for 2 min. After air drying immersion oil was applied directly onto the preparation. The cellular composition of the PEC was determined using a transmitting light microscope. This method allowed the differentiation between macrophages, mast cells, lymphocytes as well as neutrophilic and eosinophilic granulocytes.

2.3.10 Flow cytometry

All flow cytometric analysis (fluorescence-activated cell sorting, FACS) were measured using BD LSR II. The employed antibodies and the respective fluorescence conjugates or biotinylations as well as the secondary streptavidine-fluorochrome conjugates are listed in 2.1.4. If not stated otherwise, all steps were conducted on ice. 1 x 10^6 cells were filtered through cell strainer and dispensed into FACS tubes. After a wash with FACS buffer and a centrifugation step (300 g, 7 min, 4°C) the supernatants were discarded and the tube opening was tabbed on paper tissue to dry drops. This procedure is called “wash step” in this work and can be performed with different buffers. After that cells were resuspended in 100 µL FACS buffer containing 10 µg/mL rat anti-mouse Fcγ-receptor II and III and incubated on ice for 20 min. Master mixes containing the antibodies for each staining were prepared in FACS buffer according to the recommended dilutions listed in 2.1.4. Cells were washed again with FACS buffer and pelleted as described above. Supernatants were removed and 100 µL of the master mix were transferred to the cells. The tubes were vortexed briefly and incubated on ice in the dark for 30 min. If utilizing biotinylated primary antibodies, streptavidine conjugated pacific orange second dye was diluted in FACS buffer as described in 2.1.4. Cells were pelleted and supernatants were drained. 100 µL of the second dye were given to the cells and staining took place for 30 min at 4°C and in the dark. After another wash and centrifugation step as described

above cells were either resuspended in 200 µL FACS buffer and analyzed subsequently or treated with 200 µL 2% paraformaldehyde and, consequently, fixed. In the latter case samples were measured within 3 days.

2.3.11 FACS Aria cell separation

For FACS Aria cell separation cells were treated and stained in accordance with the protocol described in 2.3.10 with only a few alterations. For the staining up to 1 x 10^8 cells were incubated in 1 mL master mix containing double-concentrated antibodies or streptavidine-dye conjugates. Cells were kept under sterile conditions using a laminar flow cabinet. After complete staining cells were pelleted and resuspended to a concentration of 2 x 10^7 cells /mL in sort buffer. After sorting cells were collected in 15 mL reaction tubes containing 2 mL FCS or in sterile FACS tubes containing 1 mL FCS. The cell numbers per collection tube were counted by the instrument. Cells were washed twice with medium and used for the respective cellular assay. Re-analysis of the sorted cells were performed using the BD LSR II (BD Biosciences GmbH) instrument. Purities of the sorted cells were higher than 98%.

2.3.12 MACS cell separation

Magnetic cell separation (MACS) technology was used to purify $CD11b^+$ cells from whole splenocyte preparations as described in 2.4.4. In some cases $CD11c^+$ cells were depleted before using the same method. Throughout the separation procedure cells were kept on ice as far as possible. In brief, cells were counted, washed once in totally 50 mL with chilled MACS buffer (PBS, 0.5% (w/v) BSA, 2 mM EDTA) in a 50 mL reaction tube, and pelleted (300 g, 7 min, 4°C). Supernatants were discarded and cells were resuspended in 80 µL MACS buffer per 10^7 cells. 20 µL of the respective MACS micro beads coated with antibodies against CD11b or CD11c were added per 1 x 10^7 cells. The suspension was mixed and incubated at 4°C for 15 min. Cells were washed and centrifuged once more as described before. Supernatants were removed and the cells were adjusted to a concentration of 2 x 10^8 cells / mL MACS buffer. Depending on the number of cells MS or LS separation columns were chosen. MS columns were designed to purify up to 10^7 labeled cells from total 2 x 10^8 cells, LS columns allow the yield of 10^8 cells from total 2 x 10^9 cells. LS columns were placed into the magnetic rack MidiMACS™ Separator that was arranged under the laminar flow cabinet and attached to the MACS® MultiStand. The columns were equilibrated by rinsing with 3 mL MACS buffer. The cell suspension was applied to the column and unlabeled cells passing through the matrix were

collected. 3 wash steps, each comprising 3 mL MACS buffer, were performed. New buffer was only added when the reservoir was empty. Columns were removed and placed on a suitable collection tube (15 mL reaction tube). 5 mL MACS buffer were applied to the columns and cells were eluated by firmly pushing the plunger into the columns. When cells were used for further FACS cell sorting one MACS separation step reaching purities of about 70% of the target cells was sufficient to increase the concentration of the cells of interest. When cells were examined directly in a cellular assays the MACS purification was repeated. Therefore, the eluated cells were adjusted to 2 x 10^8 cells / mL MACS buffer and directly transferred to a new and already equilibrated MS separation column. The following steps were performed as described before for the first purification step. Thus, purities over 90% were reached. For the isolation of cells with LS separation columns adopted volumes of MACS buffer were used according to the manual of the manufacturer. The detailed cell separation procedures are described in the manufacturer's manuals for CD11b microbeads, for CD11c microbeads, and for anti-APC microbeads. The latter system included staining of the cells with anti-CD11b APC as described in 2.3.11 before purification of the labeled cells with anti-APC microbeads.

2.3.13 BrdU staining

Bromodeoxyuridine (BrdU) uses nucleotide substitution to replace thymidine with uridine in the DNA structure of dividing cells both *in vitro* and *in vivo* (Gage 2000). The more proliferation takes place the more BrdU is integrated into the DNA and the stronger FITC fluorescence signals can be detected.

BMDC differentiation cultures were supplemented with 0.01 mM BrdU (BD Biosciences GmbH) on day 9 and cultured for 24 h. The next day, cells were washed from the petri dish and stained with the respective antibodies according to the protocol described in 2.3.10 without fixation of the cells. BMDC were pelleted (300 g, 7 min, 4°C), supernatant was discarded, and cells were treated with 100 µL Cytofix / Cytoperm for 30 min at RT in the dark. Washing procedure was performed by the addition of 1 mL 1 x Perm / Wash solution followed by centrifugation of the cells (300 g, 7 min, 4°C), pouring off the supernatant, and tapping the tube opening on paper tissue to dry drops. In the next step, cells were resuspended in 100 µL PBS supplemented with 1% BSA and 0.01% Triton-X 100 (Permeabilization reagent) and incubated for 10 min on ice in the dark. Following another washing procedure as described before cells were resuspended in 100 µL Cytofix / Cytoperm and incubated at RT in the dark for 5 min. Washing procedure was performed and DNA in the cells was digested by administration of 100 µL PBS supplemented with 30 µg DNAse. After incubation for 1 h and after another washing procedure 2.5 µL anti-

BrdU mAB FITC were added to the ~ 50 µL remaining buffer over the cells and mixed properly. Labeling of the BrdU took place at RT and in the dark within 20 min. After the last washing procedure cells were resuspended in 200 µL FACS buffer and either analyzed in the flow cytometer immediately or within 2 days.

2.3.14 Combined Annexin V / 7-AAD staining

Annexin V is a member of the annexin family of intracellular proteins that binds to phosphatidylserine (PS) in a calcium-dependent manner. Usually, PS is only found on the intracellular leaflet of the plasma membrane in healthy cells and would not be accessible for the staining. During early apoptosis membrane integrity is lost and PS translocates to the external leaflet. Thus, Alexa Fluor® 647 Annexin V allows to detect early apoptotic cells (Nurden, Bihour et al. 1993; Koopman, Reutelingsperger et al. 1994; Vermes, Haanen et al. 1995).
7-AAD possesses a high DNA binding constant and is efficiently excluded by intact cells. Nevertheless, DNA of necrotic and dead cells is stained with this compound as cell membrane integrity is completely lost (Schmid, Krall et al. 1992).
BMDC were washed from the petri dish and stained with the respective antibodies according to the protocol described in 2.3.10 without fixation of the cells. BMDC were pelleted (300 g, 7 min, 4°C), supernatants were discarded, and the cells were washed once with 4 mL chilled PBS and a second time with 500 µL Annexin V binding buffer (BioLegend). 2.5 µL AlexaFluor® 647 Annexin V and 5 µL 7-AAD were mixed with 9.25 µL Annexin V binding buffer. 100 µL of this staining solution were transferred to the cells and mixed followed by 20 min incubation time at RT in the dark. 200 µL Annexin V binding buffer were added to the FACS tubes and the cells were analyzed immediately using the flow cytometry device.

2.4 Methods using mice

Animal experimentation has been approved by the local authorities (AZ:54-2532.1-32/08 and AZ:54-2531.1-22/09).

2.4.1 Housing of animals

Mice were kept in a conventional barrier animal laboratory according to the german animal protection law. Mice were exposed to a 12 h light / dark rhythm and they were fed with species specific standard diet and tap water ad libitum.

2.4.2 Anesthesia

Anesthetic was prepared freshly before use and under sterile conditions employing the laminar flow cabinet. It consisted of PBS supplemented with 0.75% ketaminehydrochloride and 0.14% xylazinehydrochloride. 4.62 mL PBS were mixed with 0.9 mL 5% ketaminehydrochloride and 0.48 mL xylazinehydrochloride. The weight of the mouse to be anesthetized was measured and 10 µL of the anesthetic were administrated i.p. per gram.

2.4.3 Cecal ligation and puncture

Sublethal CLP was used as animal model for sepsis. Mice were anesthetized with anesthetic and midline laparotomy was performed. The cecum was placed on a sterile pice of PARAFILM® M followed by ligation of the distal 30% of the appendix using lisle. After a singular cecum puncture with a 0.4 mm needle was performed the lesion in the abdominal wall was closed with metal clips. As the cecum is an endogenous source of bacterial contamination, perforation of the cecum results in bacterial peritonitis, which is followed by translocation of mixed enteric bacteria into the blood compartment causing sepsis and immunosuppression. Experiments were performed 48 h after surgery.

2.4.4 Spleen cell preparation

C57BL/6 mice were killed by cervical dislocation. Spleens were immediately taken and incubated on 900 µL chilled RPMI 1640 medium without any supplementation. The spleens were gently disrupted and 100 µL of collagenase D were added and mixed. After 15 min of incubation at 37°C in the incubator the spleen cells were isolated by pressing the organ through a cellular strainer (40 µm) into a 50 mL reaction tube using a syringe plunger. The strainer and the plunger were flushed well with medium, in order to maximize the cellular yield. Cells were washed in 50 mL medium and pelleted (300 g, 7 min, 4°C). The supernatant was discarded and the pellet was resolved in 5 mL erythrocyte lysis buffer and incubated at RT for 10 min. Cells were washed with 45 mL fresh medium followed by another centrifugation step as described above. Supernatants were removed and splenocytes were resuspended in 10 mL medium. The suspension was filtered using a cellular strainer (40 µm) and cell numbers were determined employing trypan blue solution and the protocol described in 2.3.3. Flow cytometric analysis, MACS or SORT purifications as well as stimulation experiments were performed in this work with splenocytes obtained with this method.

2.4.5 Peritoneal exudate cell preparation

Immigration of peritoneal exudate cells (PEC) was induced by injecting 1 mL PBS i.p. 16 h before the peritoneal cavity was washed out with 10 mL of cold medium and PEC were transferred into 15 mL polypropylene tubes. The cells were pelleted, washed once with cold medium, and counted using Tuerk solution. When used as feeder cells, 2 x 10^4 cells per well (96-well plate) were seeded in 100 µL medium. For stimulation experiments 2.5 x 10^5 cells were transferred in 500 µL medium to a 48 well microtiter plate and immediately supplemented with 500 µL medium for non-stimulated controls or 500 µL 2 x stimulation master mix. Cells were either used for RNA isolation after the indicated time or supernatants were collected after 48 h for ELISA or NO detection.

2.4.6 Bone marrow-derived dendritic cell generation

Bone marrow-derived denritic cells (BMDC) were generated according to the protocol of Manfred Lutz (Lutz, Kukutsch et al. 1999). In brief, mice were killed, femura and tibiae were dissected, and remaining tissue was removed. The following steps were done under the laminar airflow cabinet. The bones were sterilized by incubation in 70% EtOH for 1 min and transferred into PBS. After that both ends of the intact bones were cut by scissors and bone marrow was flushed into a 50 mL Falcon tube using 2 mL PBS and a 0.45 mm syringe. Clots within the bone marrow suspension were disrupted by pipetting up and down several times. The cells were washed once with medium, resuspended in 10 mL medium containing 10% GM-CSF supernatant from X6310 cells (see 2.3.5) per mouse, and filtered with a cellstrainer. Cells were counted using Tuerck solution. 2 x 10^6 cells were transferred into a 100 mm bacteriological petri dish and the culture vessel was filled up with 10 mL with GM-CSF-containing medium. The cell differentiation into BMDC took place in the incubator. 10 mL GM-CSF-containing medium were added on day 3. 10 mL of the medium were removed from the cultures both on day 6 and on day 8. The cells within this medium were pelleted at 300 g at 4°C for 10 min. After discarding the supernatant the pellet was resuspended in 10 mL fresh GM-CSF-containing medium and transferred back to the BMDC culture. For the experiment the BMDC from one petri dish were gently resuspended in the used medium by pipetting up and down several times. The cell suspension was transferred to a 50 mL Falcon tube and washed once with medium without GM-CSF. Cells were counted using dilutions with trypan blue solution. Flow cytometry analyses were performed with non-stimulated cells immediately after determining the yield. For stimulation experiments 2.5 x 10^5 cells were transferred in 500 µL medium to a 48 well microtiter plate and immediately supplemented with 500 µL medium for non-stimulated controls or 500 µL

2 x stimulation master mix. Stimulation occurred in medium without GM-CSF. Cells were either used for RNA isolation after the indicated time or supernatants were collected after 48 h for ELISA or NO detection.

For mixed BMDC cultures aliquots of bone marrow cells from mice different in their congenic marker were mixed at equal parts after the preparation. 2 x 10^6 cells from the mixture were employed in the BMDC generation protocol described above.

2.4.7 Generation of bone marrow chimeric mice

The generation and analysis of cells from bone marrow chimeric mice is the means of choice to examine whether hematopoietic or stromal cells are causing certain phenotypes. In this work four different combinations of bone marrow chimeric mice were generated. Bone marrow donor and bone marrow recipients were C57BL/6 mice differing in their CD45 congenic marker. CD45.2 wt as well as CD45.2 TNFR2$^{-/-}$ bm were transplanted into CD45.1 wt mice. As a control CD45.1 wt bone marrow was transplanted into CD45.2 wt and CD45.2 TNFR2$^{-/-}$ recipients. Host mice were irradiated 2 times with 5 gray from a linear accelerator, in order to destroy their hematopoietic system. Bone marrow cells from donor mice were isolated. Briefly, femura and tibiae were dissected and remaining tissue was removed. Following steps were done under the laminar airflow cabinet. The bones were sterilized by incubation in 70% EtOH for 1 min and transferred to PBS. After that both ends of the intact bones were cut by scissors and bone marrow was flushed using PBS and a 0.45 mm syringe into a 50 mL Falcon tube. Clots within the bone marrow suspension were disrupted by pipetting up and down several times. The bone marrow cells are washed twice with PBS, resuspended in 10 mL PBS, and counted. After irradiation host mice were anesthetized and 5 x 10^6 bone marrow cells were injected i.v.. After 3 weeks reconstitution was checked using venous blood samples from every mouse. 90 µL blood were mixed with 10µl 50 mM EDTA (pH8). Blood was washed once with FACS buffer and stained in 75 µL for the congenic markers CD45.1 and CD45.1 as well as for the T cell marker CD3 and the B cell marker B220. Erythrocytes were lysed by addition of 1mL 1 x BD FACS™ Lysis Solution (diluted in ddH_2O), thoroughly mixed, and incubated for 10 min at RT. Remaining cells were washed once with FACS buffer, pelleted (300 g, 7 min, 4°C), and fixed using 2% paraformaldehyde before cell composition was analyzed using flow cytometry.

After 8 weeks of reconstitution the mice with the highest degree of reconstitution were chosen for the experiments. PEC and BMDC were generated as described in 2.4.5 and 2.4.6. The cells were stimulated with LPS and IFN-γ (100ng/mL, 50ng/mL) for 48 h, in order to detect NO, cytokines, and soluble TNFR2. In addition, BMDC were investigated for the expression of the

activation markers CD80, CD86, and MHCII and PEC were checked for their composition using cytospin and Diff-Quick Differential Staining Set (Dade Behring GmbH). Furthermore, reconstitution and cell distribution were recorded using spleen cells as described in 2.4.4. Figure 6 illustrates the 4 groups of bm chimeric mice differing in the congenic markers of either the donor or the recipient bone marrow.

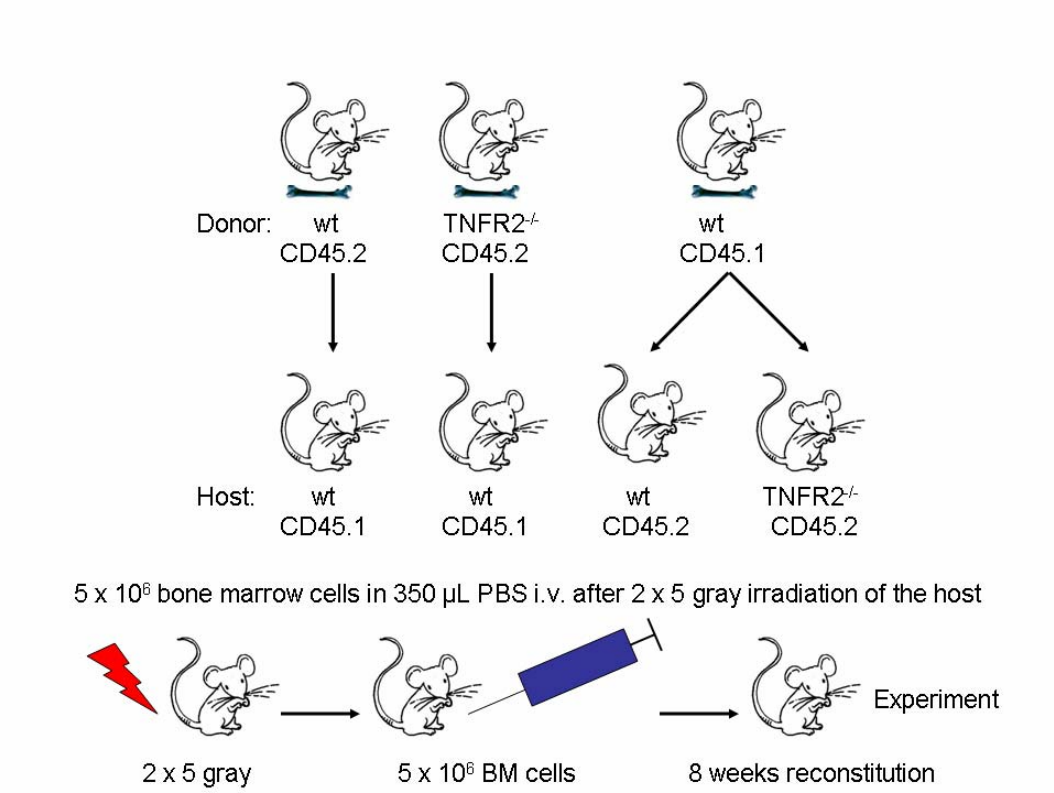

Figure 6: Generation of bm chimeric mice

2.5 Monoclonal anti-TNFR2 antibody production

2.5.1 Species

Three female TNFR2$^{-/-}$ mice were used for vaccination and termed (0), (L) and (R).

2.5.2 Vaccination

The immunization strategy is illustrated in Table 10. In brief, 100 µg TNFR2ed-V5His protein were administrated 3 times i.p. using the adjuvants Complete Freund's adjuvans (CFA) or

Incomplete Freund's adjuvans (IFA) and PBS. The spleen cells were isolated on day 44 about 60 h after the last vaccination as described in 2.4.4 using medium without FCS and without performing the erythrocyte lysing step. Cells of spleen (R) were used in the fusion of Diana Minge. Splenocytes of mice (0) and (L) were divided in two equal aliquots and stored at -80°C. The fusion described in this work was performed using one aliquot of the splenocytes from mouse (0). Monoclonal antibodies obtained from both fusions were tested for their functional properties.

Table 10: Vaccination scheme

ime [d]	Protein [1 mg/mL, PBS]	V Protein [µL]	Adjuvant	V Adjuvant [µL]
0	TNFR2ed-V5His	100	CFA	100
21	TNFR2ed-V5His	100	IFA	100
42	TNFR2ed-V5His	100	PBS	100

2.5.3 Fusion

The cell line used for the fusion with B cells from the immunized mice was the mouse myeloma cell line SP2/0-Ag14 which is a fusion cell line of a myeloma cell line from Balb/C spleen cells and the myeloma cell line P3X63AAG8 and provides reliable fusion properties using polyethylene glycol 1500 (PEG 1500) (Shulman, Wilde et al. 1978). Medium without FCS was used to wash the splenocytes prepared as described in 2.4.4 and the SP2/0-Ag14 cells before mixing both cell types in a ratio of 3 spleen cells to 1 myeloma cell (3.5×10^7 splenocytes and 1.17×10^7 myeloma cells) in a 15 mL Falcon tube. The mixed cells were pelleted for 5 min with 300 g at 4°C and the supernatant was discarded. By an additional short centrifugation step the cell pellet was completely dried. The cell pellet was dissolved by snipping the tube with the fingers. The cells were warmed up for 1 min at 37°C in the water bath before dropwise addition of 1 mL 37°C prewarmed PEG 1500 within 1 minute. Continuously rolling of the tube in this step ensured adequate interaction of PEG 1500 with the cells. After another 1 min of incubation in the water bath at 37°C 10 mL prewarmed HAT medium were added dropwise and within 5 min to the cells while continuously rolling of the Falcon tube. The cell suspension was diluted to 200 mL with HAT medium. 100 µL were transferred to each well of 20 96-well microtiter plates coated with peritoneal exudate cells the day before (see 2.4.5) resulting in a total volume of 200 µL in each well. As a control untreated Sp2/0-Ag14 cells were incubated in 200 µL HAT medium, in order to guarantee the exclusive survival and expansion of hybridomas from splenocytes and Sp2/0-Ag14 cells (Foung, Sasaki et al. 1982). The first hybridoma clones were detected after 1 week and the supernatants of those wells were tested for the specific antibody production after 10 days. After 2 weeks the cultured medium was changed stepwise from HAT

medium to HT medium and finally to normal medium. In parallel, the clones were expanded to larger cell culture vessels and finally grown in cell flasks.

2.5.4 Detection of positive hybridoma clones

In order to detect hybridoma clones that produce antibodies against TNFR2, recombinant TNFR2ed-huIgG protein was used. This ensured the exclusive detection of antibodies against TNFR2ed and not against the V5His tag of the recombinant TNFR2ed protein that was used to immunize the mice. ELISA plates were coated with 200 ng TNFR2ed-huIgG per 100 µL PBS and well at 4°C over night. The plates were washed 3 times using TBS-T and blocked with 300 µL skimmed milk powder in TBS 10% (m/v) over night at 4°C. After 3 washes with TBS-T 100 µL supernatants of the single hybridoma clones were transferred to the ELISA plate. As negative control medium was pipetted into a few wells of the ELISA plate. The serum of the mouse taken at the day of the splenectomy was diluted 1 to 5000 with PBS and 100 µL of this solution served as positive control on every ELISA plate. The samples and controls were incubated over night at 4°C before performing 3 more wash steps with TBS-T. Anti-mouse IgG γ-chain specific AP conjugated antibody was diluted 1 to 5000 in TBS containing 0.5% (m/v) skimmed milk powder and 100 µL were transferred to every well and incubated at room temperature for 2 h. The plate was washed 3 times with TBS-T before loading with 100 µL AP reaction solution (see 2.1.6) and incubation for 5 to 15 min. The reaction was stopped by the addition of 50 µL 2 M NaOH to the wells. OD was measured at 450 nm. Positivity was defined to generate an OD value that exceeds the OD value of the background at least 3 times the standard deviation of the OD value of the background. Positive clones were to be monoclonal and 3 times sucessfully tested for their positivity.

2.5.5 Subcloning

Hybridoma clones that produced antibodies against TNFR2ed-V5His were subcloned, in order to generate monoclonal cell lines. Cells were removed from the well, counted, and adjusted to a concentration of 10 cells per mL in medium. All 96-wells of a microtiter plate were filled with 100 µL of the cell suspension, in order to achieve a theoretical distribution of 1 cell per well and, consequently, to assure monoclonality. The growing clones were checked for antibody production. If all clones were positive, the most potent one was chosen, expanded, and defined to be monoclonal. If not all clones were positive, another subcloning procedure was to be performed using the most potent clone of the first plate.

2.5.6 Generation of supernatants

Positive clones were expanded and finally transferred into 175 cm² cell culture flasks containing 50 mL medium. Cells were grown in high density. After 4 days the cell suspension was removed from the flasks, the cells were pelleted in 50 mL Falcon tubes at 4 °C and 300 g for 10 min, and the supernatant was sterile-filtered and stored at 4°C. The cells were resuspended in 150 mL fresh medium and transferred into 3 new 175 cm² cell culture flasks. The procedure was repeated several times until more than 1 L supernatant was collected.

2.5.7 Protein G purification of monoclonal antibodies

Isolation and purification of monoclonal antibodies were performed as described in 2.2.3.12.

2.5.8 Functional characterization of monoclonal anti-TNFR2 antibody

Mouse anti-mouse TNFR2 mAB were either tested using the supernatant of the monoclonal hybridoma cultures or the protein G purified mAB dialysed against PBS and sterilized by filtration with 0.2 µm filters.

2.5.8.1 Determination of the IgG isotypes

IsoGold Rapid Mouse-Monoclonal Isotyping Kit™ (BioAssays) was used to determine the isotype subclasses of the newly generated mouse anti-mouse TNFR2 mAB.

2.5.8.2 ELISA for anti TNFR2 antibody characterization

ELISA tests were performed as described in 2.5.4.

2.5.8.3 Western blot for anti-TNFR2 antibody characterization

In order to characterize the newly generated mouse anti-mouse TNFR2 mAB, Western blot analyzes were performed. Therefore, SDS-PAGE and Western blot were performed with TNFR2ed-huIgG, protein standard, and 1 µg/mL TNFR2ed-V5His as described in 2.2.3.3 and 2.2.3.5. Several replicates of these blots were prepared and incubated with 10 mL of the different hybridoma cell culture supernatants. The controls were blots incubated exclusively with donkey anti-human IgG (H+L) HRP or mouse anti-V5 mAB HRP. As secondary antibody for the

hybridoma supernatants goat anti-mouse IgG (whole molecule) POX was employed. The experimental setup of one representative Western blot setting is illustrated in Figure 7.

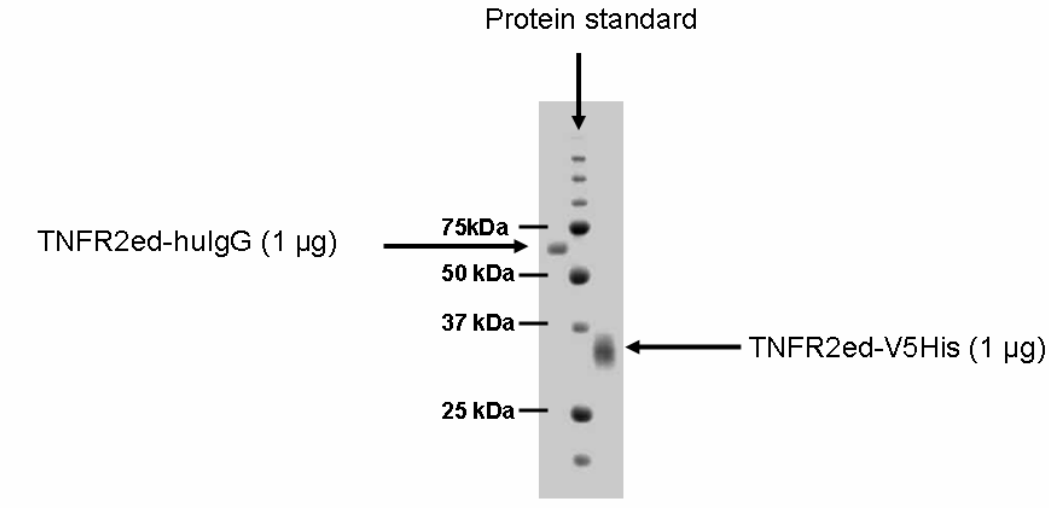

Figure 7: Mouse anti-mouse TNFR2 mAB Western blot test

2.5.8.4 Flow cytometry for anti-TNFR2 antibody characterization

The performances of anti-TNFR2 antibodies in FACS applications were investigated using transfected CHO cells overexpressing mTNFR2 (whole molecule). CHO wt and CHO TNFR2tg cells were trypsinized and removed from the culture flask. 1 - 5 x 10^5 cells were transferred into FACS tubes and washed once with FACS buffer. Cells were shortly vortexed with 500 µL supernatant from the different clones and incubated for 30 min at 4°C. After one wash step with FACS buffer FITC conjugated anti-mouse Ig antibody was adequately diluted and 100 µL were transferred to the cells. The FACS tubes were mixed and incubated at 4°C for 30 min. Non-stained cells and cells stained with an available anti-mouse TNFR2 mAB conjugated with AF647 were used as controls. After another wash step cells were fixed with 2% paraformaldehyde and analyzed using flow cytometry.

2.5.8.5 TNFR2 activation or inhibition assay for anti-TNFR2 mAB

In order to characterize the functional properties of the newly generated mouse anti-mouse TNFR2 mAB (see 2.5), fusion proteins comprising mouse TNFR2 ectracellular domain and human FAS intracellular domain (TNFR2ed-huFasid) were cloned and transduced into Wirbel wt cells using retroviral techniques (PD Dr. Wulf Schneider). In the case of agonistic antibodies for TNFR2, transduced cells should die due to the induction of apoptosis. *Vice versa*, when treated with possibly antagonistic antibodies for TNFR2, TNFR2ed-huFasid transduced cells

should be protected from apoptosis even when treated with soluble mouse TNF (Peprotech GmbH) or membrane-bound TNF. These methods were used before by Dr. Anja Krippner-Heidenreich in the human system for huTNFR1 and huTNFR2 (Krippner-Heidenreich, Tubing et al. 2002). As TNFR1 and TNFR2 are highly homologue receptors, the mentioned tests were performed in parallel with TNFR1ed-huFasid transduced cells. Thus, cross-reactivity can be examined. Figure 8 illustrates the principle of the test.

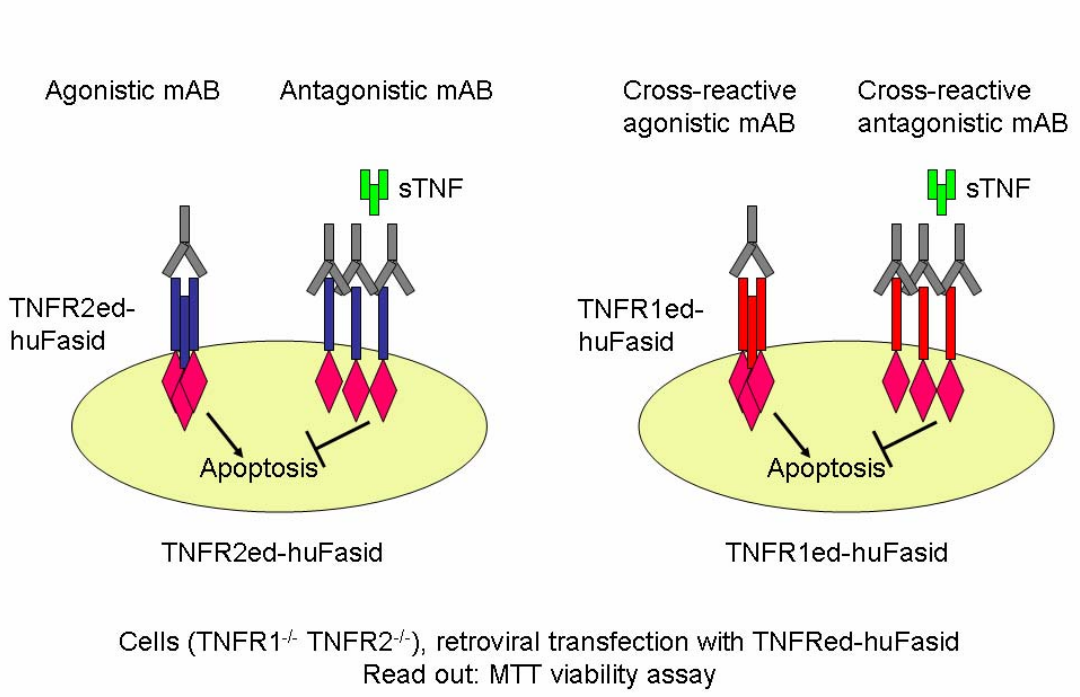

Figure 8: Agonistic / antagonistic mouse anti-mouse TNFR2 mAB test

Wirbel cells transduced with TNFR2ed-huFasid cells were always tested with the control wt cells and TNFR1ed-huFasid transduced cells. 2 x 10^4 wt cells were seeded in 100 µL medium in the wells of a 96-well plate on day 0. The next day, the supernatants were removed and the tests for either agonistic or antagonistic function were performed. All 3 types of cells were tested in triplicates. In order to detect agonistic properties, the purified antibodies were adjusted to 50 µg/mL with medium. 100 µl were transferred to the 3 types of cells. Subsequently, 100 µL of 4 µg/mL actinomycin D containing medium were added and cells were incubated for 24 h in the incubator. In order to detect antagonistic properties, cells were treated with 100 µL 50 µg/mL purified anitibodies diluted in medium for 6 h. Afterwards, 100 µL medium containing 4 µg/mL actinomycin D and either supplemented with 50 ng/mL mTNF (Peprotech GmbH) or 100 ng/mL TNC-mTNF (Prof. H. Wajant) were added and cells were incubated for 24 h. TNC-mTNF is a mutant form of TNF that has been designed for exclusive activation of TNFR2. In both types of

assays controls were performed with cells without antibody treatment. These control cells were incubated either with TNF or not. MTT assays as described in 2.2.3.9 were used to calculate the viability of the cells 24 h after the different treatments with the antibodies.

2.6 Statistical calculations

Experimental results are shown as mean values and associated standard deviations. The statistical analyzes were based on Student´s t-test. p-values < 0.05 were accepted as statistically significant.

3 Results

3.1 iNOS mRNA expression and Nitric Oxide (NO) production of TNFR2$^{-/-}$ myeloid cells

The overproduction of NO can be harmful for septic patients. Therefore, iNOS mRNA expression and NO production were investigated in different myeloid cells.

3.1.1 CD11b^{+} CD11c^{-} splenocytes after CLP

In order to get information about the relative proportion of NO producing cells in the spleens of CLP-treated mice, the frequency of CD11b^{+} CD11c^{-} cells as the main source of NO was measured in the spleens of mice at different time points after CLP. No significant differences in the kinetic of CD11b^{+} CD11c^{-} relative splenocyte proportions after CLP comparing wildtype and TNFR2$^{-/-}$ mice could be detected. Data are shown in Figure 9. Percentages of CD11b^{+} CD11c^{-} cells were slightly increased starting on day 4 until day 11.

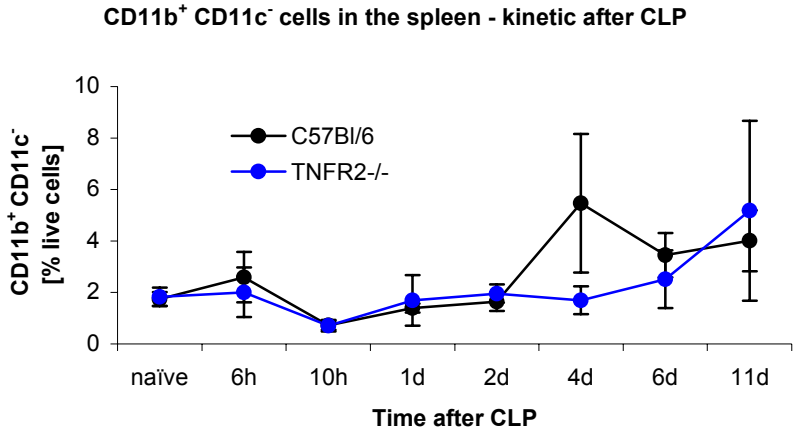

Figure 9: CD11b^{+} CD11c^{-} splenocytes after CLP – kinetic

Wildtype and TNFR2$^{-/-}$ were subjected to CLP. At the indicated time points mice were killed by cervical dislocation and spleen cells were isolated. The cells were analyzed for the content of CD11b^{+} CD11c^{-} myeloid cells using flow cytometry. Shown are the mean ± SD of 4 to 5 individual animals per group and time point.

As the absolute numbers of CD11b+ CD11c- splenocytes were not changed, the capacity of these cells to express iNOS mRNA and to produce NO was analyzed next. Figure 10 shows

that CLP was essential for iNOS mRNA expression and NO production and that both parameters were impaired in CD11b^{+} CD11c^{-} splenocytes of TNFR2$^{-/-}$ mice after CLP.

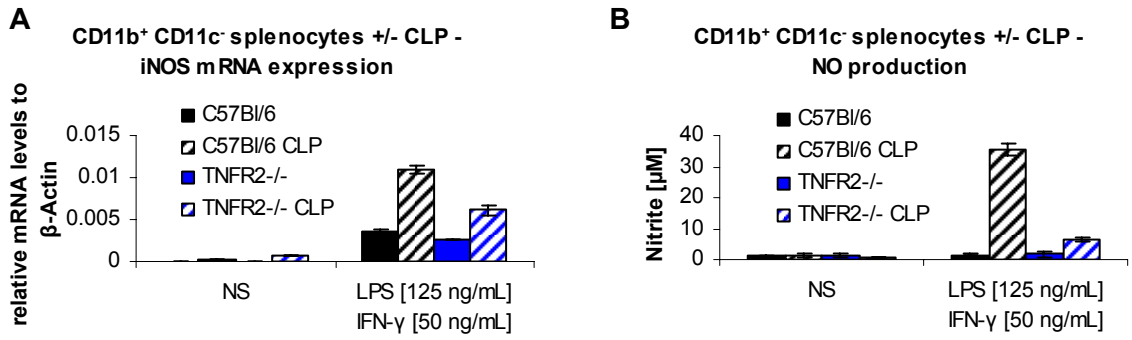

Figure 10: CLP is required to detect significant amounts of iNOS mRNA expression and NO production

Wt and TNFR2$^{-/-}$ mice were left untreated or subjected to CLP. After 2 days spleen cells were isolated and pooled. Following CD11c^{+} MACS depletion, CD11b^{+} cells were isolated using MACS technology. The purification process was repeated, in order to increase the purity. The cells were seeded at a concentration of 2.5 x 10^{5} / 48 well microtiter plate and stimulated with 125 ng/mL LPS and 50 ng/mL IFN-γ in 1 mL for 6 h (mRNA expression analysis, A) or for 48 h (NO detection, B). The data originate from one of three representative experiments, shown are the mean ± SD of 3 technical replicates per group.

Figure 11 shows the iNOS mRNA expression and NO production data based on CD11b^{+} CD11c^{-} spleen cells from mice 2 days after CLP. TNFR2$^{-/-}$ CD11b^{+} CD11c^{-} splenocytes showed reduced iNOS mRNA expression and NO production. Figure 11 contains data from several independent experiments.

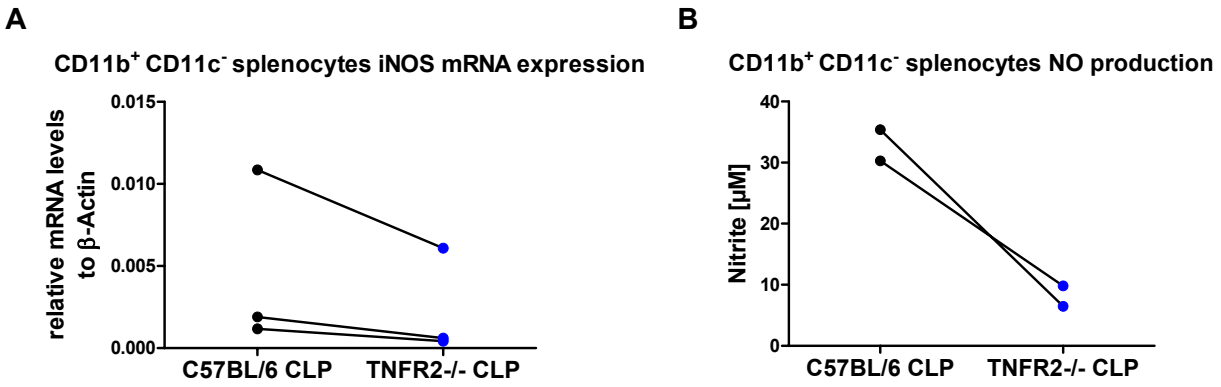

Figure 11: iNOS mRNA expression and NO production of CD11b$^+$ CD11c$^-$ splenocytes 2 days after CLP

Wt and TNFR2$^{-/-}$ splenocytes from up to 3 CLP-treated mice were isolated and pooled. Following CD11c$^+$ MACS depletion, CD11b$^+$ cells were isolated using MACS technology. The purification process was repeated, in order to increase the purity. The cells were seeded at a concentration of 2.5 x 10^5 / 48 well microtiter plate and stimulated with 125 ng/mL LPS and 50 ng/mL IFN-γ in 1 mL for 6 h (mRNA expression analysis, A) or for 48 h (NO detection, B). Every pair of dots represents one independent experiment.

3.1.2 Peritoneal exudate cells (PEC)

As the differences between TNFR2-/- and wt CD11b$^+$ CD11c$^-$ spleen cells only were apparent in CLP-treated mice, it was next examined whether myeloid cells of naïve TNFR2$^{-/-}$ mice show this phenotype, too. Therefore, wt and TNFR2$^{-/-}$ PEC from naïve mice were tested for the iNOS mRNA expression and NO production. As shown in Figure 12, TNFR2$^{-/-}$ PEC were characterized by reduced iNOS mRNA expression and significantly reduced NO production.

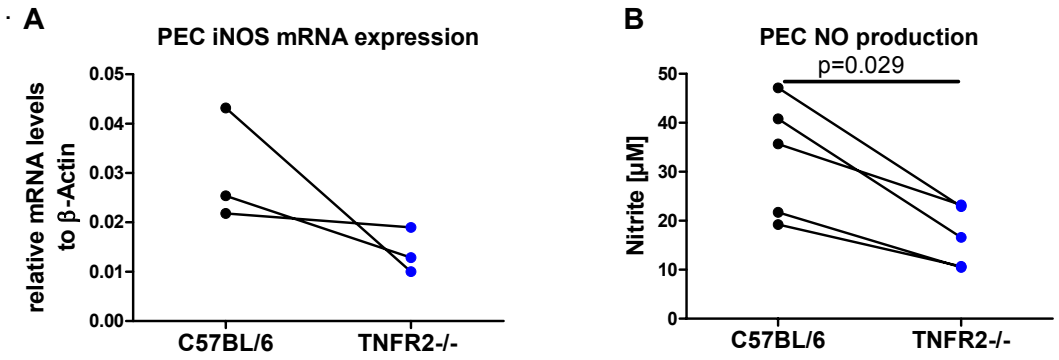

Figure 12: iNOS mRNA expression and NO production of PEC

WT and TNFR2$^{-/-}$ PEC were isolated from the peritoneal cavities of up to 3 pooled naïve mice per group. The cells were seeded at a concentration of 2.5 x 10^5 / 48 well microtiter plate and stimulated with 125 ng/mL LPS and 50 ng/mL IFN-γ in 1 mL for 6 h (mRNA expression analysis, A) or for 48 h (NO detection, B). Every pair of dots represents one independent experiment.

3.1.3 Bone marrow-derived dendritic cells (BMDC)

Another source of myeloid cells are BMDC differentiation cultures. Therefore, it was addressed next whether the deficient iNOS mRNA expression and NO production of cells from TNFR2$^{-/-}$ mice could also be detected in BMDC. Figure 13 shows that BMDC from TNFR2$^{-/-}$ mice expressed reduced iNOS mRNA levels and produced significantly reduced concentrations of NO.

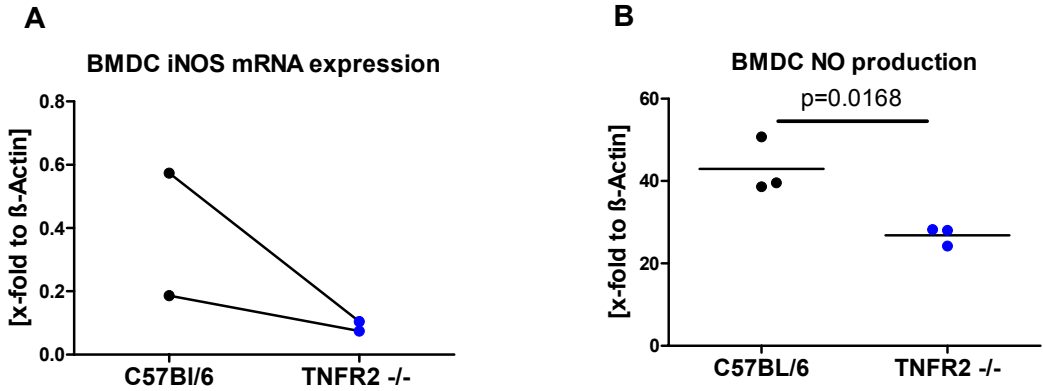

Figure 13: iNOS mRNA expression and NO production in BMDC

Wt and TNFR2$^{-/-}$ BMDC were generated according to the protocol. On day 8 cells were flushed from the petri dishes and seeded at a concentration of 2.5 x 10^5 / 48 well microtiter plate. BMDC were stimulated with 125 ng/mL LPS and 50 ng/mL IFN-γ in 1 mL for 6 h (mRNA expression analysis, A) or for 48 h (NO detection, B). Every pair of dots represents one independent experiment used for iNOS mRNA expression analysis. Data for NO production were obtained from 3 individual mice per group. The lines connect the mean values of one experiment.

3.2 The role of MDSC for the TNFR2$^{-/-}$ phenotype in myeloid cells

MDSC play a critical role in the modulation and suppression of the proliferation and effector functions of T cells. MDSC from TNFR2$^{-/-}$ mice could play an important role for the protection of these mice from the harmful effects of secondary infections in a phase of immunosuppression after CLP treatment.

3.2.1 MDSC in CD11b^{+} splenocytes

3.2.1.1 Relative proportion of MDSC

In order to find out whether altered percentages of MDSC could cause the protection of TNFR2$^{-/-}$ during sepsis, the relative proportions of MDSC (CD11b^{+} Ly6C^{+} Ly6G^{-}) were determined in the spleens of TNFR2$^{-/-}$ mice compared to wt control animals during the course of CLP-induced sepsis. No significant differences were seen comparing the splenocytes of TNFR2$^{-/-}$ and wt mice neither in naïve mice nor during sepsis as illustrated in Figure 14. There was a cell loss 6 h after CLP in both mouse strains. The initial proportion of MDSC among CD11b^{+} splenocytes was recovered after one day and strongly increased on day 11.

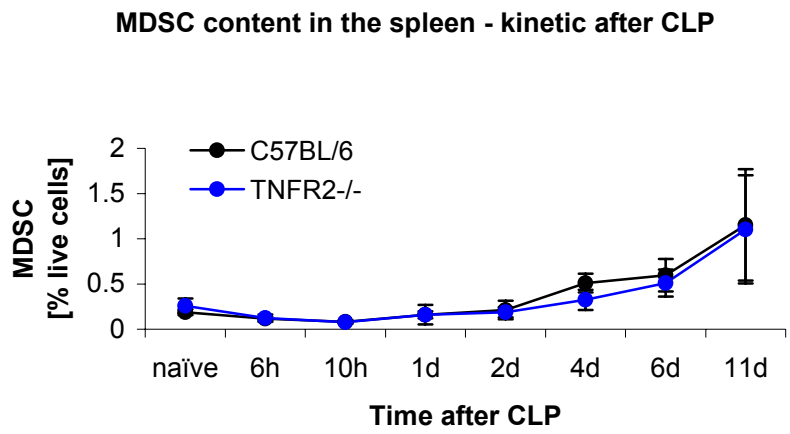

Figure 14: MDSC proportion of the live cells in the spleen – kinetic after CLP

MDSC (CD11b^{+} Ly6C^{+} Ly6G^{-}) contents in spleen cells from naïve or CLP-treated wt and TNFR2$^{-/-}$ mice were compared using flow cytometry. Shown are the mean ± SD from 3 to 5 animals per group and time point.

3.2.1.2 Nitric Oxide (NO) production of MDSC

Having shown that the percentages of MDSC in the spleens of CLP-treated TNFR2$^{-/-}$ mice were not impaired during the course of CLP induced sepsis, we next addressed the question whether the effector functions of these cells were altered. Therefore, the NO production and iNOS mRNA expression were measured in sorted subpopulations of CD11b^{+} splenocytes from naïve or CLP-treated wt and TNFR2$^{-/-}$ mice 2 days after surgery. The sorting strategy is explained in Figure 15. Results are illustrated in Figure 16. The importance of CLP for proper iNOS mRNA expression and NO production shown in 3.1.1 could be reproduced. MDSC (CD11b^{+} Ly6C^{+} Ly6G^{-}) and PMN (CD11b^{+} Ly6C^{int} Ly6G^{+}) cells of wildtype mice express high amounts of iNOS mRNA and MDSC produce significant amounts of NO.

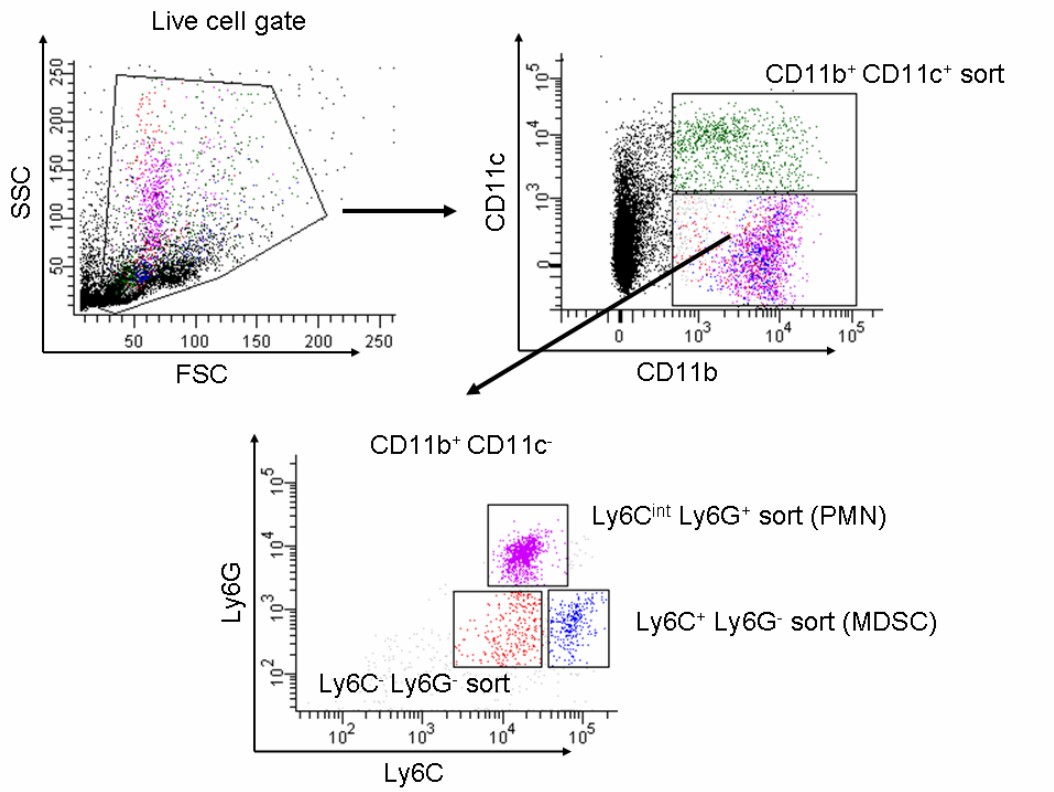

Figure 15: Sorting strategy for MDSC and other CD11b^{+} populations in splenocytes

Mice were subjected to CLP or left naïve. 2 days after CLP splenocytes were isolated and purified using CD11b^{+} MACS. Subsequently, CD11b^{+} cells were subdivided into CD11c^{+}, PMN (Ly6C^{int} Ly6G^{+}), MDSC (Ly6C^{+} Ly6G^{-}) (Zhu, Bando et al. 2007), and Ly6C^{-} Ly6G^{-} subpopulations employing FACS Aria cell sort.

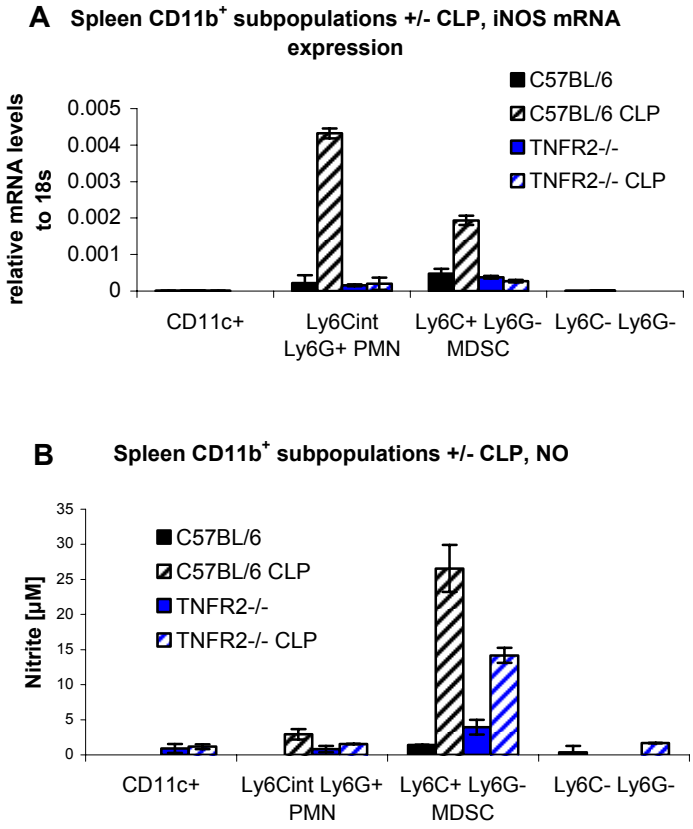

Figure 16: iNOS mRNA expression and NO production in Ly6G/C subpopulations of CD11b$^+$ splenocytes of naïve mice and 2 days after CLP

Mice were subjected to CLP or left naïve. 2 days after CLP splenocytes were isolated and purified using CD11b$^+$ MACS. Subsequently, CD11b$^+$ cells were subdivided into CD11c$^+$, PMN (Ly6C^{int} Ly6G$^+$), MDSC (Ly6C$^+$ Ly6G-), and Ly6C$^-$ Ly6G$^-$ subpopulations employing FACS Aria cell sort. 1 x 10^5 cells were stimulated in 200 µL with 125 ng/mL LPS and 50 ng/mL IFN-γ. After 6 h cells were used for iNOS mRNA expression analysis (A). Shown are the mean ± SD from 3 technical replicates of one sample. After 72 h supernatants were used for NO detection (B). Shown are the mean ± SD from 3 to 8 different cultures. The data originated from one representative experiment out of two.

3.2.2 MDSC population in bone marrow-derived dendritic cells (BMDC)

3.2.3 CD11b$^+$ cells and MDSC in bone marrow

The next aim was to investigate the frequencies of MDSC (CD11b$^+$ Ly6C$^+$ Ly6G$^-$) and PMN (CD11b$^+$ Ly6C^{int} Ly6G$^+$) in the bone marrow of wt and TNFR2$^{-/-}$ mice, in order to characterize this source of progenitor cells for BMDC differentiation cultures. The results are shown in Figure 17. The relative proportion of CD11b$^+$ cells in TNFR2$^{-/-}$ bone marrow was significantly increased. The percentages of MDSC (CD11b$^+$ Ly6C$^+$ Ly6G$^-$) and PMN (CD11b$^+$ Ly6C^{int} Ly6G$^+$) in TNFR2$^{-/-}$

bone marrow were significantly increased compared to wildtype control bone marrow. The relative proportions of MDSC ($CD11b^+$ $Ly6C^+$ $Ly6G^-$) and PMN ($CD11b^+$ $Ly6C^{int}$ $Ly6G^+$) in $TNFR2^{-/-}$ bone marrow were not impaired when referred to the $CD11b^+$ bone marrow cells.

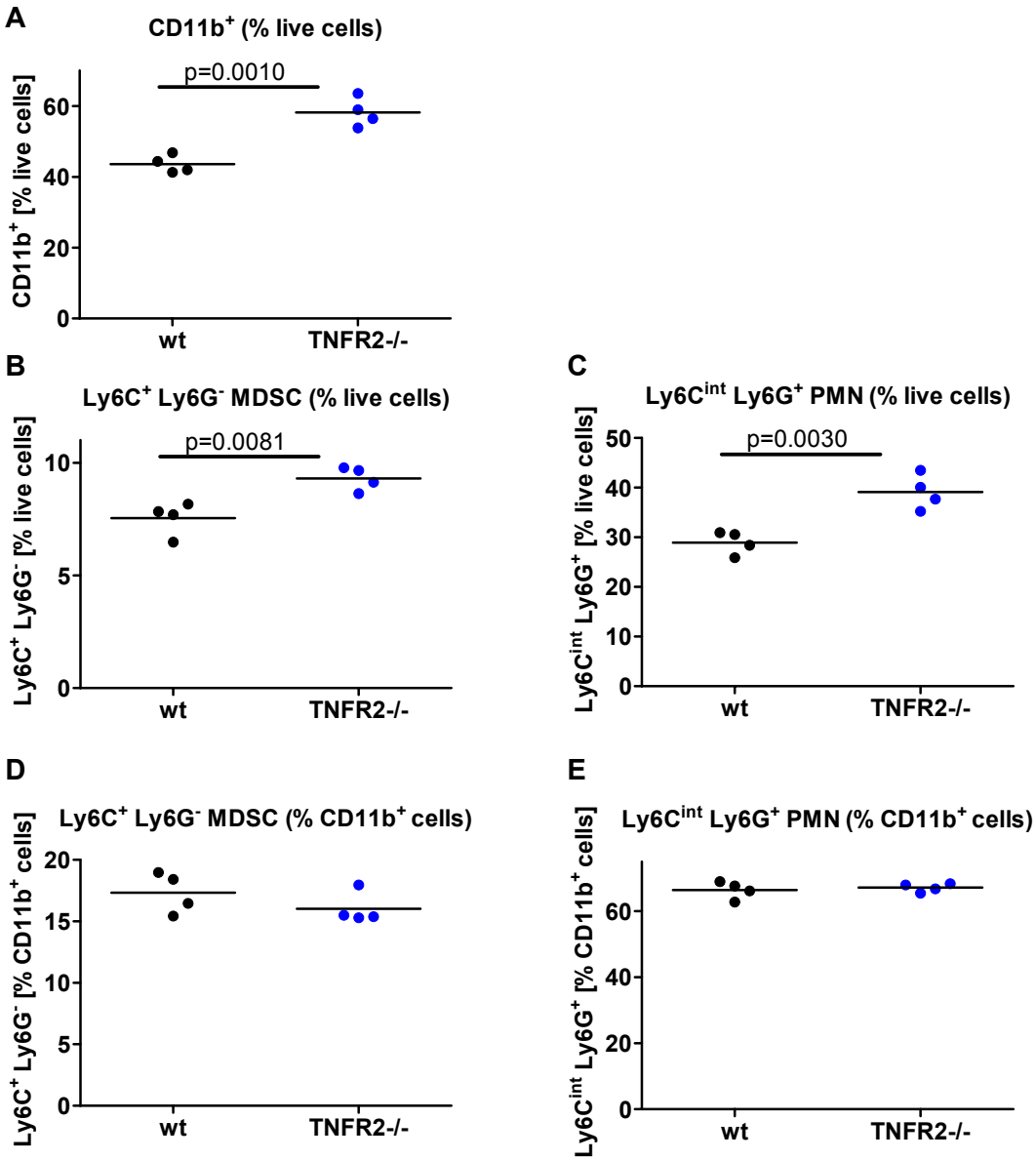

Figure 17: Expression of CD11b, Ly6C, and Ly6G in wildtype and $TNFR2^{-/-}$ bone marrow

Bone marrow cells from wildtype and $TNFR2^{-/-}$ mice were isolated and stained for CD11b, Ly6C, and Ly6G. The cells were analyzed using flow cytometry. (A) shows the percentages of $CD11b^+$ cells of live cells. The percentages of MDSC ($CD11b^+$ $Ly6C^+$ $Ly6G^-$) and PMN ($CD11b^+$ $Ly6C^{int}$ $Ly6G^+$) of live cells are illustrated in (B) and (C). The percentages of MDSC ($CD11b^+$ $Ly6C^+$ $Ly6G^-$) and PMN ($CD11b^+$ $Ly6C^{int}$ $Ly6G^+$) of $CD11b^+$ cells are illustrated in (D) and (E). Shown are the single values and the mean (horizontal line) of four different mice per group.

3.2.3.1 Differentiation and development of BMDC

In order to characterize the development of BMDC, differentiation cultures from wildtype and TNFR2$^{-/-}$ mice were examined for the expression of CD11b and CD11c at different time points. As shown in Figure 18, the expression of CD11c started to increase on day 6 and reached the plateau on day 8 with a relative proportion of 90%. The percentages of CD11b^{+} CD11c^{-} BMDC decreased reciprocally, indicating that almost 100% of the cells in BMDC cultures express CD11b and belong to the myeloid cell lineage. No difference between wt and TNFR2-/- BMDC differentiation cultures could be detected.

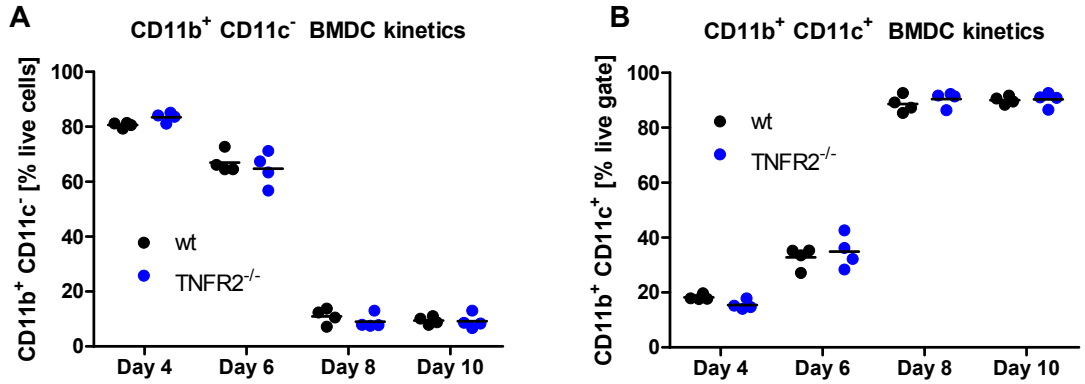

Figure 18: CD11b and CD11c distribution in BMDC – kinetics

The percentages of BMDC expressing the markers CD11b and CD11c were analyzed employing flow cytometry on different time points during the differentiation into dendritic cells. The percentages of CD11b^{+} CD11c^{-} cells are analyzed in (A) whereas the relative proportion of CD11b^{+} CD11c^{+} cells is visualized in (B). Shown are the single values and the mean (horizontal line) of four different BMDC cultures per group representing individual mice.

3.2.3.2 Frequency of MDSC

The next aim was to characterize the relative proportions of cells expressing the MDSC markers CD11b^{+}, Ly6C^{+}, and Ly6G^{-} in BMDC cultures at different time points. Throughout the differentiation into BMDC TNFR2$^{-/-}$ cultures contained significantly reduced percentages of MDSC. Data are shown in Figure 19.

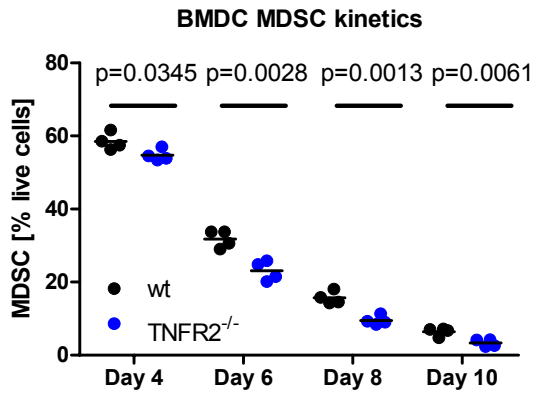

Figure 19: MDSC contents in BMDC cultures - kinetics

The percentages of BMDC expressing the MDSC markers CD11b^{+}, Ly6C^{+}, and Ly6G^{-} were analyzed employing flow cytometry at different time points during the differentiation into dendritic cells. Shown are the single values and the mean (horizontal line) of four different BMDC cultures per group representing individual mice.

3.2.3.3 Nitric Oxide (NO) production of MDSC

Having shown that BMDC differentiation cultures contain high amounts of MDSC on day 4, it was next investigated whether these cells express iNOS mRNA and produce NO and if there are differences between MDSC and PMN. BMDC subpopulations expressing the markers for MDSC (CD11b^{+} Ly6C^{+} Ly6G^{-}) and PMN (CD11b^{+} Ly6C^{int} Ly6G^{+}) were separated on day 4 using FACS aria cell sort according to the sorting strategy explained in Figure 20.

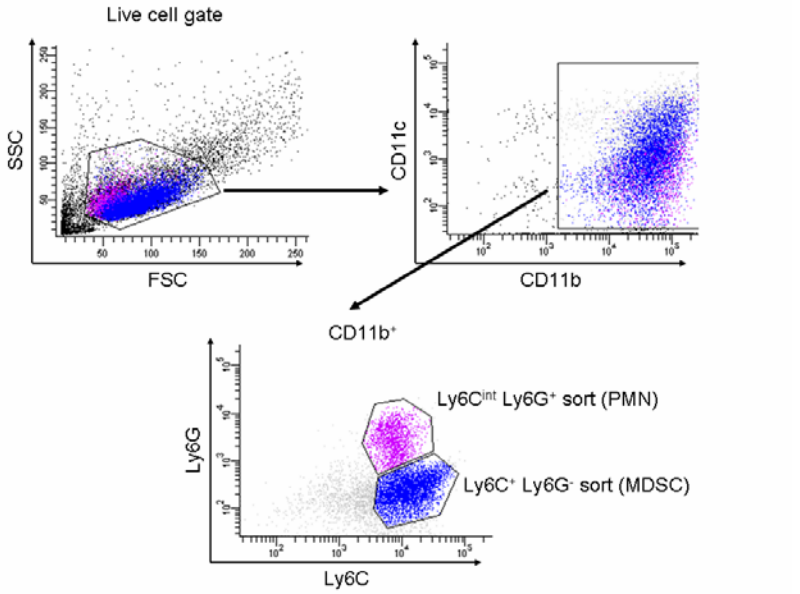

Figure 20: Sorting strategy for MDSC and PMN in BMDC cultures on day 4

BMDC were removed from the petri dish cultures on day 4 and stained for CD11b, CD11c, Ly6C, and Ly6G. The CD11b^{+} population was separated into PMN (Ly6C^{int} Ly6G^{+}) and MDSC (Ly6C^{+} Ly6G^{-}) employing FACS Aria cell sort (Zhu, Bando et al. 2007).

The iNOS mRNA expression and the NO production capacity of these different cell populations were measured. Figure 21 shows that MDSC were the main source of NO on day 4. Differences between TNFR2$^{-/-}$ and wt cultures could not be detected on the NO level but TNFR2$^{-/-}$ MDSC featured significantly reduced iNOS mRNA expression after 6 h of stimulation.

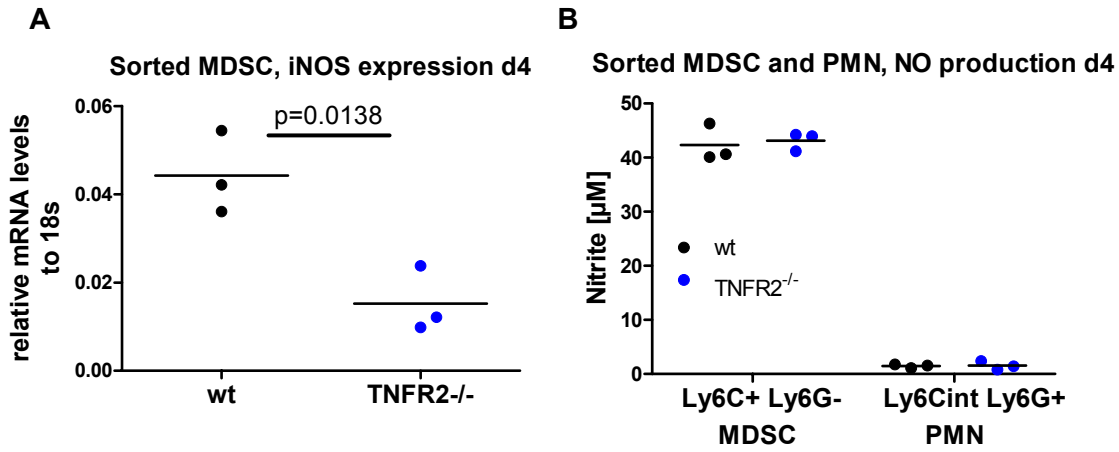

Figure 21: iNOS mRNA expression and NO production of MDSC (CD11b^{+} Ly6C^{+} Ly6G^{-}) and PMN (CD11b^{+} Ly6C^{int} Ly6G^{+}) from BMDC cultures on day 4

BMDC were stained on day 4 with anti-Ly6C FITC and anti-Ly6G PB. Cells were sorted into the two main populations (CD11b^{+} Ly6C^{+} Ly6G^{-}) and PMN (CD11b^{+} Ly6C^{int} Ly6G^{+}), adjusted to the same cell number (2.5 x 10^{5} / mL in the 48 well plate), and stimulated in 1 mL with LPS and IFN-γ (125 ng/mL, 50 ng/mL) for 6 h before iNOS mRNA expression was analyzed (A). After 48 h NO concentrations were determined in the supernatants (B). Shown are the single values and the mean (horizontal line) of three different BMDC cultures per group representing individual mice.

3.2.4 Arg1 expression of BMDC and MDSC

The next aim was to investigate the mRNA expression of Arg1 as the most prominent marker for suppressive MDSC. Arg1 mRNA expression of was measured in non-stimulated whole BMDC on day 6 and purified MDSC on day 4. Figure 22 shows that both TNFR2$^{-/-}$ BMDC and sorted TNFR2$^{-/-}$ MDSC expressed slightly decreased Arg1 mRNA levels.

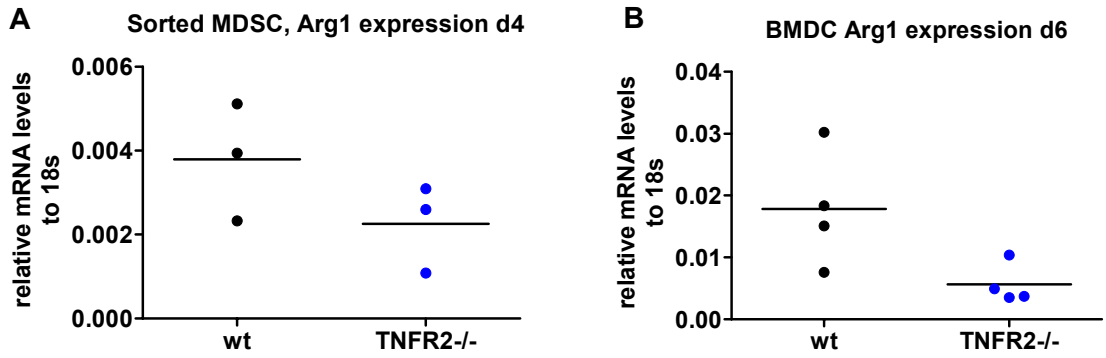

Figure 22: Arg1 mRNA expression in BMDC and MDSC

BMDC were stained on day 4 with anti-Ly6C-FITC and anti-Ly6G-PB. The MDSC populations ($CD11b^+$ $Ly6C^+$ $Ly6G^-$) were isolated employing the FACS Aria sort device. Arg1 mRNA expression was analyzed in non-stimulated cells (A). On day 6 non-stimulated whole BMDC were analyzed for the expression of Arg1 mRNA expression (B). Shown are the single values and the mean (horizontal line) of three different MDSC cultures per group (A) and four different BMDC cultures per group (B). (A) and (B) represent two different experiments.

3.3 Phenotypes of TNFR2$^{-/-}$ bone marrow-derived dendritic cells (BMDC)

3.3.1 Non-stimulated BMDC

Differences in the BMDC differentiation between the C57BL/6 wt and TNFR2$^{-/-}$ background were examined using kinetics or the time points indicated. Either expression of different markers or the concentrations of soluble TNF and soluble TNFR2 in the medium were measured. All BMDC samples were non-stimulated.

3.3.1.1 Cell numbers in BMDC cultures

First, the yields of cells in the BMDC differentiation cultures of wt and TNFR2$^{-/-}$ mice were analyzed. As illustrated in Figure 23, pure TNFR2$^{-/-}$ BMDC cultures provided significantly reduced yields of cells on day 8 and 10.

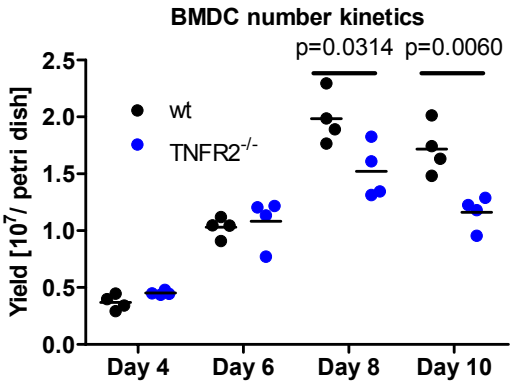

Figure 23: BMDC yields from BMDC cultures - kinetics

BMDC numbers in the petri dishes were counted on different time points during the BMDC differentiation culture period. Shown are the single values and the mean (horizontal line) of four different BMDC cultures per group representing individual mice.

3.3.1.2 Frequency of cells expressing activation markers (MHCII$^+$ CD80$^+$ CD86$^+$) in BMDC cultures

Next, the question was addressed whether the expression of activation markers is impaired in BMDC from TNFR2$^{-/-}$ mice compared to wildtype mice. TNFR2$^{-/-}$ BMDC contained higher relative proportions of cells expressing the activation markers MHCII$^+$, CD80$^+$, and CD86$^+$. This finding is visualized in Figure 24. The data are statistically significant on day 8 and 10.

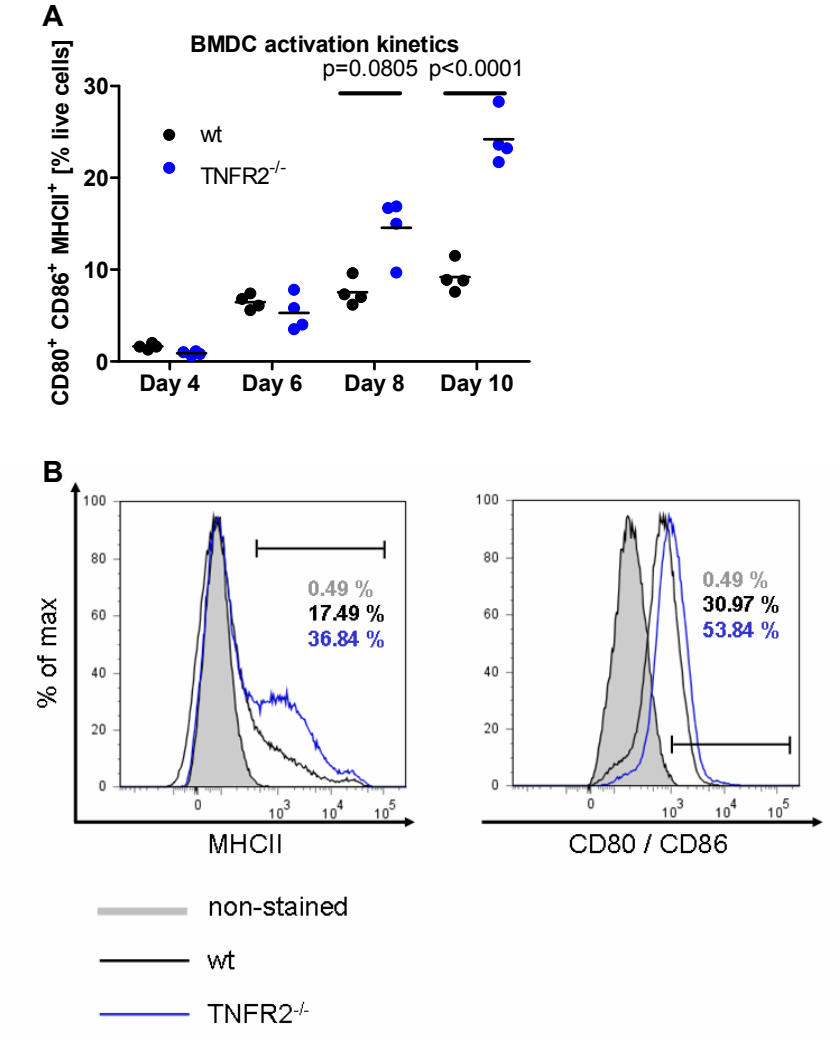

Figure 24: Activation markers – BMDC cultures kinetics

The percentage of BMDC expressing the activation markers MHCII$^+$, CD80$^+$, and CD86$^+$ were analyzed employing flow cytometry at different time points during the differentiation into dendritic cells. Shown are the single values and the mean (horizontal line) of four different BMDC cultures per group and time point representing individual mice (A). (B) illustrates the histogram of one representative culture out of four on day 10.

3.3.1.3 Frequency of MDSC in BMDC cultures

TNFR2$^{-/-}$ BMDC cultures contained lower proportions of cells expressing the MDSC markers CD11b$^+$, Ly6C$^+$, and Ly6G$^-$ throughout the BMDC differentiation culture period. This finding is shown in Figure 19. The data are statistically significant.

3.3.1.4 Proliferation in BMDC cultures

Having shown that BMDC differentiation cultures from TNFR2$^{-/-}$ mice yield reduced cell numbers compared to wildtype mice, it was next analyzed whether this is due to decreased proliferation in TNFR2$^{-/-}$ BMDC differentiation cultures. TNFR2$^{-/-}$ BMDC cultures on day 10 of the differentiation culture period contained slightly reduced percentages of cells that incorporated BrdU into the DNA indicating less proliferation. This finding is shown in Figure 25.

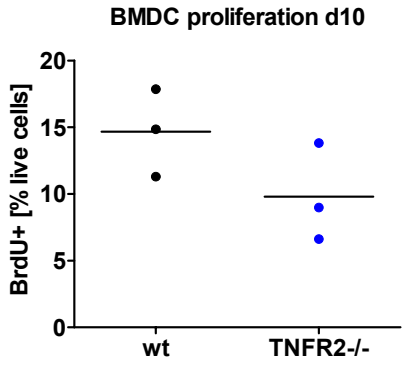

Figure 25: Proliferation in BMDC cultures

The percentages of BMDC that were positive for BrdU were analyzed employing flow cytometry on day 10. Cells were incubated with BrdU for the 24 previous hours. Shown are the single values and the mean (horizontal line) of three different BMDC cultures per group representing individual mice.

3.3.1.5 Cell death in BMDC cultures

The role of cell death for the decreased cellular yield of TNFR2$^{-/-}$ BMDC was investigated next. TNFR2$^{-/-}$ BMDC did not contain altered numbers of apoptotic and necrotic cells. Data are based on flow cytometry analysis of Annexin V^{+} and 7-AAD^{+} cells. This finding is shown in Figure 26.

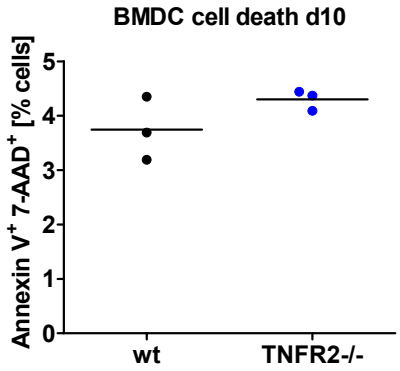

Figure 26: Cell death in BMDC cultures

The percentages of BMDC positive for Annexin V and 7-AAD were analyzed employing flow cytometry on day 10. Shown are the single values and the mean (horizontal line) of three different BMDC cultures per group representing individual mice.

3.3.1.6 TNF concentrations in BMDC cultures

Subsequently, the concentrations of soluble and biologically active TNF in BMDC differentiation cultures of wildtype and TNFR2$^{-/-}$mice were analyzed, in order to get information about the relevance of this cytokine during the BMDC differentiation. TNFR2$^{-/-}$ BMDC cultures produced significantly higher concentrations of soluble TNF on every day of the kinetic. Figure 27 shows the concentrations of soluble TNF that were not blocked by soluble TNFR2 representing the biologically active form of the cytokine. Increased TNFR1-signaling in TNFR2$^{-/-}$ BMDC differentiation cultures might occur.

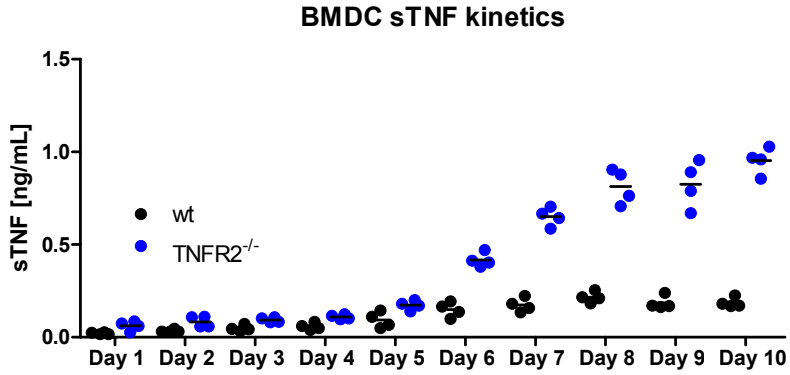

Figure 27: sTNF concentrations in BMDC cultures - kinetics

At every time point of the kinetic 0.5 mL of the supernatant were removed from each petri dish of BMDC cultures and replaced by fresh GM-CSF-containing medium. The concentrations of soluble TNF were measured employing ELISA. Shown are the single values and the mean (horizontal line) of four different BMDC cultures per group representing individual mice.

3.3.1.7 TNFR2 concentrations in BMDC cultures

Furthermore, the concentrations of soluble TNFR2 were measured in the BMDC differentiation cultures, in order to acquire informations about its possible influence on the availability of biologically active soluble TNF. Wt BMDC cultures showed high concentrations of soluble TNFR2 in the supernatant after day 3 of the BMDC differentiation cultures period as demonstrated in Figure 28.

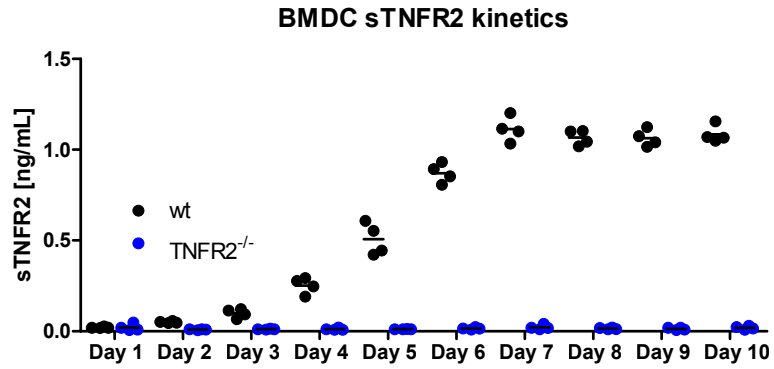

Figure 28: sTNFR2 concentrations in BMDC cultures - kinetics

At every time point of the kinetic 0.5 mL of the supernatant were removed from each petri dish of BMDC cultures and replaced by fresh GM-CSF-containing medium. The concentrations of soluble TNFR2 were measured employing ELISA. Shown are the single values and the mean (horizontal line) of four different BMDC cultures per group representing individual mice.

3.3.2 Stimulated BMDC cultures

BMDC from pure cultures were isolated and seeded in defined volumes. After stimulation with LPS and IFN-γ NO, soluble TNFR2, and the cytokines IL-6 and soluble TNF were measured.

3.3.2.1 NO production capacity in TNFR2$^{-/-}$ BMDC cultures

In order to exclude that FACS Aria sort cell separation interferes with the decreased NO production capacity of TNFR2$^{-/-}$ BMDC, BMDC were sorted after 8 days of the BMDC differentiation period and were stimulated. NO concentrations in the supernatants of TNFR2$^{-/-}$ BMDC were again significantly reduced. Data are shown in Figure 29. Reduced NO production capacity of TNFR2$^{-/-}$ BMDC has already been shown in 3.1.3. This finding served as a control experiment for further investigations using FACS aria cell sort.

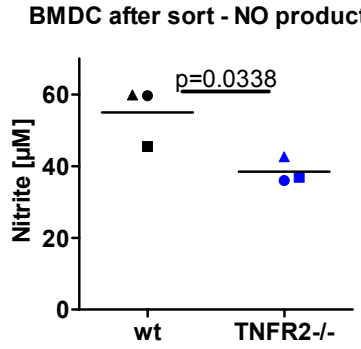

Figure 29: NO production capacity after sort in BMDC cultures

CD45.1 C57BL/6 wt and CD45.2 TNFR2$^{-/-}$ mice were used. BMDC were removed from the petri dish culture plates on day 8 and stained according to their respective congenic markers CD45.1 (C57BL/6 wt) and CD45.2 (TNFR2$^{-/-}$). Cells were subjected to FACS Aria cell separation procedure. 2.5 x 10^5 cells were stimulated in 1 mL medium with LPS and IFN-γ (125 ng/mL, 50 ng/mL). NO concentrations were measured after 48 h. Every pair of symbols represents one independent experiment and the mean values of more than three biological replicates. Shown are the single values and the mean (horizontal line) of 3 independent experiments.

3.3.2.2 IL-6 production capacity in BMDC cultures

Next, it was addressed whether the capacity to produce IL-6 is impaired in BMDC from TNFR2$^{-/-}$ mice. BMDC were stimulated and IL-6 concentrations in the supernatants were measured at different time points during the BMDC differentiation culture period. The IL-6 production capacity was significantly reduced in TNFR2$^{-/-}$ BMDC cultures throughout the kinetic as shown in Figure 30.

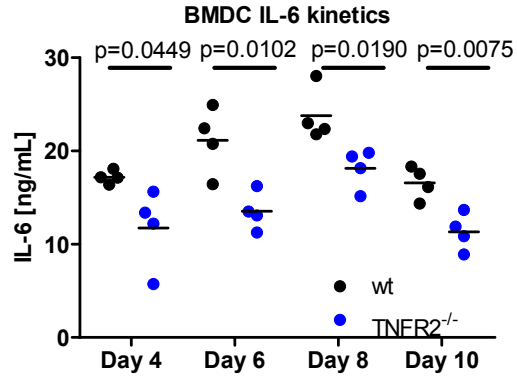

Figure 30: IL-6 production capacity in BMDC cultures - kinetics

BMDC were removed from the petri dish cultures at the time points indicated. 2.5 x 10^5 cells were seeded in 1 mL and in 48 well microtiter plates and, subsequently, stimulated with LPS and IFN-γ (125 ng/mL, 50 ng/mL). IL-6 concentrations were measured after 48 h using ELISA. Shown are the single values and the mean (horizontal line) of four different BMDC cultures per group representing individual mice.

3.3.2.3 sTNF concentrations in TNFR2$^{-/-}$ BMDC cultures

Next, it was addressed whether the concentrations of soluble TNF were also impaired after stimulation. TNF concentrations in the supernatants of stimulated BMDC were measured at different time points during the differentiation. The concentrations of soluble TNF were significantly increased in TNFR2$^{-/-}$ BMDC cultures after day 4 as shown in Figure 31.

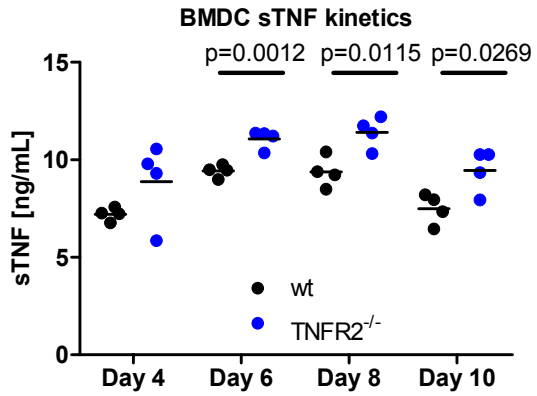

Figure 31: sTNF concentrations in BMDC cultures - kinetics

BMDC were removed from the petri dish cultures at the time points indicated. 2.5 x 10^5 cells were seeded in 1 mL and in 48 well microtiter plates and, subsequently, stimulated with LPS and IFN-γ (125 ng/mL, 50 ng/mL). Soluble TNF concentrations were measured after 48 h using ELISA. Shown are the single values and the mean (horizontal line) of four different BMDC cultures per group representing individual mice.

3.3.2.4 sTNRF2 concentrations in BMDC cultures

In parallel, soluble TNFR2 concentrations were measured in the supernatants of stimulated BMDC at different time points during the differentiation. The soluble TNFR2 concentrations were significantly increased in TNFR2$^{-/-}$ BMDC cultures after day 4 as shown in Figure 32.

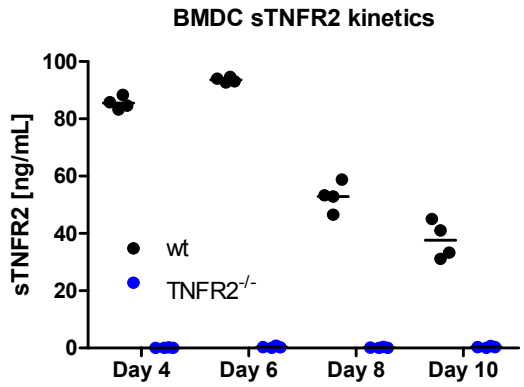

Figure 32: sTNFR2 concentrations in BMDC cultures - kinetics

BMDC were removed from the petri dish cultures at the time points indicated. 2.5 x 10^5 cells were seeded in 1 mL and in 48 well microtiter plates and, subsequently, stimulated with LPS and IFN-γ (125 ng/mL, 50 ng/mL). Soluble TNFR2 concentrations were measured after 48 h using ELISA. Shown are the single values and the mean (horizontal line) of four different BMDC cultures per group representing individual mice.

3.3.3 Mixed and non-stimulated BMDC cultures

In order to address whether different culture conditions in terms of soluble TNF and soluble TNFR2 influence the phenotypes seen in TNFR2-/- BMDC cultures, both populations were differentiated in the same petri dish, in order to guarantee identical conditions. Mixed BMDC cultures were obtained by preparing bone marrow cells from one wildype and one TNFR2$^{-/-}$ mouse and mixing equal numbers of these cells. Hence, the resulting mixed culture should consist of 50% wt and 50% TNFR2$^{-/-}$ bone marrow cells. These cultures were differentiated into BMDC. At the indicated time points the two populations in the mixed BMDC cultures were investigated using flow cytometry or FACS Aria cell sort device.

3.3.3.1 Cell proportions in mixed BMDC cultures

In order to find out, whether the reduced yield of BMDC of TNFR2$^{-/-}$ mice is due to missing intrinsic signaling or depending on altered culture conditions, the frequencies of the respective population in mixed BMDC differentiation cultures were analyzed at different time points. Figure 33 illustrates that TNFR2$^{-/-}$ BMDC were present in an above-average frequency in mixed cultures on day 3. In contrast to this, the percentage of TNFR2$^{-/-}$ BMDC decreased steadily and reached significantly lower levels compared to the wt BMDC on day 8 and day 10. These

findings correspond to the results from BMDC generated in separated BMDC differentiation cultures shown in Figure 23.

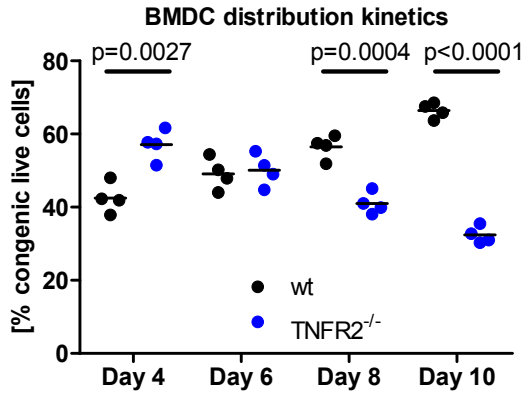

Figure 33: BMDC distribution in mixed cultures - kinetics

Mixed BMDC were analyzed for the distribution of CD45.1 wt and CD45.2 TNFR2$^{-/-}$ cells at the time points indicated using flow cytometry. Shown are the single values and the mean (horizontal line) of four different mixed BMDC cultures per group representing individual mice.

3.3.3.2 Frequency of cells expressing activation markers (MHCII$^+$ CD80$^+$ CD86$^+$) in mixed BMDC cultures

Afterwards, the influence of TNFR2$^{-/-}$ BMDC culture conditions on the activation of the developing BMDC should be figured out. Therefore the frequencies of activated cells in the two different populations of mixed BMDC differentiation cultures were examined at different time points. The relative proportions of activated cells in the TNFR2$^{-/-}$ BMDC population of mixed BMDC cultures started lower on day 4 and day 6 but were significantly increased on day 10. Data are interpreted in Figure 34. These findings correspond to the results from BMDC generated in separated BMDC differentiation cultures shown in Figure 24.

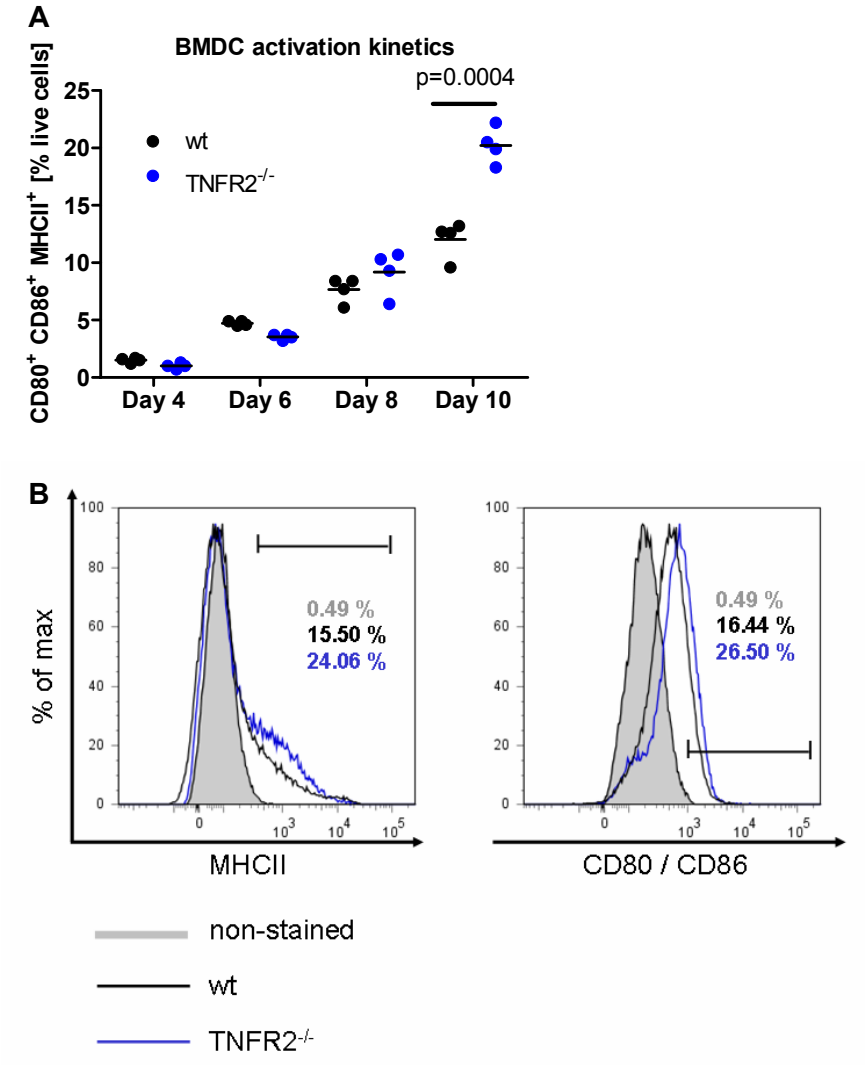

Figure 34: Activation markers expression in mixed BMDC cultures - kinetics

Mixed BMDC were analyzed for the percentages of activated cells ($MHCII^+$ $CD80^+$ $CD86^+$) in the two populations that were distinguished by their congenic markers. Measurements were done at the time points indicated using flow cytometry. Shown are the single values and the mean (horizontal line) of four different BMDC cultures per group and time point representing individual mice (A). (B) illustrates the histogram of one representative culture out of four on day 10.

3.3.3.3 Frequency of MDSC in mixed BMDC cultures

Moreover, the frequencies of cells expressing the markers of MDSC ($CD11b^+$ $Ly6C^+$ $Ly6G^-$) in the two different populations of mixed BMDC differentiation cultures were examined at different time points. The relative proportions of MDSC in the $TNFR2^{-/-}$ population of mixed cultures were significantly decreased after day 4. Data are shown in Figure 35. These findings correspond to the results from BMDC generated in separated BMDC differentiation cultures shown in Figure 19.

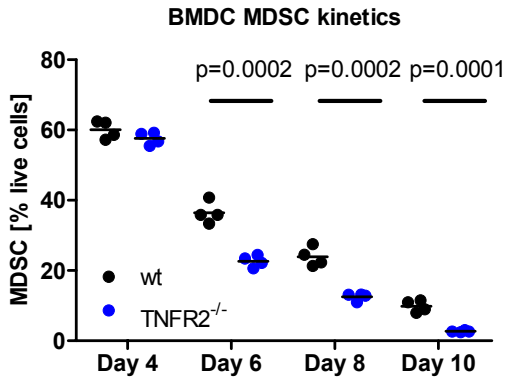

Figure 35: MDSC in mixed BMDC cultures - kinetics

Mixed BMDC were analyzed for the percentages of MDSC ($CD11b^+$ $Ly6C^+$ $Ly6G^-$) in the two BMDC populations that were distinguished by their congenic markers. Measurements were done at the time points indicated using flow cytometry. Shown are the single values and the mean (horizontal line) of four different mixed BMDC cultures per group representing individual mice.

3.3.3.4 Proliferation of mixed BMDC cultures

The proliferation was measured in the two populations of mixed BMDC differentiation cultures. The relative proportions of proliferating cells in the $TNFR2^{-/-}$ population of mixed cultures were slightly decreased on day 10. The data are shown in Figure 36. These findings correspond to the results from BMDC generated in separated BMDC differentiation cultures shown in Figure 25.

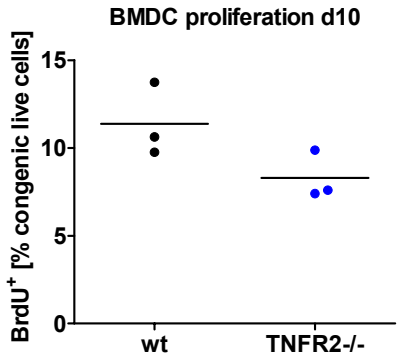

Figure 36: Proliferation in mixed BMDC cultures

Mixed BMDC were analyzed for the percentage of proliferating cells (anti-BrdU FITC) in the two BMDC populations that were distinguished by their congenic markers. Measurements were performed on day 10 using flow cytometry. Cells were incubated with BrdU for the 24 previous hours. Shown are the single values and the mean (horizontal line) of three different mixed BMDC cultures per group representing individual mice.

3.3.3.5 Cell death in mixed BMDC cultures

In parallel, the frequencies of dead cells in the two populations of mixed BMDC differentiation cultures were analyzed. The relative proportions of dead cells in the TNFR2$^{-/-}$ population of mixed cultures were comparable to the percentages in the wt population. Data are illustrated in Figure 37. These findings correspond to the results from BMDC generated in separated BMDC differentiation cultures shown in Figure 26.

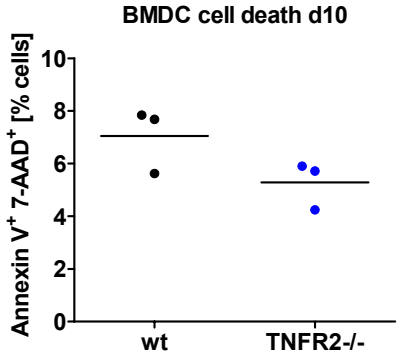

Figure 37: Cell death in mixed BMDC cultures

Mixed BMDC were analyzed for the percentages of apoptotic and necrotic cells (Annexin V$^+$ 7-AAD$^+$) in the two BMDC populations that were distinguished by their congenic markers. Measurements were performed on day 10 using flow cytometry. Shown are the single values and the mean (horizontal line) of three different mixed BMDC cultures per group representing individual mice.

3.3.4 Mixed BMDC cultures, sorted and stimulated

Mixed BMDC cultures were separated after 8 days of co-culture according to their congenic markers using FACS Aria sort device. The cells were subsequently stimulated with LPS and IFN-γ for 48 h before supernatants were removed and analysis were performed.

3.3.4.1 NO production in mixed BMDC cultures

First, the NO production capacities in the two separated pupulations of mixed BMDC differentiation cultures were analyzed. TNFR2$^{-/-}$ BMDC recovered from mixed cultures showed significantly reduced amounts of NO in the supernatants after stimulation. This is demonstrated in Figure 38. These findings correspond to the results from BMDC generated in separated BMDC differentiation cultures shown in Figure 13 and Figure 29.

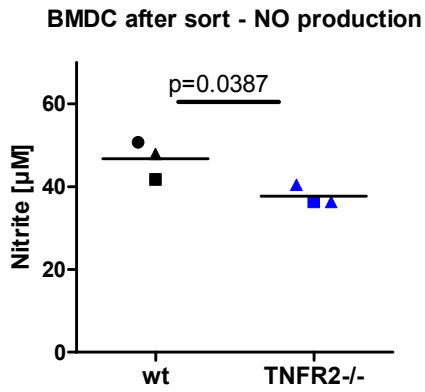

Figure 38: NO production of sorted BMDC grown in mixed cultures

The two BMDC populations in mixed BMDC cultures were sorted on day 8 according to their congenic markers using FACS Aria sort. 2.5 x 10^5 cells were stimulated in 1 mL medium with LPS and IFN-γ (125 ng/mL, 50 ng/mL). NO concentrations were measured after 48 h. Every pair of symbols represents one independent experiment and the mean value of more than three biological replicates. Shown are the single values and mean (horizontal line) of three independent experiments.

3.3.4.2 IL-6 production in mixed BMDC cultures

Additionaly, the IL-6 production capacities in the two separated pupulations of mixed BMDC differentiation cultures were analyzed. The TNFR2$^{-/-}$ BMDC recovered from mixed BMDC cultures showed significantly reduced amounts of IL-6 in the supernatants after stimulation. This is shown in Figure 39. These findings correspond to the results from BMDC generated in separated BMDC differentiation cultures shown in Figure 30.

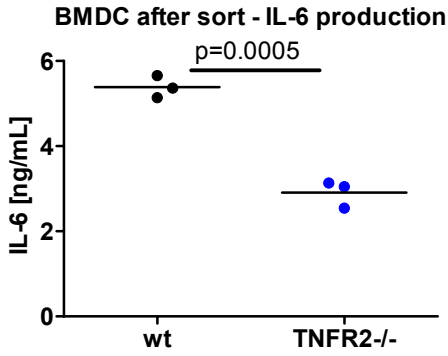

Figure 39: IL-6 production of sorted BMDC grown in mixed cultures

The two BMDC populations in mixed BMDC cultures were sorted on day 8 according to their congenic markers using FACS Aria sort. 2.5 x 10^5 cells were stimulated in 1 mL medium with LPS and IFN-γ (125 ng/mL, 50 ng/mL). IL-6 concentrations were measured after 48 h. Shown are the single values and the mean (horizontal line) of three technical replicates of one experiment.

3.4 Bone marrow chimeric mice

Bone marrow chimeric mice were generated to examine TNFR2$^{-/-}$ hematopoietic cells grown in wildtype hosts and and wildtype hematopoietic cells grown in TNFR2$^{-/-}$ hosts.

3.4.1 Reconstitution

Eight weeks after bone marrow transplantation mice were killed and the rates of reconstitution were checked in the spleens. As shown in Figure 40, about 80% reconstitution of the donor bone marrow could be achieved. The distributions of CD4 and CD8 T cells as well as B-cells were not changed in the 4 different groups and were similar to naïve animals.

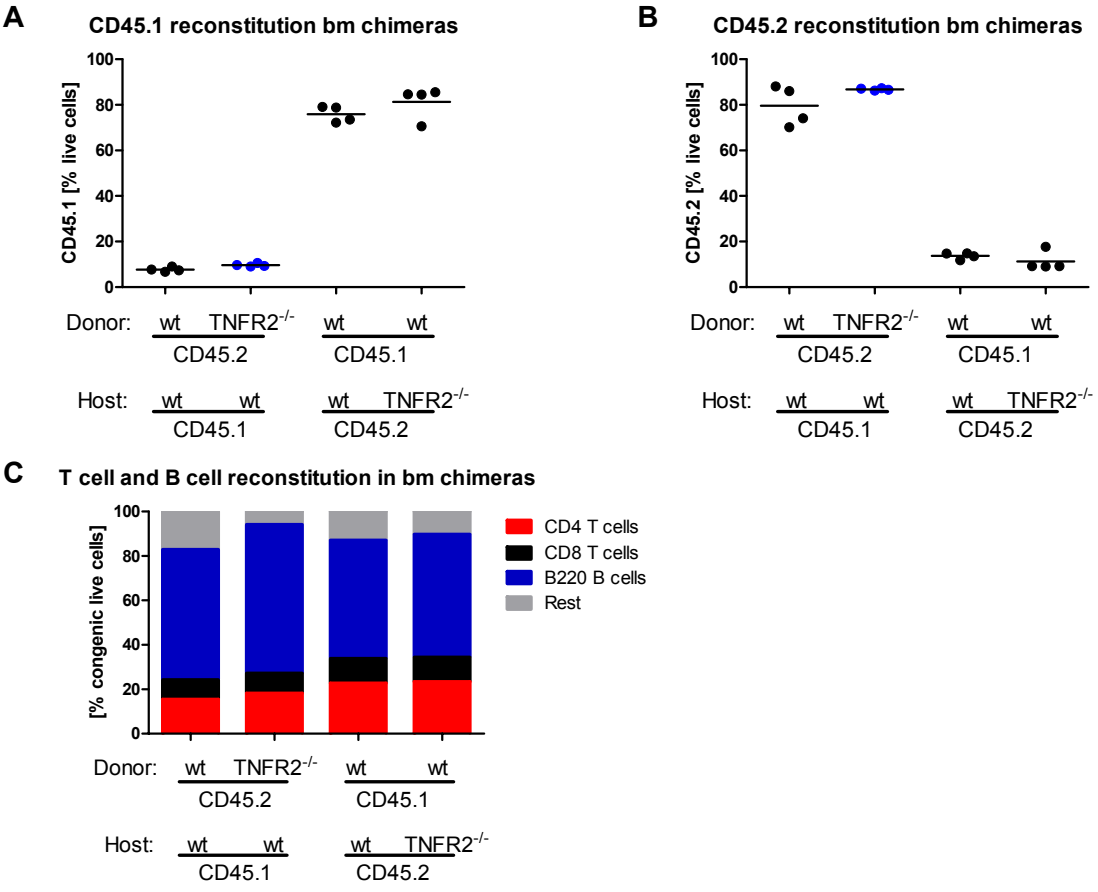

Figure 40: Reconstitution of bm chimeric mice

Spleen cell suspensions were prepared and stained according to the congenic markers CD45.1 (A) and CD45.2 (B) of donor and host, respectively. In order to guarantee a natural spleen cell composition, additional stainings for CD4 T cells, CD8 T cells and B cells (B220) were performed and analyzed using flow cytometry (C). Shown are the single values and the mean (horizontal line) of four individual animals per group (A and B) and the mean of the pecentages of the different cells of four individual mice per group (C).

3.4.2 PEC cell distribution and NO production

First, PEC from bm chimeric mice were analyzed for the cellular composition and the NO production capacity. As shown in Figure 41 the cell distributions of PEC in the different chimeras were similar. However, no difference in the NO production could be detected anymore in PEC from wildtype mice that were reconstituted with TNFR2$^{-/-}$ bone marrow.

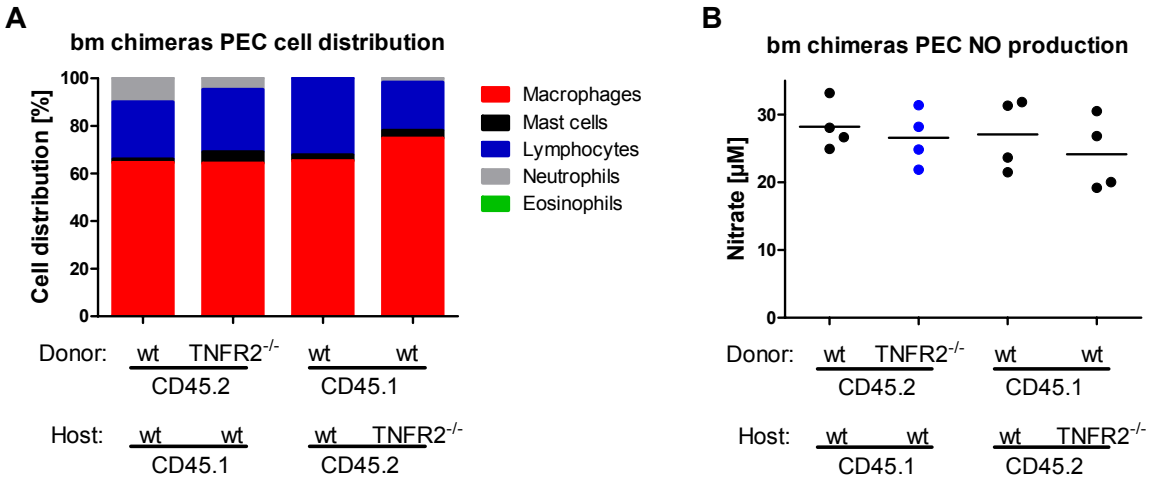

Figure 41: bm chimeras – PEC distribution and NO production

PEC were generated from bm chimeric mice and analyzed for the distribution of various cell types (A). Additionally, 2.5 x 10^5 cells were stimulated in 1 mL medium with LPS and IFN-γ (125 ng/mL, 50 ng/mL), in order to measure NO after 48 h (B). Shown are the mean of four individual mice per group (A) and single values and mean (horizontal line) of four individual mice per group (B).

3.4.3 BMDC from bm chimeric mice

BMDC were generated from bm chimeric mice according to the protocol and tested on day 8.

3.4.3.1 Frequency of cells expressing activation markers (MHCII$^+$ CD80$^+$ CD86$^+$) in BMDC cultures from bm chimeric mice

The frequencies of activated cells in BMDC differentiation cultures of bm chimeric mice expressing the activation markers MHCII$^+$, CD80$^+$, and CD86$^+$ on day 8 are shown in Figure 42. Significantly increased percentages of mature and activated cells were found in BMDC differentiation cultures of wildtype mice that were reconstituted with TNFR2$^{-/-}$ bone marrow. These findings correspond to the results from BMDC generated in separated BMDC differentiation cultures shown in Figure 24.

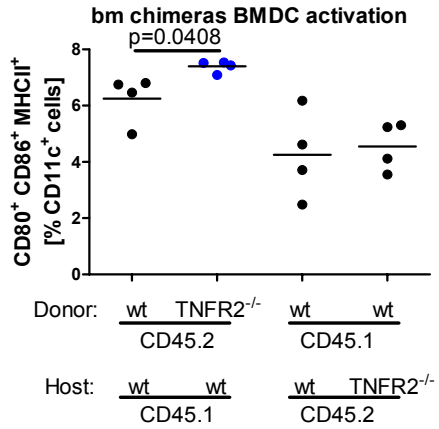

Figure 42: Activation markers of BMDC from bm chimeric mice

The percentages of BMDC expressing the activation markers MHCII, CD80, and CD86 were analyzed employing flow cytometry on day 8. Shown are the single values representing individual mice and the mean (horizontal line) of four different BMDC cultures per group.

3.4.3.2 Nitric Oxide (NO) production of BMDC from bm chimeric mice

Besides, the NO production capacity was investigated in BMDC differentiation cultures of bm chimeric mice on day 8 after stimulation with LPS and IFN-γ. Figure 43 shows that BMDC from wildtype mice reconstituted with TNFR2$^{-/-}$ bone marrow produced significantly reduced amounts of NO. These findings correspond to the results from BMDC generated in separated BMDC differentiation cultures shown in Figure 13 and Figure 29.

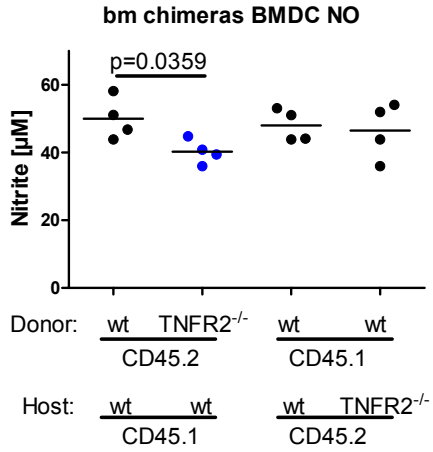

Figure 43: NO production of BMDC from bm chimeric mice

BMDC were removed from the petri dish on day 8 of BMDC differentiation culture. 2.5 x 10^5 cells were seeded in 1 mL and in 48 well microtiter plates and, subsequently, stimulated with LPS and IFN-γ (125 ng/mL, 50 ng/mL). NO concentrations were measured after 48 h using Griess reagent. Shown are the single values representing individual mice and the mean (horizontal line) of four different BMDC cultures per group.

3.4.3.3 IL-6 production of BMDC cultures from bm chimeric mice

Moreover, the IL-6 production capacity was examined in BMDC differentiation cultures of bm chimeric mice on day 8 after stimulation with LPS and IFN-γ. Figure 44 shows that BMDC from wildtype mice reconstituted with TNFR2$^{-/-}$ bone marrow produced significantly reduced amounts of IL-6. These findings correspond to the results from BMDC generated in separated BMDC differentiation cultures shown in Figure 30.

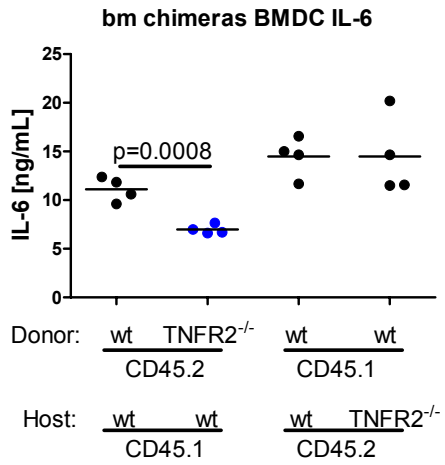

Figure 44: IL-6 production of BMDC from bm chimeric mice

BMDC were removed from the petri dish on day 8 of the culture. 2.5 x 10^5 cells were seeded in 1 mL and in 48 well microtiter plates and, subsequently, stimulated with LPS and IFN-γ (125 ng/mL, 50 ng/mL). IL-6 concentrations were measured after 48 h using ELISA. Shown are the single values representing individual mice and the mean (horizontal line) of four different BMDC cultures per group.

3.4.3.4 sTNF concentrations in BMDC cultures from bm chimeric mice

Additionally, the soluble TNF concentrations were measured in BMDC differentiation cultures of bm chimeric mice on day 8 after stimulation with LPS and IFN-γ. Figure 45 shows that BMDC from wildtype mice reconstituted with TNFR2$^{-/-}$ bone marrow produced slightly increased concentrations of soluble TNF in the supernatant. These findings correspond to the results from BMDC generated in separated BMDC differentiation cultures shown in Figure 31.

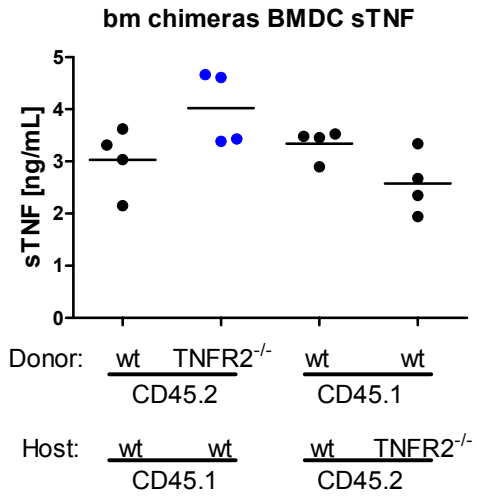

Figure 45: sTNF concentrations in the supernatants of BMDC from bm chimeric mice

BMDC were removed from the petri dish on day 8 of the culture. 2.5 x 10^5 cells were seeded in 1 mL and in 48 well microtiter plates and, subsequently, stimulated with LPS and IFN-γ (125 ng/mL, 50 ng/mL). Soluble TNF concentrations were measured after 48 h using ELISA. Shown are the single values representing individual mice and the mean (horizontal line) of four different BMDC cultures per group.

3.4.3.5 sTNFR2 concentrations in BMDC cultures from bm chimeric mice

In parallel, the TNFR2 concentrations were measured in BMDC differentiation cultures of bm chimeric mice on day 8 after stimulation with LPS and IFN-γ. BMDC from wildtype mice reconstituted with $TNFR2^{-/-}$ bone marrow expressed hardly any soluble TNFR2 compared to the wildtype control BMDC indicating almost complete reconstitution. Data are shown in Figure 46. These findings correspond to the results from BMDC generated in separated BMDC differentiation cultures shown in Figure 32.

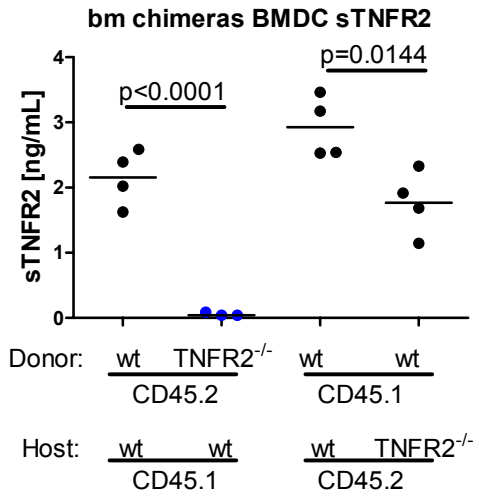

Figure 46: sTNFR2 concentrations in the supernatants of BMDC from bm chimeric mice

BMDC were removed from the petri dish on day 8 of the culture. 2.5 x 10^5 cells were seeded in 1 mL and in 48 well microtiter plates and, subsequently, stimulated with LPS and IFN-γ (125 ng/mL, 50 ng/mL). Soluble TNFR2 concentrations were measured after 48 h using ELISA. Shown are the single values representing individual mice and the mean (horizontal line) of four different BMDC cultures per group.

3.5 Generation of mouse anti-mouse TNFR2 mAB

3.5.1 Cloning of recombinant TNFR2ed-huIgG and TNFR2ed-V5His-tagged proteins

First, vectors for the expression of two different recombinant TNFR2ed fusion were cloned. The cloning strategy for TNFR2ed proteins tagged with the Fc part of human IgG or V5His was based on a vector cloned by Dr. Andrea Hauser (Hauser, Hehlgans et al. 2007). pMT/Bip/V5-His (DesMTA) hygro vector was generated by integration of the hygromycine cassette from pCoHygro vector via the restriction enzyme sites AccI and SapI. TNFR2 extracellular domain was cloned into pMT/Bip/V5-His hygro via BamH1 Not1 using the primers shown in Table 2 resulting in the expression of TNFR2ed-V5His.

The sequence for TNFR2ed-huIgG was integrated via Spe and Nos restriction sites. In the latter case a stop codon was generated after the human Fc portion. Thus, the V5His tag was not attached to the protein. All vectors were verified using gene sequencing. The predicted molecular weight for the TNFR2ed-V5His protein was 29.11 kDa and 53.43 kDa for the TNFR2ed-huIgG protein.

3.5.2 Expression of TNFR2ed-huIgG and TNFR2ed-V5His-tagged proteins

DS-2 cells were transfected with pMT/Bip/V5-His (DesMTA) hygro plasmids for TNFR2ed-huIgG or TNFR2ed-V5His. 0.3 mg/mL hygromycine was used for selection and during the expansion of the successfully transfected cells. Protein expression was induced, supernatants were collected, and proteins were isolated as described in 2.2.3.10 and 2.2.3.11. After dialysis against PBS protein concentrations were adjusted to 1 mg/mL and serial dilutions were performed followed by the analysis using SDS page and Western blot. Figure 47 shows that the recombinant proteins had the predicted molecular weight of ~ 53.5 kDa for TNFR2ed-huIgG and ~ 30 kDa for TNFR2ed-V5His (A, B) and were successfully modified with the respective tag (C and D). Cross-reactivity of the used antibodies for huIgG and V5His was excluded.

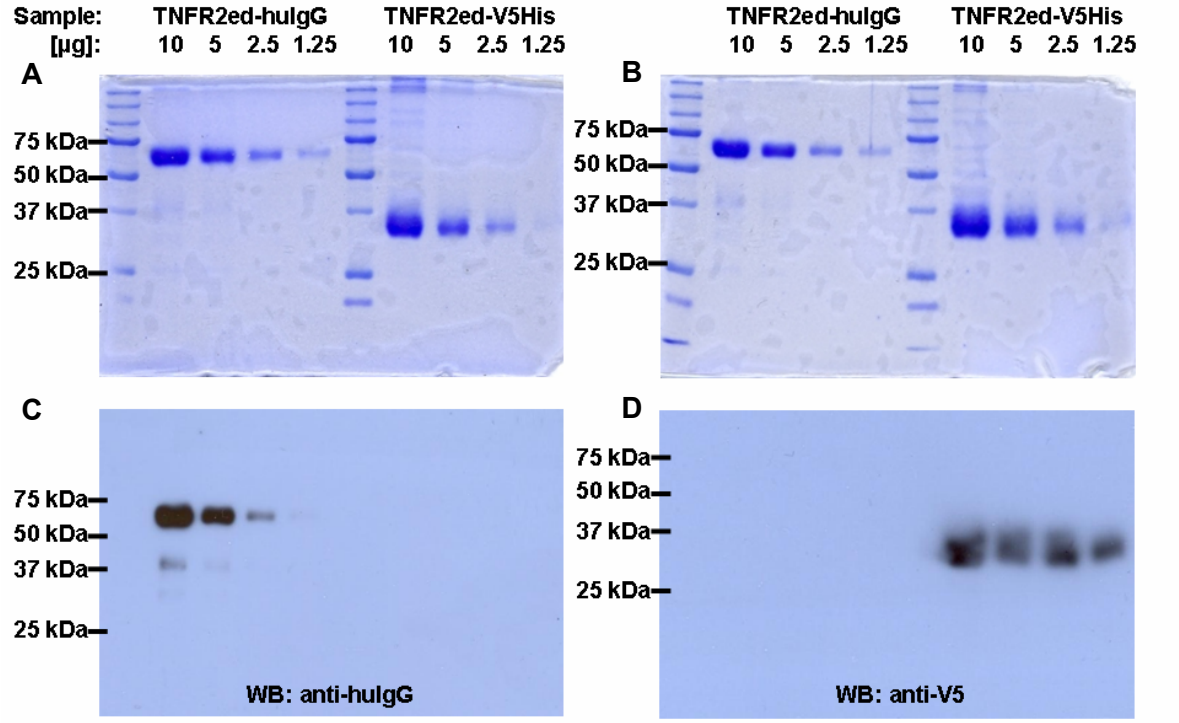

Figure 47: SDS page and Western blot of TNFR2ed proteins tagged with huIgG or V5His

SDS-PAGE was performed using 10, 5, 2.5, and 1.25 µg of recombinant TNFR2ed-huIgG and TNFR2ed-V5His per lane. A and B show the coomassie stained SDS gels used for Western blot (C, D). huIgG-tagged TNFR2ed was selectively detected in a Western blot with donkey anti-human IgG (H+L) HRP (C). V5His-tagged TNFR2 was exclusively detected when incubating the Western blot with the primary antibody anti-V5 mAB (mouse) and the secondary antibody goat anti-mouse IgG (whole molecule) POX.

3.5.3 Test for biological activity of TNFR2ed-huIgG / V5His constructs

Next, it was examined whether recombinant TNFR2ed proteins were functionally active. In this case preincubation of both TNFR2 constructs with TNF should reduce the biologically active TNF concentrations available for L-929^{m} cell kill as described in 2.2.3.8 and 2.2.3.9. Figure 48 shows that both TNFR2ed-huIgG and TNFR2ed-V5His were able to bind soluble TNF and effected protection in TNF dependent L-929^{m} cell cytotoxicity assay.

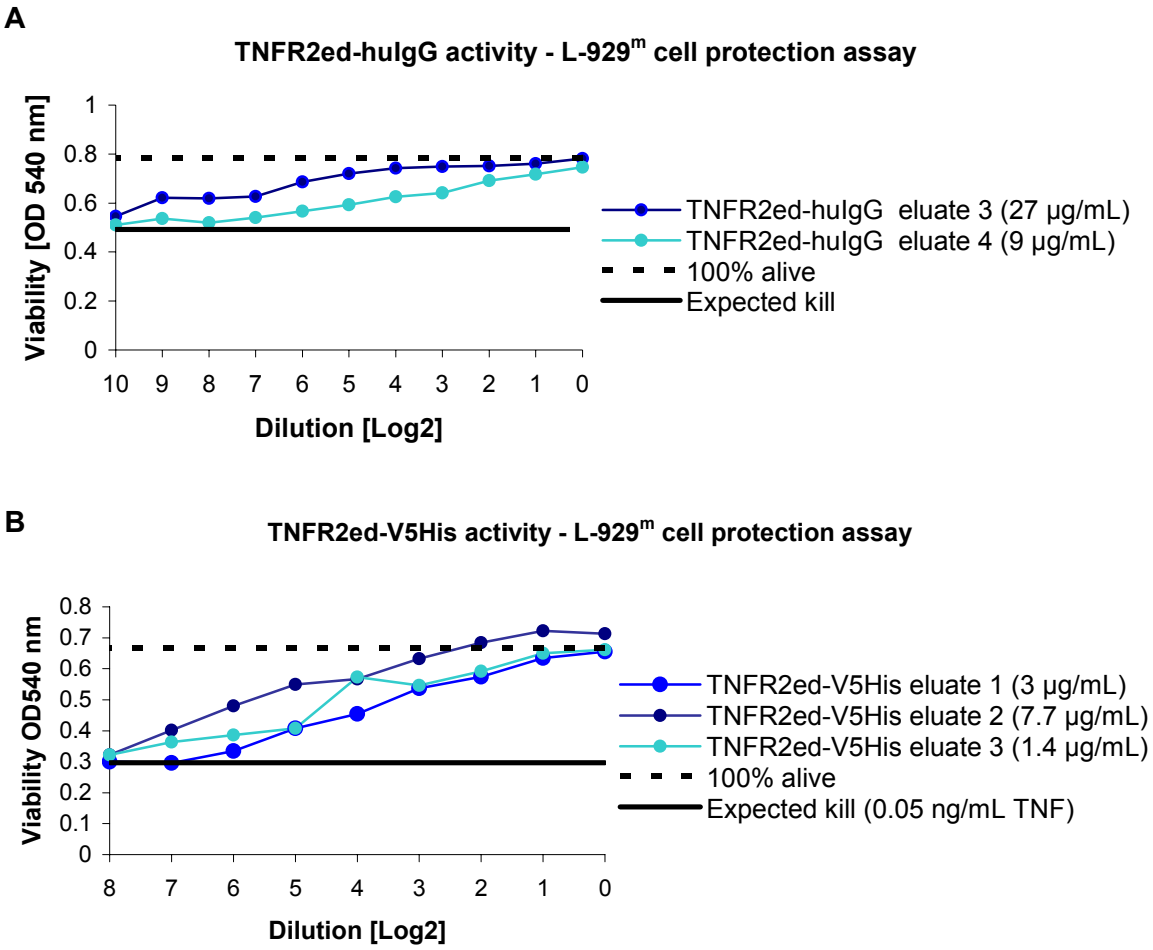

Figure 48: Test for biological activity of recombinant TNFR2ed proteins tagged with huIgG or V5His

Different fractions of sterile recombinant TNFR2ed-huIgG (fractions 3 and 4) (A) and TNFR2ed-V5His (fractions 1, 2, and 3) (B) eluates were diluted to the indicated concentrations in medium containing 0.05 ng/mL TNF and 2 µg/mL actinomycin D. After 2 h of incubation at 37 °C 200 µL of the respective solutions were transferred to L-929^{m} cells seeded for the TNF cytotoxicity assay the day before. After 24 h the viability of the differentially treated cells was measured using MTT assay. Cells treated with neither TNFR2ed nor TNF were used as 100% alive controls as well as cells treated only with TNF for TNF-induced kill. Shown are single values

3.5.4 Immunization of TNFR2$^{-/-}$ mice and test of serum titer

TNFR2$^{-/-}$ mice (0, L, R) were immunized with TNFR2ed-V5His according to the protocol listed in 2.5.2. The immunized mice developed considerable levels of anti-TNFR2ed IgG titers as shown in Figure 49.

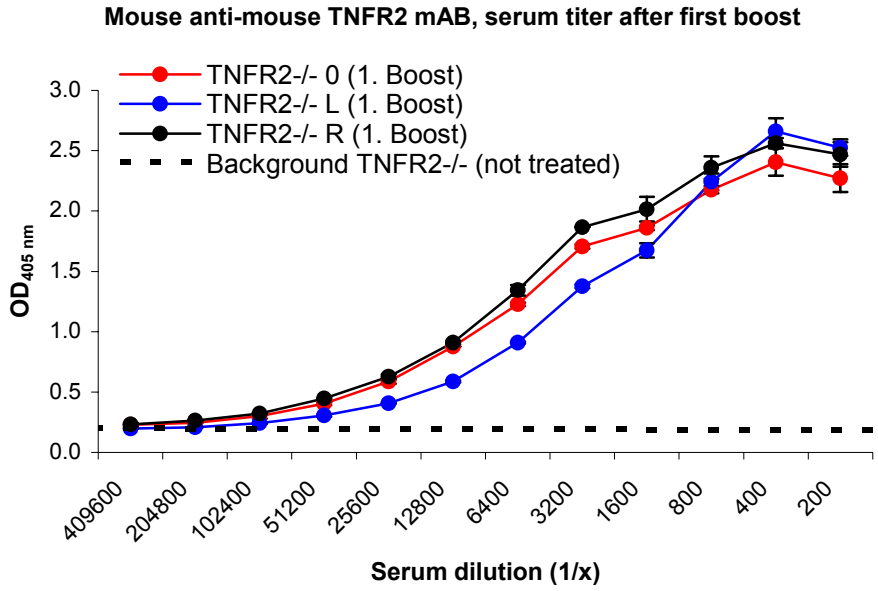

Figure 49: Serum levels of mouse anti-mouse TNFR2 antibodies after the first boost
Three days after the first boost blood was taken from the immunized mice and serum was prepared. Serum levels of mouse anti-mouse TNFR2 antibodies IgG (γ-chain specific) were determined using ELISA. Shown are the mean ± SD of three technical replicates.

3.5.5 Fusion and characterization of mouse anti-mouse TNFR2 mAB

3.5.5.1 Fusion

Two days after the second boost spleen cells were fused with SP2/0-Ag14 cells as described in 2.5.3. Ten days after the fusion about 90% of the wells contained viable hybridoma clones. The supernatants of all wells from 20 96-well microtiter plates were checked for binding TNFR2ed-huIgG using ELISA. 14 clones were defined as positive as OD values exceeded the background OD more than 3-fold the standard deviation of the background. By the following intense testing and subcloning 5 hybridoma clones expressing monoclonal antibodies were identified and expanded for the generation of large amounts of supernatant. Antibodies were either tested using the supernatants or protein G purified fractions.

3.5.5.2 ELISA

Supernatants of five hybridoma cultures were identified to bind to TNFR2ed-huIgG and hybridomas were named II D12, II G11, XIII A4, XVIII A9, XIX H10. In addition, in some test systems clone DJ2008 generated in cooperation with Diana Minge was tested, too. Figure 50 shows that supernatants of the hybridomas contained high amounts of mouse anti-mouse TNFR2 mAB IgG. After purification on protein G columns high OD values could be reached only by application of high concentrations of the respective antibody and, hence, titers were low. This is illustrated in Figure 50.

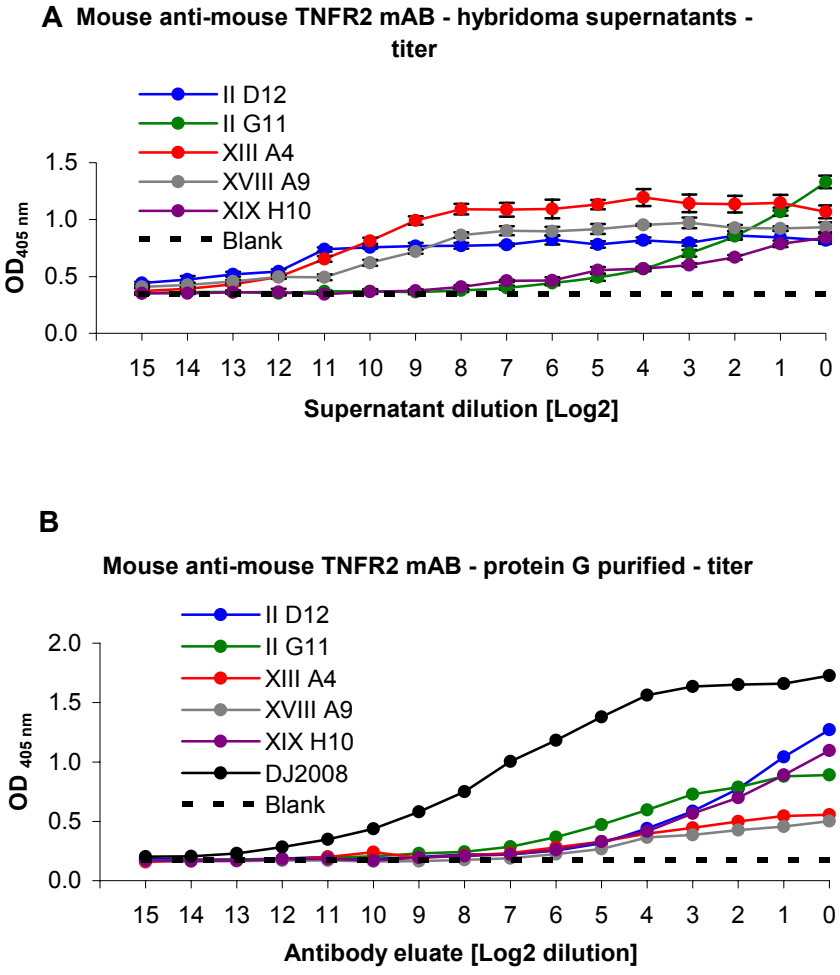

Figure 50: Titer test of mouse anti-mouse TNFR2 mAB – hybridoma supernatants and Protein G purified mAB

A titer test was performed employing ELISA and log2 dilutions of the hybridoma supernatants (A) or of protein G purified antibodies starting with 100 µg/mL (B). Detection was performed using goat anti-mouse IgG (γ-chain specific) AP. Shown are the mean ± SD of three technical replicates (A) and single values (B).

3.5.5.3 Isotype test

As the ELISA detection system for mouse anti-mouse TNFR2 clones was γ-chain specific, only IgG antibodies were detected. The isotypes of the 6 generated mouse anti-mouse TNFR2 mAB were tested using IsoGold rapid mouse-monoclonal isotyping kit™ and either supernatant or eluate as substrate. All clones were found to be of the IgG1 isotype.

3.5.5.4 SDS-PAGE

Mouse anti-mouse TNFR2 mAB were purified from about 1 L supernatant of the monoclonal hybridoma cultures using protein G as described in 2.2.3.12. Eluate fractions were analyzed in SDS-PAGE, in order to evaluate the content of protein. Figure 51 exemplarily shows the SDS-gel of the hybridoma clone XIII A4. According to the strength of the antibody bands, different eluate fractions were pooled followed by dialysis against PBS and determination of the protein content using the BCA-kit.

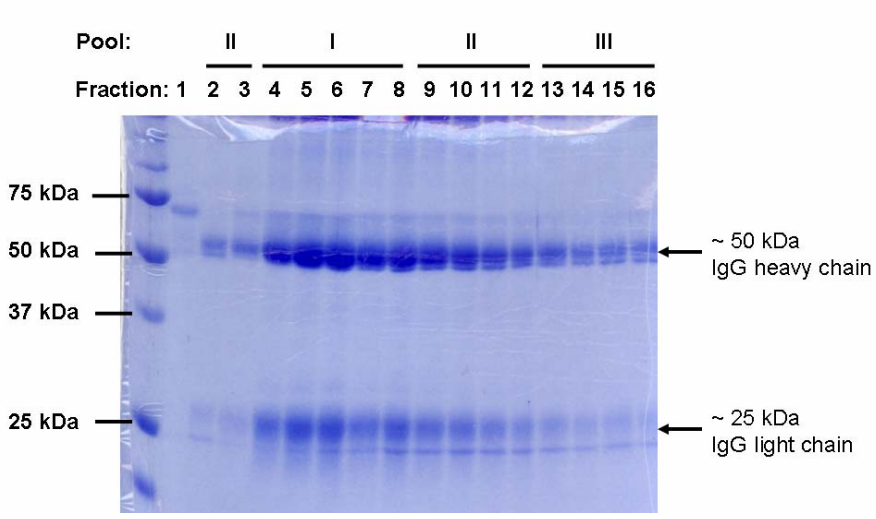

Figure 51: SDS-PAGE analysis of the antibody content in different fractions of protein G eluates
10 µL of the eluate fractions (1 – 16) were analyzed by SDS-PAGE for their protein content and combined in three pools for dialysis against PBS and determination of the absolute protein concentration.

3.5.5.5 Western blot

The protein G purified mouse anti-mouse TNFR2 mAB were tested for staining in Western blot analysis. Figure 52 shows that all newly generated mAB detected both TNFR2ed-huIgG and TNFR2ed-V5His. Thus, cross-reactivity with the V5His tag used for immunization of the mice could be excluded.

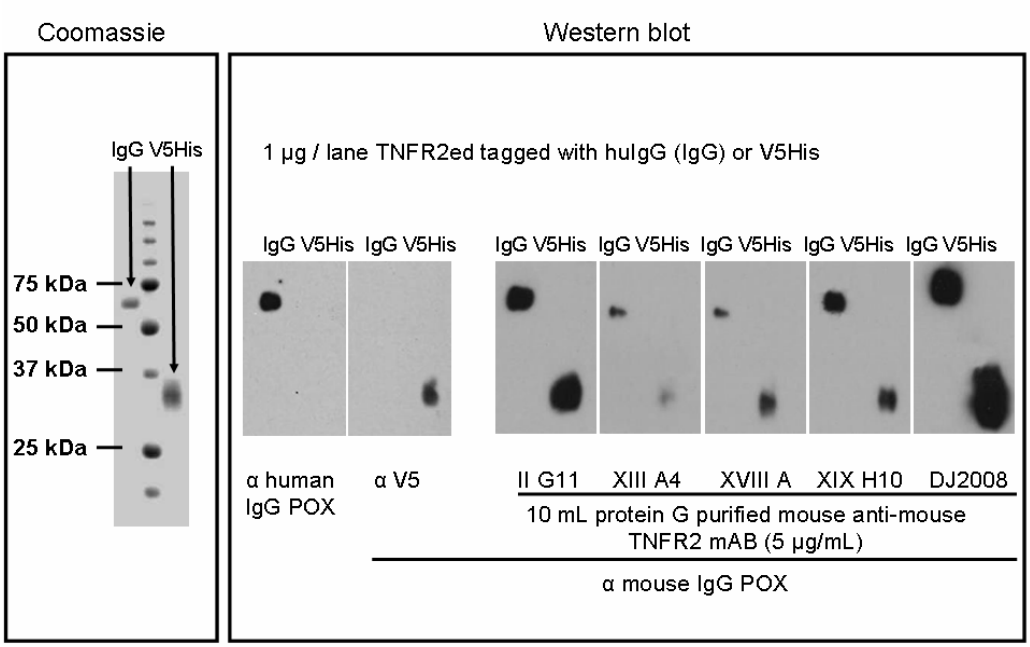

Figure 52: Performance of mouse anti-mouse TNFR2 mAB in Western blot analysis

1 µg of TNFR2ed-huIgG and TNFR2ed-V5His were loaded on several SDS gels and run on SDS-PAGE. One SDS gel was directly stained with coomassie whereas the other gels were used for Western blot. Western blot membranes were incubated with 10 mL 5 µg/mL mouse anti-mouse mAB in TBS containing 1% skimmed milk powder each over night. Several washes were performed followed by the incubation step with the secondary antibody anti-mouse IgG POX. Following several wash steps bound antibodies were analyzed using chemiluminescence. As control one membrane was incubated with anti-human IgG POX. Another control membrane was incubated with anti-V5 antibody (mouse) followed by the secondary antibody anti-mouse IgG POX.

3.5.5.6 Flow cytometry

CHO cells were transfected with pcDNA3.1 plasmid designed for the expression of mouse TNFR2 as described in 2.1.9. Performance of mouse anti-mouse TNFR2 mAB in flow cytometry was examined using wt CHO cells and CHO cells expressing mouse TNFR2 (TNFR2tg). As shown in Figure 53, 44.7% of the transfected cells were positive for commercially available TNFR2 staining mAB AF647.

The cells were incubated with the supernatants of the mouse anti-mouse TNFR2 mAB hybridomas followed by incubation with FITC labeled anti-mouse IgG AB. Clone XVIII A9 showed weak binding to the receptor expressed on the cell membrane (2.2%). Clone XIX H10 detected 10.1% of the cells as positive for TNFR2. Cross-reactivity or unspecific binding of the supernatants to the cells could be excluded as CHO wt cells exhibited almost no signal neither

using commercially available anti-TNFR2 AF647 mAB nor the supernatants of the mouse anti-mouse TNFR2 mAB hybridomas.

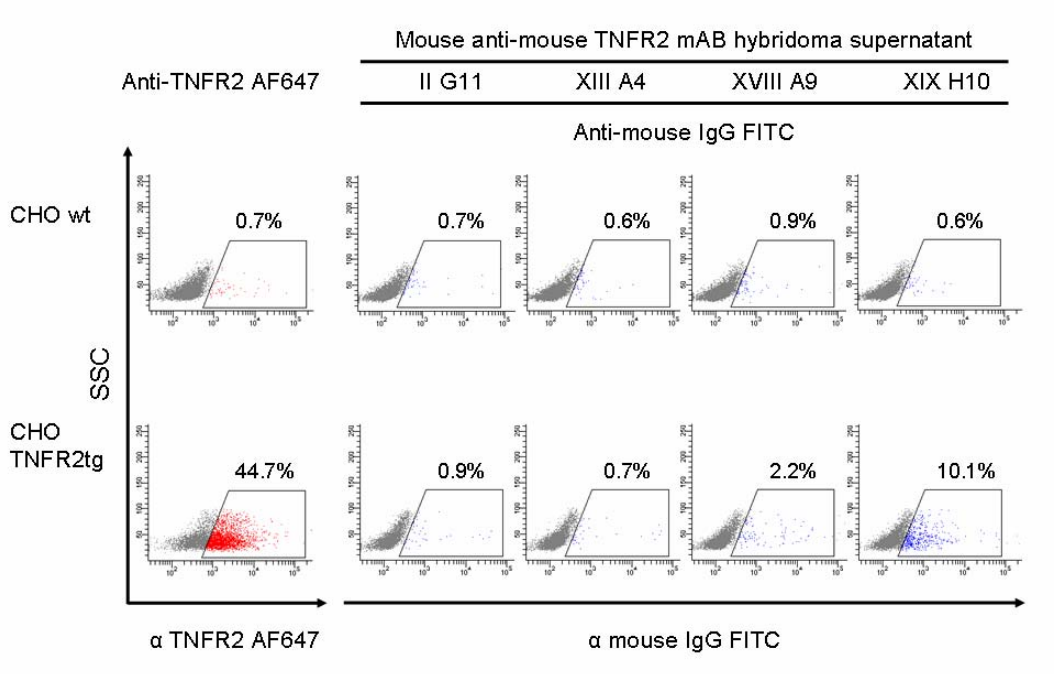

Figure 53: Performance of mouse anti-mouse TNFR2 mAB in flow cytometry

Both CHO wt and CHO cells tranfected with mouse TNFR2 were used. Cells were removed from the tissue flasks. 5 x 10^5 cells were stained with the commercially available anti-TNFR2 AF647 mAB as control for successful binding to the recombinant protein. Cells were stained with 2 mL supernatant of the newly generated mouse anti-mouse TNFR2 mAB hybridomas for 30 min. Cells were washed with FACS buffer and stained with the secondary antibody anti-mouse IgG FITC for 30 min. After another wash with FACS buffer the cells were analyzed using flow cytometry.

3.5.5.7 Transduction of Wirbel cells with TNFR1/2ed-huFasid

Wirbel cells were retrovirally transduced with pQCXIP plasmids expressing TNFR1ed-huFasid and TNFR2ed-huFasid obtained from Dr. Wulf Schneider. In brief, TNFR1ed and TNFR2ed, respectively, were cloned into the vector using the Bam and EcoRV restriction enzymes. The intracellular portion of human Fas was inserted using EcoRV and Xho restriction sites. Cells were grown in medium supplemented with 1.5 µg/mL puromycine for the selection. Transfection efficiencies were determined using flow cytometry as shown in Figure 54. 13.1% of TNFR1ed-huFasid and 71.4% of TNFR2ed-huFasid transduced cells were positive for the respective receptor.

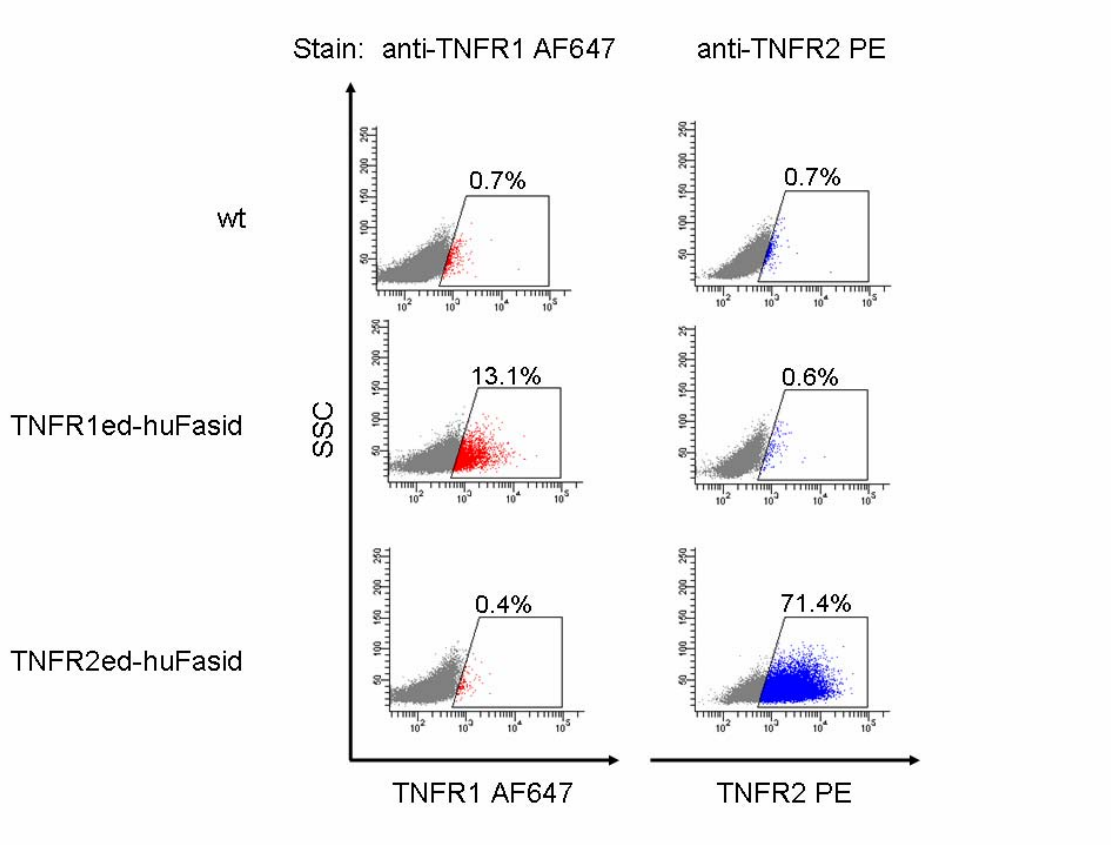

Figure 54: Expression analysis of TNFR1ed and TNFR2ed fused to human Fasid in retrovirally transduced Wirbel cells

Wirbel wt cells and TNFR1ed-huFasid as well as TNFR2ed-huFasid cells were grown and stained with anti-TNFR1 APC or anti-TNFR2 PE, respectively. The expressions of the recombinant proteins were analyzed using flow cytometry.

The sensibilities of TNFR1ed-huFasid and TNFR2ed-huFasid transduced cells for mouse and human TNF were examined. Results are shown in Figure 55. Wt Wirbel cells were not influenced by human and mouse TNF. TNFR1ed-huFasid expressing cells were highly susceptible to both types of TNF. TNFR2ed-huFasid expressing could only be killed by mouse TNF. The induction of apoptosis was less pronounced and only apparent in the presence of high concentrations of mouse TNF.

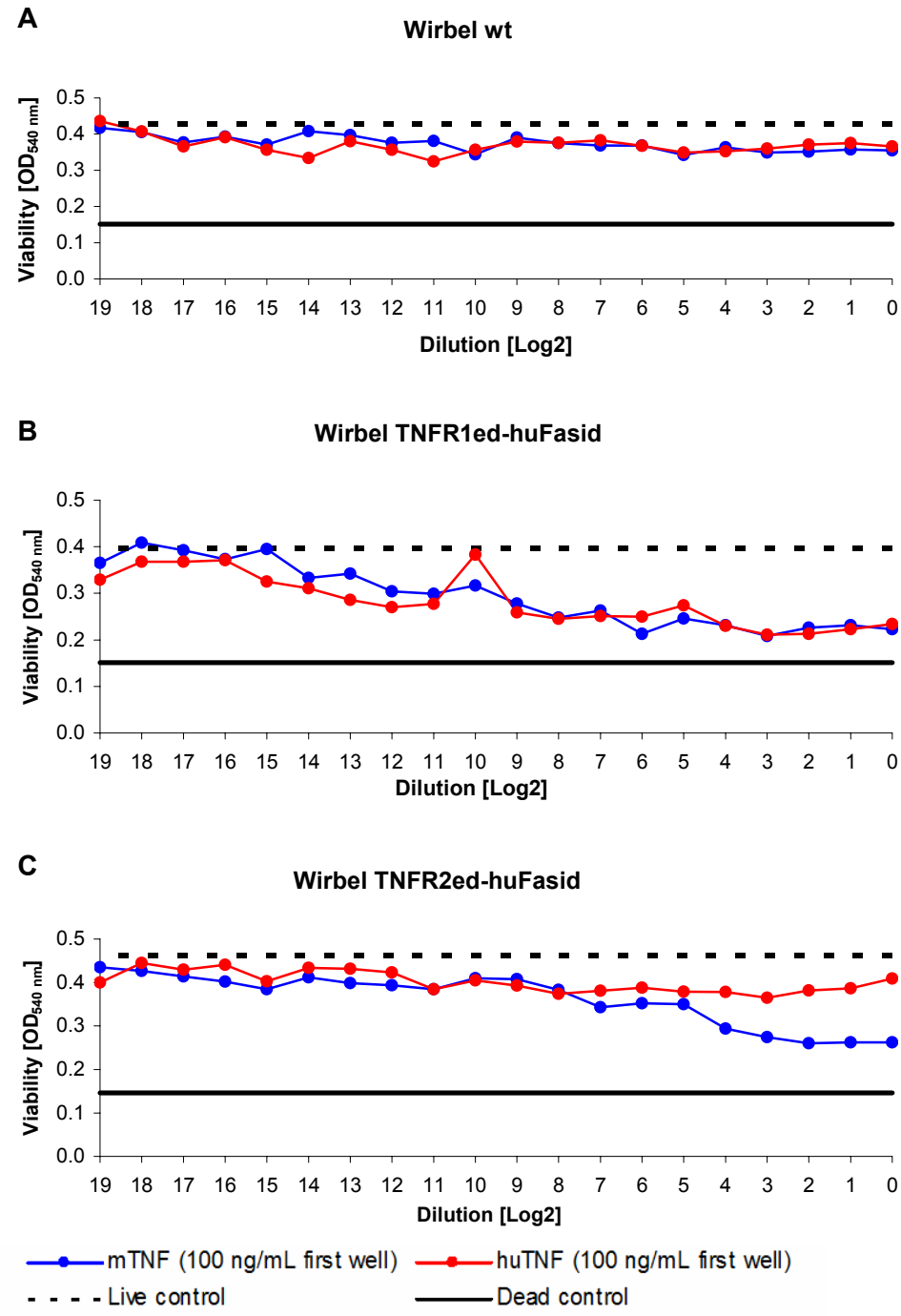

Figure 55: Cytotoxicity assay on TNFR1ed- and TNFR2ed-huFasid transduced Wirbel cells – mouse and human TNF

Wirbel cells (2 x 10^4) were seeded in 100 µL per well of 96-well plates. After 24 h supernatants were discarded and cells were treated with serial dilutions of mouse and human TNF starting with 100 µg/mL in 200 µL medium containing 2 µg/mL actinomycin D. After 24 h MTT assays were performed for viability analysis. Viabilities of Wirbel wt (A), TNFR1ed-huFasid expressing cells (B), and TNFR2ed-huFasid expressing cells (C) are shown. Dots represent single values.

3.5.5.8 Test for agonistic properties

Wirbel cells expressing TNFR2ed-huFasid were used to test for agonistic properties of the newly generated mouse anti-mouse TNFR2 mAB. In brief, mAB dependent induction of apoptosis was examined as shown in Figure 56. Apoptosis could neither be induced in TNFR2ed-huFasid expressing Wirbel cells nor in the control experiments using Wirbel wt and Wirbel cells transduced with TNFR1ed-huFasid.

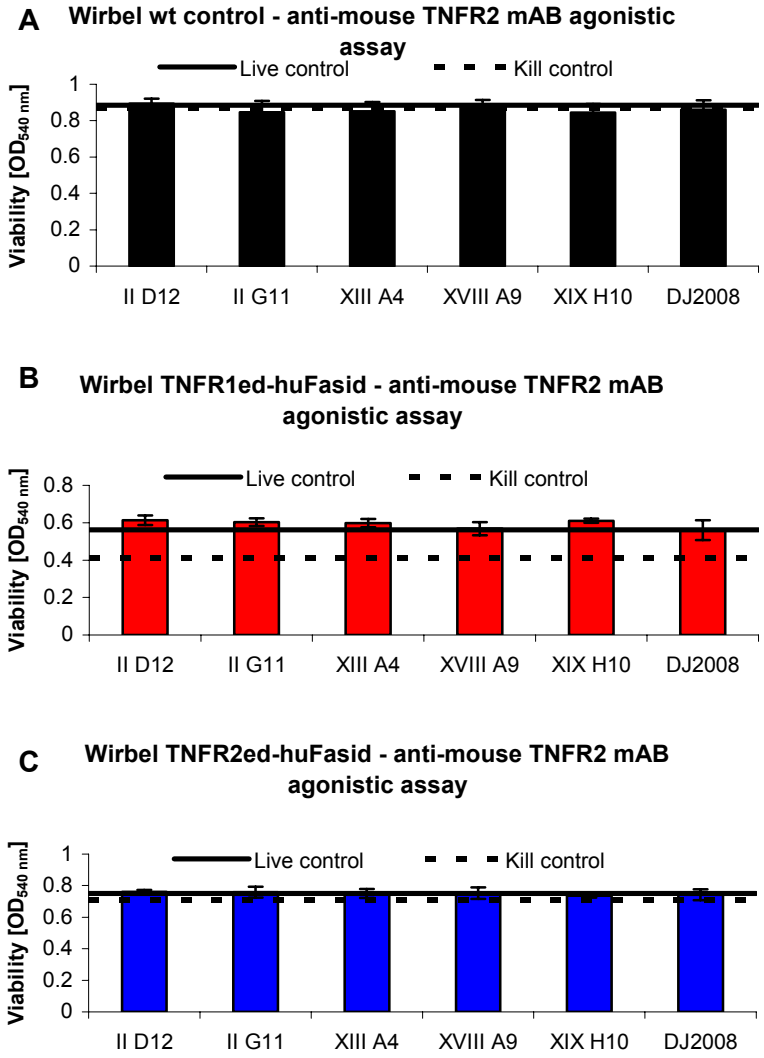

Figure 56: Mouse anti-mouse TNFR2 mAB test for agonistic activity

Wt Wirbel cells (A) and Wirbel cells transduced with TNFR1ed-huFasid (B) or TNFR2ed-huFasid (C) were seeded in medium (2 x 10^4 cells / 96-well) and treated after 24 h with 200 µL 25 µg/mL mouse anti-mouse mAB in medium supplemented with 2 µg/mL actinomycin D. Cells were incubated for 24 h before assessment of the cell viability employing MTT. Control cells were not treated with mAB and either incubated in pure medium (live control) or in medium containing 25 ng/mL mouse TNF (kill control). Shown are the mean values ± SD of three technical replicates per group.

3.5.5.9 Test for antagonistic properties

Wirbel cells expressing TNFR2ed-huFasid were used to test for antagonistic properties of the newly generated mouse anti-mouse TNFR2 mAB. In brief, cells were preincubated with TNFR2 mAB before TNF challenge. Data are shown in Figure 57.

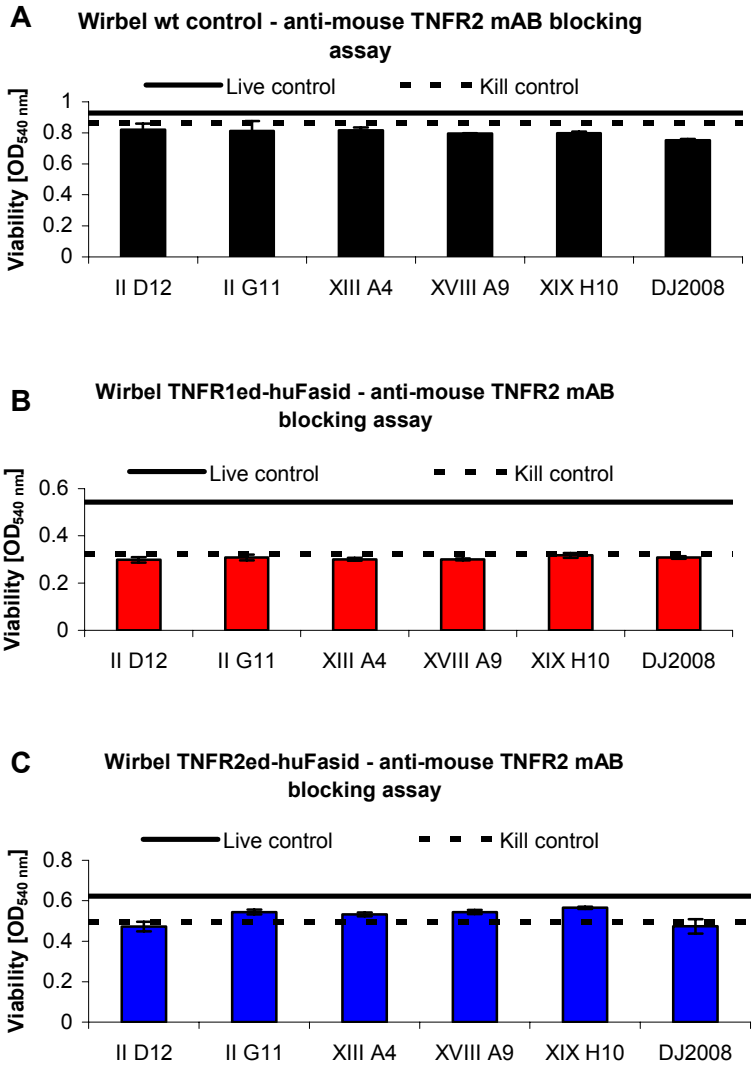

Figure 57: Mouse anti-mouse TNFR2 mAB test for antagonistic activity

Wirbel cells (2 x 10^4) both wt (A), transduced with TNFR1ed-huFasid (B), or TNFR2ed-huFasid (C) were seeded in medium and pretreated after 24 h with 100 µL 50 µg/mL mouse anti-mouse TNFR2 mAB in medium. 6 h later cells were challenged with 100 µL 50 ng/mL mouse TNF in medium supplemented with 4 µg/mL actinomycin D. Cells were incubated in the resulting 200 µL medium containing 25 µg/mL mAB and 25 ng/mL mouse TNF and 2 µg/mL actinomycin D for 24 h before assessment of the cell viability employing MTT. Control cells were not treated with mAB and either incubated in pure medium (live control) or in medium containing TNF (kill control). Shown are the mean values ± SD of three technical replicates per group.

As expected, Wirbel wt control cells could not be killed. Antagonistic cross-reactivity with TNFR1ed-huFasid could be excluded as well. Marginal protection from TNF-induced apoptosis could be reached by the treatment of TNFR2ed-huFasid transduced Wirbel cells with the mouse anti-mouse TNFR2 mAB clones II G11, XIII A4, XVIII A9, and XIX H10. However, the grade of induced apoptosis using mouse TNF was very faint for TNFR2ed-huFasid transduced cells and, thus, significant evidence for TNFR2 blocking properties of the six candidate mAB could not be achieved. Therefore, TNC-mTNF mutant TNF (Prof Wajant) was used as positive control. Figure 58 shows that this recombinant TNF mutant induces a strong kill in TNFR2ed-huFasid expressing cells indicating high affinity to TNFR2. Pretreatment of the TNFR2ed-huFasid transduced cells with mouse anti-mouse TNFR2 mAB did not reduce the induced kill indicating no antagonistic properties of these mAB.

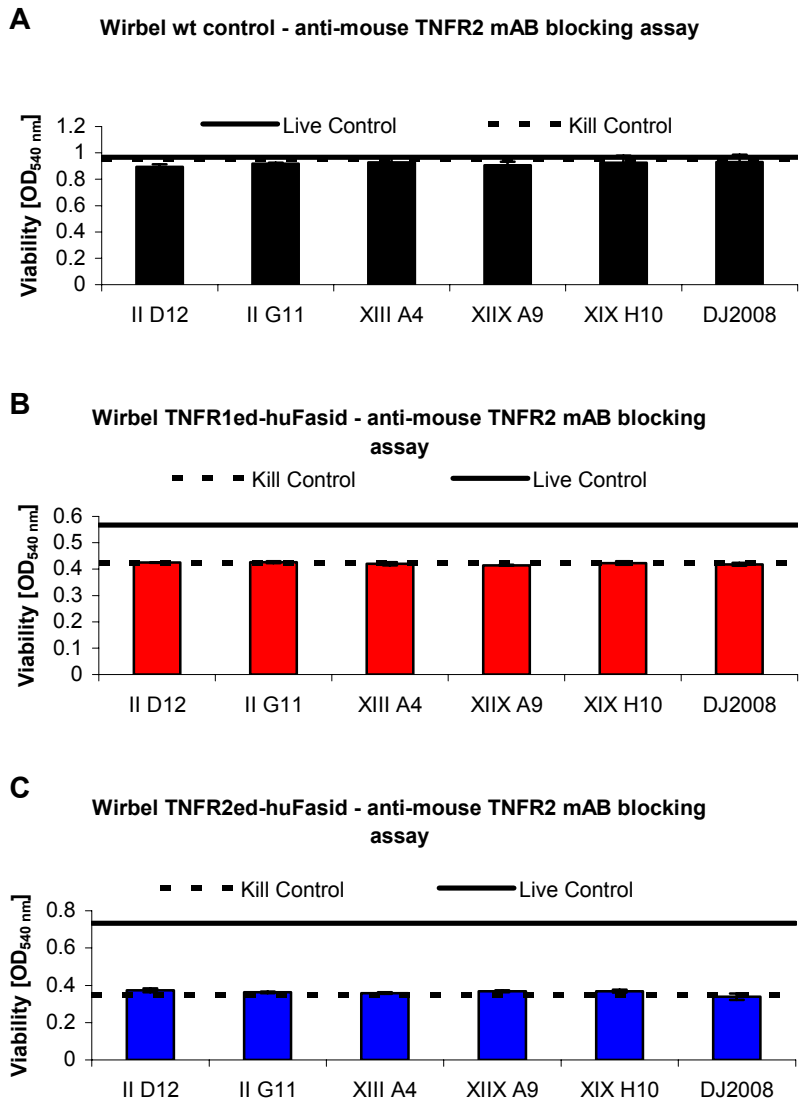

Figure 58: Mouse anti-mouse TNFR2 mAB test for antagonistic activity using TNC-mTNF

Wirbel cells (2 x 10^4) both wt (A), transduced with TNFR1ed-huFasid (B), or TNFR2ed-huFasid (C) were testet according to the experimental setup described in the legend of Figure 57. The kill was induced with 50 ng/mL TNC-mTNF mutant. Shown are the mean values ± SD of three technical replicates per group.

4 Discussion

Severe sepsis, septic shock, and immunosuppression represent some of the most serious pathologies causing morbidity and mortality in intensive care. During the last few years the trend of their incidences has increased as a consequence of the rising life expectancy of the population, especially in the western civilization (Angus, Linde-Zwirble et al. 2001; Martin, Mannino et al. 2003).

Therefore, great efforts are being made in basic sepsis research aiming at the development of new drugs and therapeutical strategies, in order to reduce multi-organ failure and to make the immune system more apt to react adequately to secondary infections.

This thesis is based on the findings of Dr. Theo Sterns that TNFR2$^{-/-}$ mice are protected from lethal effects of secondary infections in the phase of immunoparalysis after CLP (Sterns, Pollak et al. 2005). Therefore, either the TNFR2-signaling on specific cells, reverse signaling of TNFR2 to membrane-bound TNF, or the TNF-neutralizing functions of soluble TNFR2 leading to diminished TNFR1-signaling must be the reasons for the severe pathology of secondary infections in CLP-treated wildtype mice. It has to be taken into consideration that either direct signaling during sepsis could be causal for the protection of TNFR2$^{-/-}$ mice or that this effect could be caused by changes in the immune system that occurred earlier in the life of the animals. The latter comprises epigenetic changes caused by the three possible modes of TNFR2 action discussed above as well as continuous low dose TNF-signaling via TNFR1 in TNFR2$^{-/-}$ mice due to the lack of antagonizing soluble TNFR2. The lack of TNF-neutralizing soluble TNFR2 could lead to TNF tolerance and could be the reason for the findings of Dr. Theo Sterns. These hypothetical causes are discussed in the following chapters based on the novel findings of this work.

4.1 Characterization of CD11b^{+} cells of TNFR2$^{-/-}$ mice

4.1.1 Splenocytes in the animal model of CLP

Initially, the phenotypcial and functional status of splenocytes, especially CD11b^{+} CD11c^{-} cells and MDSC, was investigated after CLP and compared between wildtype and TNFR2$^{-/-}$ mice. It is known that numbers and percentages of mature DC and CD4 T cells are reduced one day after CLP (Hotchkiss and Karl 2003; Ding, Chung et al. 2004). The total numbers of splenocytes that could be recovered were slightly reduced in mice on day 1 and 2 after CLP. This effect was overcome on day 4 as splenomegaly started to develop. On day 11 after CLP the weight of the

spleens and the yield of cells exceeded the naïve levels up to 10-fold (data not shown). Figure 9 and Figure 14 show that the percentages of $CD11b^+$ $CD11c^-$ cells were not drastically influenced by CLP within the first 2 days and, starting on day 4, went up to 5% on day 11. The content of MDSC within the $CD11c^+$ splenocyte population was drastically reduced 6 h, 10 h, and 1 day after CLP. This loss was compensated on day 2. From then on, MDSC proportions in the spleen rose until day 11 after CLP. This phenomenon has already been published earlier (Delano, Scumpia et al. 2007). The loss of cells in the $CD11b^+$ $CD11c^-$ population is comparable to the the loss in absolute numbers of splenocytes while the contribution of $CD11b^+$ cells to the splenomegaly is slightly increased. MDSC, however, are more than proportionally affected by cell loss immediately after CLP and contribute overproportionally to the splenomegaly in particular. Differences between wildtype and $TNFR2^{-/-}$ mice could not be revealed. As shown in Figure 16, MDSC were the source of NO in LPS and IFN-γ stimulated $CD11b^+$ splenocytes from CLP-treated mice. $TNFR2^{-/-}$ splenic MDSC produced significantly reduced levels of NO. These data, in combination with Figure 10, demonstrate that a previous CLP is required for NO production upon stimulation with LPS and IFN-γ

4.1.2 Functional characterization of MDSC

As already described, the relative proportion of MDSC in the splenocytes of $TNFR2^{-/-}$ mice was not impaired compared to wt mice but the capacity to express iNOS mRNA and to produce NO was reduced (Figure 11). In BMDC differentiation cultures on day 4 it was the MDSC population as well that produced the majority of NO upon stimulation with LPS and IFN-γ. While differences in the absolute NO concentration in the supernatants after 48 h were not detected, significantly reduced iNOS mRNA expression after stimulation for 6 h was found (Figure 21). As shown in Figure 19, almost no MDSC were found in BMDC cultures on day 10 when almost all cells were DC as they expressed CD11c. The questions, which cell type produces NO in BMDC upon stimulation on day 10, could not be answered in this work. Both Ly6C and Ly6G were downregulated during BMDC differentiation. The two distinct populations of MDSC ($Ly6C^+$ $Ly6G^-$) and PMN ($Ly6C^{int}$ $Ly6G^+$) merged in the FACS profile. Nevertheless, as shown in Figure 19, the percentages of MDSC in $TNFR2^{-/-}$ BMDC on day 10 were still significantly decreased. Assuming this population being the most potent source of NO, the differences between $TNFR2^{-/-}$ and wt BMDC in terms of NO production could be explained by the cell numbers of MDSC. However, it is unlikely that the few cells of the not well defined MDSC population on day 10 exclusively produced NO thereby contributing to the difference between wildtype and $TNFR2^{-/-}$ BMDC.

On day 6 TNFR2$^{-/-}$ BMDC expressed slightly decreased Arg1 mRNA (Figure 22). This effect was not due to the different proportion of MDSC in the cultures as purified and cell number adjusted MDSC on day 4 also expressed slightly reduced Arg1 mRNA levels. Since Arg1 expression is the most prominent marker for the activity of MDSC, a decreased capacity for Arg1 expression of TNFR2$^{-/-}$ MDSC can be assumed.

4.1.3 iNOS mRNA expression and NO production

As shown in chapter 3.1.1, iNOS mRNA expression and NO production were impaired in CD11b^{+} CD11c^{-} splenocytes of TNFR2$^{-/-}$ mice 2 days after CLP compared to wildtype mice. CLP was required for iNOS mRNA expression and NO production. The differences between wildtype and TNFR2$^{-/-}$ splenocytes can be assigned to the MDSC population (see 3.2.1.2) in terms of iNOS mRNA expression and NO production. The fact that only MDSC of CLP-treated mice were able to express iNOS mRNA and to produce NO leads to two different possibilities: either new cells immigrate to the spleen or other cells differentiate *in situ* into the MDSC phenotype as a consequence of the CLP treatment.

Myeloid cells derived from other sources were examined for these parameters, too. As shown in Figure 12 and Figure 13, PEC and BMDC of TNFR2$^{-/-}$ mice featured exactly the same phenotype of reduced iNOS mRNA expression and NO production even in naïve mice. As a result of this finding BMDC were used for further investigation of the underlying causes for this phenotype and its physiological role.

NO is thought to be one of the main mediators in severe sepsis. There are several functions of NO inducing both systemic and cellular reactions. Three different nitric oxide synthetases are known: neuronal NOS (nNOS) derived NO acts as a neurotransmitter and a hormone and is expressed in 2% of cerebral cortical neurons as well as in dendrites and axons (Snyder and Bredt 1991). Epithelial NOS (eNOS) derived NO regulates the vascular tone and plays a critical role in the regulation of blood pressure and supply (Kirkeboen, Naess et al. 1992). iNOS derived NO mediates the non-specific cytotoxicity against bacteria, protozoa, and tumor cells. iNOS mRNA expression and NO production are increased in smooth muscle cells, in macrophages as well as parenchymal cells during septic shock as a consequence of high concentrations of bacterial components like LPS or cytokines such as IL-1β, IL-2, IL-6, TNF, and IFN-γ (Kirkeboen and Strand 1999). NO concentrations in the plasma of septic mice are drastically increased (Nathan and Xie 1994; Lush, Cepinskas et al. 2001). Anti-inflammatory cytokines like IL-4, IL-8, IL-10, and TGF-β, which are produced among others by T_H2 cells, are known to diminish the NO production capacity of certain cells (Nussler and Billiar 1993).

As TNFR2$^{-/-}$ myeloid cells produce less NO, these reduced levels could protect the mice from vasodilation as well as tissue and organ damage. A less hazardous effect on the organism caused by NO could be the reason for the protection of TNFR2$^{-/-}$ mice from a secondary infection. In this case CLP would not affect the vital functions to the extent compared to wildtype mice. However, in contrast to this, TNFR2$^{-/-}$ mice do not exhibit improved survival after CLP (Ebach, Riehl et al. 2005).

When iNOS mRNA is expressed in myeloid cells, they persistently produce large amounts of NO (Morris and Billiar 1994). More recently, it was discovered that parenchymal cells are responsible for large amounts of systemic NO during sepsis, too (Bultinck, Sips et al. 2006). This occurs particularly in the intestines of CLP-treated mice. Under hypoxic and acidic conditions nitrite can be reduced to the vasodilating NO and serves as an important vascular storage compound for NO (Lundberg and Weitzberg 2005). The various origins of NO question the influence of iNOS-derived NO in animal models of septic shock. Specific iNOS inhibition in CLP-treated mice generated divergent outcomes. Contrary to non-specific NO inhibition, specific iNOS inhibitors did not cause hazardous effects and sometimes even protected the animals from multi-organ failure or death. Contrary to this, iNOS-deficient mice were not protected against endotoxemia, sepsis, or TNF-induced shock but showed increased mortality (Cobb, Hotchkiss et al. 1999). Anti-apoptotic and anti-oxidative properties of iNOS-derived NO could be causal for this protective effect (Li and Wogan 2005; Cauwels and Brouckaert 2007) as it has been reported that NO protects from lipid peroxidation (Rubbo, Radi et al. 1994).

All these data suggest a very complex system of NO functions causing both deleterious and protective effects. The consequences of NO exposure depend on the concentration, the physiological conditions of the organism, and the timing. However, TNFR2$^{-/-}$ systems do not exhibit absolute abrogation of iNOS induced NO and this reduced NO production could be the reason for protection in secondary infections. There could be levels of NO sufficient to induce the positive effects of this low molecular weight mediator but not high enough to cause severe multi-organ damage or extreme vasodilation. Besides, reduced NO production saves the L-arginine amounts and, hence, could protect T cells from shortage of this important amoni acid. This reduced NO production of TNFR2$^{-/-}$ mice could balance the effects of MDSC and, as a result, could save TNFR2$^{-/-}$ mice from unresponsiveness to secondary infections during CLP-induced immunosuppression.

4.1.4 Characterization of BMDC

Bone marrow is the source of precursor cells for BMDC. Therefore, bone marrow cells from wildtype and TNFR2$^{-/-}$ mice were analyzed directly after preparation for the expression of CD11b, Ly6C, and Ly6G. As shown in Figure 17, the percentages of CD11b^{+} cells in TNFR2$^{-/-}$ bone marrow were significantly increased. MDSC (CD11b^{+} Ly6C^{+} Ly6G^{-}) and PMN (CD11b^{+} Ly6C^{int} Ly6G^{+}) bone marrow cells of TNFR2$^{-/-}$ mice were statistically increased compared to wildtype controls, too. Interestingly, the relative proportions of MDSC and PMN bone marrow cells of TNFR2$^{-/-}$ mice were not impaired in the CD11b^{+} cell population.

BMDC were used as a cellular model for the TNFR2$^{-/-}$ CD11b^{+} cellular phenotype that has been seen in different myeloid cells and especially in splenic MDSC after CLP. Additionally to the NO deficit upon stimulation with LPS and IFN-γ, other parameters were also analyzed. Non-stimulated naïve BMDC featured four main phenotypes.

First: TNFR2$^{-/-}$ BMDC cultures yield reduced cell numbers compared to the wildtype control cultures on day 8 and 10 suggesting either reduced proliferation or increased apoptosis (Figure 23). Kinetics revealed that early in the differentiation towards BMDC, the TNFR2$^{-/-}$ cultures contained even more cells compared to the wildtype control. Staining for apoptosis (Annexin V) and necrosis (7-AAD) (Figure 26) indicated that the percentages of dying cells ranged between 3.5% and 4.5% on day 10 equally in both cultures. Interestingly, TNFR2$^{-/-}$ BMDC showed reduced proliferation (Figure 25). 24 h of incubation with BrdU from day 9 until day 10 revealed a proliferation of 10% in TNFR2$^{-/-}$ BMDC cultures compared to 15% in the wildtype control. In order to reach statistical significance, further experiments need to be performed. Another hint for the hypothesis that TNFR2 is delivering proliferation signals is the finding that TNFR1$^{-/-}$ BMDC showed significantly increased proliferation as only TNFR2 is available for TNF-signaling in these cultures (data not shown). There are several reports that support this conclusion besides the finding that total cell yields in TNFR2$^{-/-}$ BMDC cultures are reduced. TNFR1$^{-/-}$ BMDC have been shown to be long-living (Funk, Walczak et al. 2000). The conclusion would be that TNFR2-signaling is necessary for proliferation and delivers a survival signal. There are several reports on this phenomenon for cytotoxic T cell proliferation, too (Brown and Thiele 2000; Brown, Lee et al. 2002). This fact might be confirmed by the finding that TNFR2$^{-/-}$ mice had reduced spleen weights and reduced total numbers of splenocytes (unpublished data). This phenomenon could not be ascribed to a certain cell type as it equally affected CD4 and CD8 T cells, B cells, macrophages, and dendritic cells. Another possible reason for the reduced cell yields in TNFR2$^{-/-}$ BMDC cultures could be induction of apoptosis via increased levels of biologically active TNF in TNFR2$^{-/-}$ BMDC cultures as the TNF antagonist soluble TNFR2 is missing (Figure 27 and Figure 28). Whether missing TNFR2-signaling, reverse signaling, or

higher concentrations of biologically active TNF is causal for the reduced BMDC yield in TNFR2$^{-/-}$ cultures, will be elucidated later.

Second: the percentages of mature DC expressing CD80, CD86, and MHCII were significantly increased in TNFR2$^{-/-}$ BMDC cultures as shown in Figure 24. This effect became visible during the GM-CSF driven differentiation on day 8. On day 10 it was enhanced and about 25% of TNFR2$^{-/-}$ BMDC cultures exhibited an activated state compared to 10% in wildtype controls. It has been shown with TNFR2-deficient cells that TNFR2-signaling is required for the processing of p100 (Rauert, Wicovsky et al. 2010). In support of this, it has been reported that BMDC and splenic DC from mice lacking p100 contain higher percentages of cells expressing MHCII, CD80, and CD86 (Speirs, Lieberman et al. 2004). p100, a member of the NF-κB family, is processed upon stimulation of the NF-κB pathyway into the transcription factor p52. Consequently, the missing TNFR2-signaling could lead to decreased processing of the NF-κB member p100 and impaired processing into p52. This would reduce immunomodulatory effects of p52 leading to higher activation and maturation in terms of expression of MHCII and costimulatory molecules CD80 and CD86. Activated BMDC express more costimulatory molecules like CD80 and CD86. In combination with the upregulation of MHCII, both antigen presentation and CD4 T cell proliferation should be improved. When TNFR2$^{-/-}$ BMDC loaded with ovalbumine (OVA) were incubated together with CFSE-labeled OVA-specific T cells from OTII mice, the proliferation was slightly enhanced compared to wildtype control BMDC as antigen-presenting cells (data not shown). This has also been shown with splenic DC of TNFR2$^{-/-}$ mice (personal communication: Dr. Elisabeth Martin).

Interestingly, these results can be interpreted as defective p100-processing in cells devoid of TNFR2 intrinsic signaling. OVA incubated BMDC of mice lacking p100 were reported to induce significantly increased OTII T cell proliferation (Speirs, Lieberman et al. 2004).

Mature BMDC do not proliferate any further (data not shown). The higher percentages of activated BMDC could be explained by assuming an equal capacity for the generation of activated BMDC and by taking the reduced proliferation of non-activated cells into consideration. Another possible reason for the higher grade of activation in TNFR2$^{-/-}$ BMDC could be the concentration and availability of biologically active TNF during the generation of BMDC. As shown in Figure 27, TNFR2$^{-/-}$ BMDC cultures express about 1 ng/mL TNF in the late phase of differentiation into mature BMDC. TNF induces the maturation and activation of BMDC (Brunner, Seiderer et al. 2000).

Third: the levels of biologically active TNF were significantly increased in TNFR2$^{-/-}$ BMDC cultures during the whole differentiation process and started to rise drastically on day 6 (Figure 27). On day 10 the concentrations of biologically active TNF present in the cultures amounted to

1 ng/mL compared to 0.2 ng/mL in the wildtype control cultures. This is due to high amounts of soluble TNFR2 present in the cultures of wildtype BMDC as shown in Figure 28. The concentrations of this TNF antagonist rose on day 3 and reached a plateau on day 7 with about 1.2 ng/mL. It has been shown by several other groups that altered TNF concentrations influence the percentages of activated mature BMDC (Brunner, Seiderer et al. 2000; Ritter, Meissner et al. 2003). Whether this is the only reason for the altered maturation in TNFR2$^{-/-}$ BMDC cultures or whether missing TNFR2-signaling, forward or reverse, contributes to this finding, will be discussed later.

Fourth: the percentages of cells expressing surface markers for MDSC (CD11b^{+} Ly6C^{+} Ly6G^{-}) were examined throughout the GM-CSF-induced differentiation into BMDC. As shown in Figure 19, the proportion of MDSC on day 3 was about 60%. Until day 10 the population steadily decreased and almost disappeared. TNFR2$^{-/-}$ BMDC cultures contained significantly reduced percentages of MDSC at all times during the BMDC differentiation culture. This effect could be caused by the reduced proliferation of this cellular population. Additionally, naïve TNFR2$^{-/-}$ BMDC on day 6 expressed significantly reduced Arg1 mRNA compared to wildtype BMDC (Figure 22). Whether missing TNFR2-signaling, reverse signaling, or higher concentrations of biologically active TNF is causal for the reduced MDSC proportion in TNFR2$^{-/-}$ cultures, will be discussed later.

BMDC of wildtype and TNFR2$^{-/-}$ mice stimulated with LPS and IFN-γ were investigated, too. The cell type responsible for the reduced NO production in BMDC cultures on day 4 was found to be MDSC since MDSC were responsible for the complete NO production (Figure 21). Interestingly, there was no difference in the NO production of TNFR2$^{-/-}$ and wildtype control BMDC whereas the concentrations of NO after 48 h stimulation of stimulation were comparable to the values that can be found in mature BMDC cultures stimulated for 48 h on day 10. On day 10 of BMDC differentiation culture the NO production capacity of TNFR2$^{-/-}$ BMDC was significantly reduced (Figure 13). This finding indicates that the reduced capacity to produce NO in TNFR2$^{-/-}$ BMDC on day 10 could be due to the reduced proportions of MDSC as MDSC are the only source of NO on day 4 and in the spleen of mice 2 days after CLP (Figure 16 and Figure 21). The sorting procedure of BMDC did not interfere with the impaired NO production of BMDC from TNFR2$^{-/-}$ mice (Figure 29).

The concentrations of IL-6 were also significantly reduced in TNFR2$^{-/-}$ BMDC cultures after stimulation (Figure 30) as already seen in TNFR2$^{-/-}$ PEC (data not shown). IL-6 is a pleitropic cytokine which has been reported to be involved in the differentiation and maturation of DC and BMDC. IL-6 blocks the maturation of BMDC and keeps them in an immature state. Besides, IL-6-mediated STAT3 activation is required for the suppression of LPS-induced DC maturation

(Park, Nakagawa et al. 2004) possibly explaining the higher grade of activated BMDC in TNFR2$^{-/-}$ cultures. However, no significant IL-6 concentrations can be found in the supernatants of non-stimulated BMDC (data not shown) but is found after TLR signaling. The relevance of IL-6 could be more important in the context of sepsis as a consequence of high dose bacterial components.

Furthermore, there are indications that IL-6 switches the monocyte differentiation and maturation to the direction of macrophages rather than to DC thereby being an essential factor in the molecular control of antigen-presenting cell development (Chomarat, Banchereau et al. 2000). IL-6 concentrations have been shown to correlate with the severity of CLP-induced sepsis. However, IL-6$^{-/-}$ mice are not protected from CLP-induced mortality (Remick, Bolgos et al. 2005). IL-6 induces the expression and release of acute phase proteins from the liver. When the harmful role of the complement activation product C5a in the early phase of CLP-caused severe sepsis or after *in vivo* LPS treatment was investigated intensively, IL-6 was found to be responsible for the strong upregulation of C5a receptor (C5aR) in multiple organs of septic mice. The blockade of C5aR considerably increased the survival of these mice (Riedemann, Guo et al. 2002). Protective effects of the antibody-based blockade of IL-6 in mice during CLP-induced sepsis have also been reported and were linked with decreased C5aR expression (Riedemann, Neff et al. 2003). The protection of CLP-treated TNFR2$^{-/-}$ mice from immunoparalysis after a secondary infection could be based on this decreased IL-6 production. This would lead to a reduced release of acute phase proteins like C5a and to a reduced expression of C5aR. This mechanism could contribute to the protection of the TNFR2$^{-/-}$ organism from multi-organ failure. IL-6 expression is regulated by the NF-κB signaling pathway (Libermann and Baltimore 1990; Baeuerle and Henkel 1994). As it is possible for both TNFR1 and TNFR2 to activate the NF-κB pathway, an influence of the concentrations of biologically active TNF could be relevant. Nevertheless, neither in TNFR2$^{-/-}$ BMDC nor in the wildtype control BMDC detectable concentrations of IL-6 protein could be found in the supernatants without stimulation (data not shown). This implicates that either TNF tolerance due to the persistent exposure to high concentrations of biologically active TNF or the influence of the stimulation with LPS and IFN-γ could be required to make the difference in IL-6 production obvious. In both cases, missing TNFR2-signaling or increased TNFR1-signaling in TNFR2$^{-/-}$ BMDC might be the reason. As TNFR1$^{-/-}$ BMDC produce significantly increased levels of IL-6 compared to wildtype controls (data not shown), the conclusion would be that TNFR2-signaling is essential for adequate IL-6 production. Whether direct TNFR2-signaling or reverse signaling is the crucial signaling pathway, will be discussed later.

The differentiation of CD4 T cells into T_H17 cells *in vivo* requires the presence of IL-23 which consists of a p19 and a p40 subunit. The latter is also part of IL-12 and its production is significantly decreased in various myeloid cells of TNFR2$^{-/-}$ mice (personal communication: Dr. Elisabeth Martin). *In vitro* differentiation into T_H17 cannot be induced by IL-23 but only by using a combination of IL-6 and TGF-β. Therefore, the combination of both cytokines supports the *in vivo* development of T_H17 cells (Zhou, Ivanov et al. 2007). As TNFR2$^{-/-}$ cells express decreased amounts of IL-6 and IL-12, the number of T_H17 cells is to be expected to be reduced. Preliminary experiments support this notion (data not shown).

4.1.4.1 BM chimeric mice

In order to elucidate whether the described phenotypical characteristics of TNFR2$^{-/-}$ myeloid cells are due to missing intrinsic TNFR2-signaling or caused by increased TNFR1-signaling as a consequence of the missing TNF antagonist soluble TNFR2, bone marrow chimeric mice were generated. Wildtype host environmental conditions were generated for a TNFR2$^{-/-}$ hematopoietic system and *vice versa*. On the one hand, TNFR2$^{-/-}$ myeloid cells develop, differentiate, and mature in a wildtype host organism with soluble TNFR2 which can reduce the amounts of biologically active TNF in the system. On the other hand, wildtype hematopoietic cells reconstitute the immune system in TNFR2$^{-/-}$ mice free of TNFR2 except for the indigenious production by the transferred hematopoietic cells. In order to discriminate between donor and host cells, the CD45 congenic system was used. CD45.1 wildtype mice were reconstituted with CD45.2 TNFR2$^{-/-}$ bone marrow and *vice versa*. Control experiments with CD45.1 wildtype mice that were reconstituted with CD45.2 wildtype bone marrow were performed as well as the reciprocal combinations. The reconstitution efficiencies were checked at the day of the experiment and ranged between 80% and 90% (Figure 40).

BMDC from CD45.1 wildtype mice that were reconstituted with CD45.1 TNFR2$^{-/-}$ bone marrow maintained the known phenotypes of TNFR2$^{-/-}$ BMDC that were described and discussed above in this work. BMDC of wildtype mice carrying a TNFR2$^{-/-}$ hematopoietic system contained significantly higher proportions of activated cells expressing CD80, CD86, and MHCII (Figure 38). The NO and IL-6 concentrations in the supernatants of these cells after stimulation with LPS and IFN-γ were significantly decreased (Figure 43 and Figure 44) and contained significant higher amounts of soluble TNF whereas soluble TNFR2 concentrations were negligible compared to the control BMDC cultures (Figure 45 and Figure 46). In summary, BMDC cultures from a TNFR2$^{-/-}$ donor and a wildtype host featuring a TNFR2$^{-/-}$ hematopoietic system generated similar results as BMDC cultures of TNFR2$^{-/-}$ mice. These data strongly indicate that the

expression of TNFR2 on hematopoietic cells is required for the observed phenotypes of TNFR2$^{-/-}$ myeloid cells described above which points to a TNFR2-signaling effect. BMDC from wildtype mice that were reconstituted with TNFR2$^{-/-}$ bone marrow miss the antagonizing effects of soluble TNFR2 produced from the hematopoietic cells. As a consequence, high biologically available concentrations of TNF could lead to increased TNFR1-signaling. This would argue for an environmental TNF effect. Moreover, the possible influence of reverse signaling in this context cannot be excluded, either. Consequently, the data from bm chimeric mice are no absolute proof of the relevance of missing intrinsic signals via TNFR2 as a reason for the phenotypes described for TNFR2$^{-/-}$ myeloid cells.

PEC from wildtype mice that were reconstituted with TNFR2$^{-/-}$ bone marrow only showed a slight and not significant reduction of NO production after stimulation with LPS and IFN-γ (Figure 41) which is in contrast to the NO production of PEC from TNFR2$^{-/-}$ mice. This points to a TNF effect via TNFR1 in TNFR2$^{-/-}$ mice as a consequence of enhanced TNF levels due to the missing antagonist soluble TNFR2. This result supports other findings of our working group: when stimulated with the TLR9 ligand CpG, the IL-12 production capacity was impaired in splenic DC from TNFR2$^{-/-}$ mice. IL-12 is a prominent cytokine that is induced in T_H1 reactions and stabilizes this type of immune response. It has been reported that the IL-12 production capacity, induced by TLR ligands, is drastically decreased in DC of mice 2 days after CLP (Flohe, Agrawal et al. 2006). Thus, the reduced IL-12 production capacity of post-septic wildtype and naïve TNFR2$^{-/-}$ splenic DC were similar. This phenotype, however, was not seen in DC from wildtype mice reconstituted with TNFR2$^{-/-}$ bone marrow (personal communication: Dr. Elisabeth Martin) indicating an environmental rather than cell-intrinsic effect of TNFR2. In addition, TNF pretreatment of macrophages has been shown to reduce the expression of IL-12 (IL12p40) drastically upon stimulation with LPS and IFN-γ (Zakharova and Ziegler 2005). These effects were mainly due to TNFR1-signaling. Eight hours pretreatment with TNF were sufficient to induce this reduction of IL-12 production. Mice subjected to CLP treatment produce high amounts of TNF. As a consequence of TNFR1-signaling, the capacity to express IL-12p40 is drastically decreased. TNFR2$^{-/-}$ mice lack the antagonizing soluble TNFR2, hence, higher TNF levels diminish the IL-12p40 production capacity in splenic DC of both naïve and CLP-treated animals. In cells of naïve TNFR2$^{-/-}$ mice this phenomenon could be caused either by endogenous TNF production during the stimulation with CpG or by the chronic or repetitive exposure to relatively high TNF levels during the life of the experimental mice. However, these considerations, as well as the methods discussed until now, do not exclude the possibility of reverse signaling. TNFR2$^{-/-}$ splenic DC and PEC could be triggered in a wildtype environment by membrane-bound or soluble TNFR2. As soluble TNFR2 is able to bind to membrane TNF,

TNFR2$^{-/-}$ cells could be coated with soluble TNFR2 from naïve hosts that were reconstituted with TNFR2$^{-/-}$ bone marrow. Consequently, soluble TNFR2 could be transferred into the experimental culture systems including the stimulation with TLR ligands. This could lead to both reverse signaling and interference with the concentrations of biologically active soluble TNF in these cultures.

4.1.4.2 BMDC from mixed cultures

To directly approach the question whether missing intrinsic TNFR2-signaling, increased TNFR1 concentrations caused by the lack of the TNF-antagonizing TNFR2, or missing reverse signaling is the reason for the phenotypes seen in TNFR2$^{-/-}$ myeloid cells, mixed BMDC cultures were used. Wildtype and TNFR2$^{-/-}$ bone marrow cells were isolated and differentiated into BMDC either in cultures derived from the respective mice or in cultures which contained bone marrow cells from both mouse lines mixed in equal parts. BMDC cultures consisting of 50% wildtype and 50% TNFR2$^{-/-}$ bone marrow cells feature identical conditions for cells derived from both types of mice, especially in terms of soluble TNF and soluble TNFR2 concentrations. Additionally, the possible requirement of membrane-bound or soluble TNFR2 for reverse signaling with membrane-bound TNF is also provided for TNFR2$^{-/-}$ and wildtype BMDC in mixed cultures. Hence, the probability of cellular contact with another cell expressing TNFR2 should be the same for all cells.

First, naïve cells from such mixed cultures were analyzed for the expression of surface markers and the development of congenic markers for wildtype and TNFR2$^{-/-}$ BMDC, respectively. As shown in Figure 33, the ratio of TNFR2$^{-/-}$ BMDC on day 3 was significantly increased compared to wildtype cells. This phenomenon was reverted and, finaly, the ratio of TNFR2$^{-/-}$ BMDC in mixed BMDC cultures was significantly reduced on day 10. The TNFR2$^{-/-}$ population in mixed cultures showed an equal degree of apoptotic cells but slightly decreased proliferation on day 10 (Figure 36 and Figure 37). Interestingly, BMDC cultures consisting of mixed cells of TNFR1$^{-/-}$ and wildtype mice showed equal proliferation of the two populations while pure TNFR1$^{-/-}$ BMDC showed significantly increased proliferation as discussed before. This leads to the conclusion that it is the TNFR2-signaling that promotes the proliferation of BMDC. In TNFR1$^{-/-}$ BMDC higher TNF levels are to be assumed compared to wildtype cultures as antagonizing membrane-bound or soluble TNFR1 is not available and only TNFR2 is present in these cultures. Contrary to this, in mixed TNFR1 and wildtype cultures TNFR2 molecules on both wildtype and TNFR1$^{-/-}$ cells are activated equally and, consequently, the proliferation rate is equal.

The percentages of $CD80^+$ $CD86^+$ $MHCII^+$ activated cells in mixed BMDC cultures were significantly higher in the $TNFR2^{-/-}$ BMDC fractions (Figure 34). In contrast, the percentages of cells expressing the MDSC marker $CD11b^+$, $Ly6C^+$, and $Ly6G^-$ were significantly reduced in the $TNFR2^{-/-}$ BMDC populations (Figure 35). These phenotypes were seen in pure $TNFR2^{-/-}$ BMDC as well and remained stable in mixed BMDC cultures. This represents a very strong indication for a missing intrinsic TNFR2 signal responsible for the phenotype seen in $TNFR2^{-/-}$ BMDC.

Moreover, wildtype and $TNFR2^{-/-}$ BMDC from pure and mixed BMDC cultures were separated according to their congenic markers. Independent of the culture system, $TNFR2^{-/-}$ BMDC produced significantly reduced NO and IL-6 levels (Figure 38 and Figure 39) compared to the wildtype BMDC. Clearly, $TNFR2^{-/-}$ BMDC, sorted from mixed cultures, expressed higher amounts of TNF compared with wildtype BMDC. Thus, it cannot be entirely excluded that TNF, produced in the sorted BMDC cultures, could influence the outcome of NO and IL-6 production via TNFR1 signaling. This demonstrates the limitations of this experimental setup which is based on the separation of cells grown in mixed cultures followed by stimulation of the separated cells, in order to analyze the concentrations of produced mediators. It could partly be overcome by the determination of intracellular TNF, IL-6, and NO production upon stimulation of mixed cultures, but even then it cannot be entirely excluded.

However, these data from mixed cultures together with the flow cytometry-based data show that neither TNFR1-signaling due to the lack of the TNF antagonist TNFR2 and enhanced TNF levels in the cultures nor missing reverse signaling activating membrane TNF via TNFR2 are the reasons for the $TNFR2^{-/-}$ phenotype of myeloid cells described in this work.

Nevertheless, the results from mixed BMDC cultures with bone marrow cells from wildtype as well as $TNFR2^{-/-}$ mice provide very strong evidence against an influence of the milieu on the $CD11b^+$ phenotypic and functional characteristics shown for $TNFR2^{-/-}$ cells.

Another hypothesis that epigenetic modifications as a consequence of chronic exposure to high amounts of TNF in $TNFR2^{-/-}$ mice could be the reason for the above-mentioned observations in $TNFR2^{-/-}$ myeloid cells also exists. As TNF is usually not detectable in healthy organisms, the overexposure to TNF in naïve $TNFR2^{-/-}$ mice has not been shown yet. However, it has been shown that LPS pretreatment of wildtype mice switches splenic DC into a tolerant state in respect to IL-12 production following *ex vivo* restimulation with CpG (preliminary data from our working group). LPS pretreatment induces TNF production and, consequently, TNF tolerance. As LPS is a very potent endotoxin with several side effects besides TNF induction, the experiment needs to be repeated with TNF pretreatment. However, epigenetic modifications cannot be excluded as the underlying reason for the observed phenotypes described in this work. In order to elucidate this question, methylation studies on the histone architecture in the

promoter regions of iNOS, IL-6, and IL-12 are planned. Furthermore, TNFR2 could be downregulated in hematopoietic cells using siRNA approaches or blocked using antagonistic mediators such as mAB. When the shown cellular phenotypes for TNFR2$^{-/-}$ myeloid cells could be induced in these cells immediately after the knock-down or blockade of TNFR2, this would be another indication that the phenotypes that were seen are caused by missing intrinsic TNFR2-signaling.

4.2 Mouse anti-mouse TNFR2 mAB with agonistic or antagonistic properties

In order to clarify whether the effects seen in TNFR2$^{-/-}$ mice are due to the loss of TNFR2-signaling or caused by higher TNF levels resulting from the absence of soluble TNFR2 as inhibitor for biologically functional TNF, specific activation or blockade of TNFR2 can be used as another approach. There is no specific agonistic or antagonistic ligand known for mouse TNFR2, so far. Monoclonal antibodies with special functional properties have been used for many years to selectively activate or block cytokine activation via their receptors. Furthermore, *in vivo* treatment with monoclonal antibodies can be used to eliminate the cells expressing the respective receptor that is recognized by the antibody. The use of mouse anti-mouse antibodies would enable the *in vivo* application as intraspecies-antibodies are not immunogenic.

Mouse anti-mouse TNFR2 mAB were generated. In order to guarantee adequate immunity against the antigen, TNFR2$^{-/-}$ mice were immunized with the extracellular domain of TNFR2. These mice lack TNFR2 and, therefore, T and B cells with TNFR2-specific T and B cell receptors are not negatively selected during the differentiation in the thymus and the bone marrow.

An immunization protocol was used aiming at the class switch from primarily IgM to high titers of IgG. TNFR2$^{-/-}$ mice were immunized and the splenocytes were fused with SP2/0-Ag14 cells. Five monoclonal hybridoma cell lines producing mouse anti-mouse TNFR2 mAB were identified in this work and tested together with the antibodies of another positive hybridoma for TNFR2 generated earlier. The mAB were positive in binding TNFR2 in ELISA and Western blot analysis. Only one mAB stained TNFR2-expressing cells in FACS analysis (Figure 53). All mouse anti-mouse TNFR2 mAB are IgG1-type immunoglobulins.

Thus, 6 different mAB were available for agonistic and antagonistic tests in a TNFR2-signaling assay. As TNFR1 and TNFR2 show high similarity in their extracellular domains, agonistic and antagonistic tests had to be performed in parallel with a TNFR1 and TNFR2 specific system, in order to detect cross-reactivity. Therefore, a test system that was described by Dr. A. Krippner-

Heidenreich in the human system was adapted to the mouse system. Fusion proteins of TNFR1 or TNFR2 extracellular domain and huFas intracellular domains were cloned and retrovirally transduced into TNFR-free cells.

Both types of transduced cells died when incubated with mouse TNF due to the Fas-induced apoptosis upon binding TNF to the extracellular domains of the two TNF receptor constructs. Cells transduced with the TNFR2 construct were less sensible to mouse TNF compared to cells expressing the TNFR1 construct (Figure 55). This can be explained by the finding that TNFR2 is primarily activated by membrane-bound TNF. Therefore, the recombinant mouse TNF does not provide the optimal spatial density and aggregation conditions needed for efficient activation of TNFR2. As expected, human TNF only activated the TNFR1 construct leading to apoptosis of these cells. Nevertheless, apoptosis in neither TNFR1 construct-transduced nor in TNFR2 construct-carrying cells could be induced by incubation with the 6 newly generated monoclonal mouse anti-mouse TNFR2 antibodies (Figure 56) indictaing no agonistic properties. The positive control mouse TNF induced sufficient apoptosis in TNFR1 construct transduced cells whereas it was less efficient in TNFR2 construct expressing cells. Consequently, the TNFR2 extracellular huFas intracellular system is perhaps not sensitive enough to detect agonistic mAB properties (Figure 55).

Preincubation of TNFR1 construct transduced cells with mouse anti-mouse TNFR2 mAB did not affect the apoptosis that was induced by the addition of TNF indicating that the antibodies do not cross-react with TNFR1 (Figure 57). TNFR2 construct-expressing cells were not protected by preincubation with the mouse anti-mouse TNFR2 mAB from TNF-induced apoptosis. Sufficient apoptosis in TNFR2 construct expressing cells was only achieved by the use of TNC-mTNF (Prof. H. Wajant) as the TNC motif induces the polymerization of the TNF molecules and, thus, better activation of TNFR2. However, Figure 58 shows that no blocking function of the 6 mouse anti-mouse TNFR2 mAB was detectable.

Interestingly, the group of Prof. H. Wajant (University of Würzburg) has recently produced TNF mutants that selectively activate mouse TNFR2 (personal communication, data not shown). As human TNF selectively activates TNFR1, the specific activation of both mouse TNF receptors *in vivo* and *in vitro* would be possible. Nevertheless, there is no reagent available to block TNFR2 as the most important tool to understand the mechanism behind the cellular phenotypes described in this work.

5 Conclusion

The results shown and discussed in this work reveal several cellular phenotypes of TNFR2$^{-/-}$ myeloid cells and allow to draw conclusions about the function of TNFR2 in general and especially in sepsis. It was shown that CLP is required to induce iNOS mRNA expression and NO production in CD11b^{+} CD11c^{-} cells upon stimulation with LPS and IFN-γ and that the lack of TNFR2 results in a reduction of both iNOS mRNA expression and NO production. This cellular phenotype was also found in other myeloid cells such as PEC and BMDC from naïve mice. BMDC were used as a cellular model for further investigations. TNFR2$^{-/-}$ BMDC produce reduced concentrations of IL-6 upon stimulation with LPS and IFN-γ. These findings indicate that TNFR2-signaling is required for adequate NO and IL-6 production.

It turned out that missing TNFR2 decreased the proliferation in these cells leading to reduced cell yields at day 10 of the BMDC differentiation culture. In combination with data from TNFR1$^{-/-}$ BMDC TNFR2 expression was shown to be required for adequate proliferation. TNFR2$^{-/-}$ BMDC cultures showed reduced proportions of MDSC throughout the cultivation period. TNFR2$^{-/-}$ BMDC as well as TNFR2$^{-/-}$ BMDC sorted for the MDSC marker Ly6C^{+} Ly6G^{-} showed reduced Arg1 mRNA expression indicating an important role of TNFR2 in the generation and function of MDSC. TNFR2 signaling seems to be essential for adequate generation of MDSC and could contribute to the suppressive functions of these cells in dampening inflammation *in vivo*. The hypothesis that TNFR2$^{-/-}$ cells *ex vivo* or *in vitro* contain a higher percentage or more activated MDSC could not be proven.

TNFR2$^{-/-}$ BMDC cultures contained increased proportions of activated (MHCII^{+} CD80^{+} CD86^{+}) cells at day 8 and day 10 indicating less suppression of T cell proliferation and, simultaneously, improved antigen presentation and, thus, better activation of T cells. These are strong indications for a dampening function of TNFR2 in the immune system as its presence seems to be required for the downregulation of activation molecules.

Whether direct TNFR2-signaling or indirect effects via enhanced TNFR1-signaling as a consequence of the missing TNF antagonist soluble TNFR2 are responsible for the phenotypes of TNFR2$^{-/-}$ myeloid cells has been investigated using bone marrow chimeric mice and mixed BMDC cultures. It has been shown that the phenotypes of TNFR2$^{-/-}$ myeloid cells remain stable in BMDC from wildtype host mice that were reconstituted with TNFR2$^{-/-}$ bone marrow and, thus, generating wildtype conditions for a TNFR2$^{-/-}$ hematopoietic system. These phenotypes also persisted in TNFR2$^{-/-}$ BMDC in mixed BMDC differentiation cultures initially containing wildtype and TNFR2$^{-/-}$ bone marrow in equal proportions. This culture method generates equal environmental conditions for both types of BMDC. As TNFR2$^{-/-}$ BMDC of both bone marrow

chimeric mice and mixed BMDC differentiation cultures maintained the phenotypes found for TNFR2$^{-/-}$ BMDC, this is a very strong indication for a missing intrinsic signaling via TNFR2 and, thus, confirms the hypothesis of an important role of direct TNFR2-signaling in the immune system. Additionally, these results reveal that reverse signaling via soluble or membrane-bound TNFR2 as ligand and membrane-bound TNF as receptor can be excluded as the reason for these phenotypes as the conditions are equal for TNFR2$^{-/-}$ and wildtype BMDC in mixed BMDC differentiation cultures.

However, epigenetic promoter or histone modifications could also be the cause for the TNFR2$^{-/-}$ phenotypes described in this work since altered TNFR1-signaling in TNFR2$^{-/-}$ mice cannot be excluded completely as the TNF antagonist soluble TNFR2 is missing in these mice.

Mouse anti-mouse TNFR2 mAB were generated and tested for binding as well as agonistic and antagonistic properties. The antibodies performed positive in ELISA and Western blot and one clone also stained TNFR2-expressing cells in FACS analysis. However, neither agonistic nor antagonistic functions could be detected in a cytotoxicity assay established to detect specific TNFR2 activation by using cells expressing the extracellular domain of TNFR2 fused to the intracellular domains of human Fas.

6 References

Aderka, D., H. Englemann, et al. (1991). "Increased serum levels of soluble receptors for tumor necrosis factor in cancer patients." Cancer Res **51**(20): 5602-5607.

Aderka, D., A. Wysenbeek, et al. (1993). "Correlation between serum levels of soluble tumor necrosis factor receptor and disease activity in systemic lupus erythematosus." Arthritis Rheum **36**(8): 1111-1120.

Aggarwal, B. B. (2003). "Signalling pathways of the TNF superfamily: a double-edged sword." Nat Rev Immunol **3**(9): 745-756.

Aktan, F. (2004). "iNOS-mediated nitric oxide production and its regulation." Life Sci **75**(6): 639-653.

Al-Lamki, R. S., J. Wang, et al. (2001). "Expression of tumor necrosis factor receptors in normal kidney and rejecting renal transplants." Lab Invest **81**(11): 1503-1515.

Alexander, H. R., B. C. Sheppard, et al. (1991). "Treatment with recombinant human tumor necrosis factor-alpha protects rats against the lethality, hypotension, and hypothermia of gram-negative sepsis." J Clin Invest **88**(1): 34-39.

Alonso-Ruiz, A., J. I. Pijoan, et al. (2008). "Tumor necrosis factor alpha drugs in rheumatoid arthritis: systematic review and metaanalysis of efficacy and safety." BMC Musculoskelet Disord **9**: 52.

Angus, D. C., W. T. Linde-Zwirble, et al. (2001). "Epidemiology of severe sepsis in the United States: analysis of incidence, outcome, and associated costs of care." Crit Care Med **29**(7): 1303-1310.

Arnaout, M. A., S. K. Gupta, et al. (1988). "Amino acid sequence of the alpha subunit of human leukocyte adhesion receptor Mo1 (complement receptor type 3)." J Cell Biol **106**(6): 2153-2158.

Ashkenazi, A. and V. M. Dixit (1998). "Death receptors: signaling and modulation." Science **281**(5381): 1305-1308.

Ayala, A. and I. H. Chaudry (1996). "Immune dysfunction in murine polymicrobial sepsis: mediators, macrophages, lymphocytes and apoptosis." Shock **6 Suppl 1**: S27-38.

Ayres, S. M. (1985). "SCCM's new horizons conference on sepsis and septic shock." Crit Care Med **13**(10): 864-866.

Baeuerle, P. A. and T. Henkel (1994). "Function and activation of NF-kappa B in the immune system." Annu Rev Immunol **12**: 141-179.

Balk, R. A. and R. C. Bone (1989). "The septic syndrome. Definition and clinical implications." Crit Care Clin **5**(1): 1-8.

Balk, R. A. and J. E. Parrillo (1992). "Prognostic factors in sepsis: the cold facts." Crit Care Med **20**(10): 1373-1374.

Barnden, M. J., J. Allison, et al. (1998). "Defective TCR expression in transgenic mice constructed using cDNA-based alpha- and beta-chain genes under the control of heterologous regulatory elements." Immunol Cell Biol **76**(1): 34-40.

Barreda, D. R., P. C. Hanington, et al. (2004). "Regulation of myeloid development and function by colony stimulating factors." Dev Comp Immunol **28**(5): 509-554.

Bazzoni, F. and B. Beutler (1995). "How do tumor necrosis factor receptors work?" J Inflamm **45**(4): 221-238.

Bennett, M., K. Macdonald, et al. (1998). "Cell surface trafficking of Fas: a rapid mechanism of p53-mediated apoptosis." Science **282**(5387): 290-293.

Beutler, B. and C. van Huffel (1994). "Unraveling function in the TNF ligand and receptor families." Science **264**(5159): 667-668.

Bevilacqua, M. P., J. S. Pober, et al. (1986). "Recombinant tumor necrosis factor induces procoagulant activity in cultured human vascular endothelium: characterization and comparison with the actions of interleukin 1." Proc Natl Acad Sci U S A **83**(12): 4533-4537.

Black, R. A. (2002). "Tumor necrosis factor-alpha converting enzyme." Int J Biochem Cell Biol **34**(1): 1-5.

Black, R. A., C. T. Rauch, et al. (1997). "A metalloproteinase disintegrin that releases tumour-necrosis factor-alpha from cells." Nature **385**(6618): 729-733.

Bone, R. C., C. J. Grodzin, et al. (1997). "Sepsis: a new hypothesis for pathogenesis of the disease process." Chest **112**(1): 235-243.

Bradley, J. R. (2008). "TNF-mediated inflammatory disease." J Pathol **214**(2): 149-160.

Bradley, J. R. and J. S. Pober (1996). "Prolonged cytokine exposure causes a dynamic redistribution of endothelial cell adhesion molecules to intercellular junctions." Lab Invest **75**(4): 463-472.

Bradley, J. R., S. Thiru, et al. (1995). "Disparate localization of 55-kd and 75-kd tumor necrosis factor receptors in human endothelial cells." Am J Pathol **146**(1): 27-32.

Bronte, V. and P. Zanovello (2005). "Regulation of immune responses by L-arginine metabolism." Nat Rev Immunol **5**(8): 641-654.

Brunner, C., J. Seiderer, et al. (2000). "Enhanced dendritic cell maturation by TNF-alpha or cytidine-phosphate-guanosine DNA drives T cell activation in vitro and therapeutic anti-tumor immune responses in vivo." J Immunol **165**(11): 6278-6286.

Buessow, S. C., R. D. Paul, et al. (1984). "Influence of mammary tumor progression on phenotype and function of spleen and in situ lymphocytes in mice." J Natl Cancer Inst **73**(1): 249-255.

Bultinck, J., P. Sips, et al. (2006). "Systemic NO production during (septic) shock depends on parenchymal and not on hematopoietic cells: in vivo iNOS expression pattern in (septic) shock." FASEB J **20**(13): 2363-2365.

Buras, J. A., B. Holzmann, et al. (2005). "Animal models of sepsis: setting the stage." Nat Rev Drug Discov **4**(10): 854-865.

Burke, F., M. S. Naylor, et al. (1993). "The cytokine wall chart." Immunol Today **14**(4): 165-170.

Bustin, S. A. (2000). "Absolute quantification of mRNA using real-time reverse transcription polymerase chain reaction assays." J Mol Endocrinol **25**(2): 169-193.

Carswell, E. A., L. J. Old, et al. (1975). "An endotoxin-induced serum factor that causes necrosis of tumors." Proc Natl Acad Sci U S A **72**(9): 3666-3670.

Chandrasekharan, U. M., M. Siemionow, et al. (2007). "Tumor necrosis factor alpha (TNF-alpha) receptor-II is required for TNF-alpha-induced leukocyte-endothelial interaction in vivo." Blood **109**(5): 1938-1944.

Chen, X., M. Baumel, et al. (2007). "Interaction of TNF with TNF receptor type 2 promotes expansion and function of mouse CD4+CD25+ T regulatory cells." J Immunol **179**(1): 154-161.

Chomarat, P., J. Banchereau, et al. (2000). "IL-6 switches the differentiation of monocytes from dendritic cells to macrophages." Nat Immunol **1**(6): 510-514.

Cline, M. J. and M. A. Moore (1972). "Embryonic origin of the mouse macrophage." Blood **39**(6): 842-849.

Cobb, J. P., R. S. Hotchkiss, et al. (1999). "Inducible nitric oxide synthase (iNOS) gene deficiency increases the mortality of sepsis in mice." Surgery **126**(2): 438-442.

Cope, A. P., D. Aderka, et al. (1992). "Increased levels of soluble tumor necrosis factor receptors in the sera and synovial fluid of patients with rheumatic diseases." Arthritis Rheum **35**(10): 1160-1169.

Corredor, J., F. Yan, et al. (2003). "Tumor necrosis factor regulates intestinal epithelial cell migration by receptor-dependent mechanisms." Am J Physiol Cell Physiol **284**(4): C953-961.

Deitch, E. A. (2005). "Rodent models of intra-abdominal infection." Shock **24 Suppl 1**: 19-23.

Di Santo, E., C. Meazza, et al. (1997). "IL-13 inhibits TNF production but potentiates that of IL-6 in vivo and ex vivo in mice." J Immunol **159**(1): 379-382.

Ding, Y., C. S. Chung, et al. (2004). "Polymicrobial sepsis induces divergent effects on splenic and peritoneal dendritic cell function in mice." Shock **22**(2): 137-144.

Docke, W. D., F. Randow, et al. (1997). "Monocyte deactivation in septic patients: restoration by IFN-gamma treatment." Nat Med **3**(6): 678-681.

Ebach, D. R., T. E. Riehl, et al. (2005). "Opposing effects of tumor necrosis factor receptor 1 and 2 in sepsis due to cecal ligation and puncture." Shock **23**(4): 311-318.

Echtenacher, B., W. Falk, et al. (1990). "Requirement of endogenous tumor necrosis factor/cachectin for recovery from experimental peritonitis." J Immunol **145**(11): 3762-3766.

Echtenacher, B. and D. N. Mannel (2002). "Requirement of TNF and TNF receptor type 2 for LPS-induced protection from lethal septic peritonitis." J Endotoxin Res **8**(5): 365-369.

Echtenacher, B., D. N. Mannel, et al. (1996). "Critical protective role of mast cells in a model of acute septic peritonitis." Nature **381**(6577): 75-77.

Eder, J. (1997). "Tumour necrosis factor alpha and interleukin 1 signalling: do MAPKK kinases connect it all?" Trends Pharmacol Sci **18**(9): 319-322.

Eissner, G., S. Kirchner, et al. (2000). "Reverse signaling through transmembrane TNF confers resistance to lipopolysaccharide in human monocytes and macrophages." J Immunol **164**(12): 6193-6198.

Enzan, H. (1986). "Electron microscopic studies of macrophages in early human yolk sacs." Acta Pathol Jpn **36**(1): 49-64.

Erickson, S. L., F. J. de Sauvage, et al. (1994). "Decreased sensitivity to tumour-necrosis factor but normal T-cell development in TNF receptor-2-deficient mice." Nature **372**(6506): 560-563.

Eskandari, M. K., G. Bolgos, et al. (1992). "Anti-tumor necrosis factor antibody therapy fails to prevent lethality after cecal ligation and puncture or endotoxemia." J Immunol **148**(9): 2724-2730.

Fadok, V. A., D. L. Bratton, et al. (1998). "Macrophages that have ingested apoptotic cells in vitro inhibit proinflammatory cytokine production through autocrine/paracrine mechanisms involving TGF-beta, PGE2, and PAF." J Clin Invest **101**(4): 890-898.

Feldmann, M. and R. N. Maini (2001). "Anti-TNF alpha therapy of rheumatoid arthritis: what have we learned?" Annu Rev Immunol **19**: 163-196.

Ferran, C., F. Dautry, et al. (1994). "Anti-tumor necrosis factor modulates anti-CD3-triggered T cell cytokine gene expression in vivo." J Clin Invest **93**(5): 2189-2196.

Fesik, S. W. (2000). "Insights into programmed cell death through structural biology." Cell **103**(2): 273-282.

Fleming, T. J., M. L. Fleming, et al. (1993). "Selective expression of Ly-6G on myeloid lineage cells in mouse bone marrow. RB6-8C5 mAb to granulocyte-differentiation antigen (Gr-1) detects members of the Ly-6 family." J Immunol **151**(5): 2399-2408.

Foung, S. K., D. T. Sasaki, et al. (1982). "Production of functional human T-T hybridomas in selection medium lacking aminopterin and thymidine." Proc Natl Acad Sci U S A **79**(23): 7484-7488.

Funk, J. O., H. Walczak, et al. (2000). "Cutting edge: resistance to apoptosis and continuous proliferation of dendritic cells deficient for TNF receptor-1." J Immunol **165**(9): 4792-4796.

Gabrilovich, D. I. and S. Nagaraj (2009). "Myeloid-derived suppressor cells as regulators of the immune system." Nat Rev Immunol **9**(3): 162-174.

Gage, F. H. (2000). "Mammalian neural stem cells." Science **287**(5457): 1433-1438.

Ganopolsky, J. G. and F. J. Castellino (2004). "A protein C deficiency exacerbates inflammatory and hypotensive responses in mice during polymicrobial sepsis in a cecal ligation and puncture model." Am J Pathol **165**(4): 1433-1446.

Gearing, A. J., P. Beckett, et al. (1994). "Processing of tumour necrosis factor-alpha precursor by metalloproteinases." Nature **370**(6490): 555-557.

Goldie, A. S., K. C. Fearon, et al. (1995). "Natural cytokine antagonists and endogenous antiendotoxin core antibodies in sepsis syndrome. The Sepsis Intervention Group." JAMA **274**(2): 172-177.

Gordon, S. (2002). "Pattern recognition receptors: doubling up for the innate immune response." Cell **111**(7): 927-930.

Gordon, S. (2003). "Alternative activation of macrophages." Nat Rev Immunol **3**(1): 23-35.

Gordon, S. and P. R. Taylor (2005). "Monocyte and macrophage heterogeneity." Nat Rev Immunol **5**(12): 953-964.

Gray, G. A., C. Schott, et al. (1991). "The effect of inhibitors of the L-arginine/nitric oxide pathway on endotoxin-induced loss of vascular responsiveness in anaesthetized rats." Br J Pharmacol **103**(1): 1218-1224.

Greifenberg, V., E. Ribechini, et al. (2009). "Myeloid-derived suppressor cell activation by combined LPS and IFN-gamma treatment impairs DC development." Eur J Immunol **39**(10): 2865-2876.

Grell, M. (1995). "Tumor necrosis factor (TNF) receptors in cellular signaling of soluble and membrane-expressed TNF." J Inflamm **47**(1-2): 8-17.

Grell, M., H. Wajant, et al. (1998). "The type 1 receptor (CD120a) is the high-affinity receptor for soluble tumor necrosis factor." Proc Natl Acad Sci U S A **95**(2): 570-575.

Guillou, P. J. (1993). "Biological variation in the development of sepsis after surgery or trauma." Lancet **342**(8865): 217-220.

Gumley, T. P., I. F. McKenzie, et al. (1995). "Tissue expression, structure and function of the murine Ly-6 family of molecules." Immunol Cell Biol **73**(4): 277-296.

Harashima, S., T. Horiuchi, et al. (2001). "Outside-to-inside signal through the membrane TNF-alpha induces E-selectin (CD62E) expression on activated human CD4+ T cells." J Immunol **166**(1): 130-136.
Hauser, A., T. Hehlgans, et al. (2007). "Characterization of TNF receptor type 2 isoform in the mouse." Mol Immunol **44**(14): 3563-3570.
Hehlgans, T. and K. Pfeffer (2005). "The intriguing biology of the tumour necrosis factor/tumour necrosis factor receptor superfamily: players, rules and the games." Immunology **115**(1): 1-20.
Hober, D., S. Benyoucef, et al. (1996). "High plasma level of soluble tumor necrosis factor receptor type II (sTNFRII) in asymptomatic HIV-1-infected patients." Infection **24**(3): 213-217.
Hoflich, C. and H. D. Volk (2002). "[Immunomodulation in sepsis]." Chirurg **73**(11): 1100-1104.
Hollenberg, N. K. (2002). "Defective nitric oxide production and functional renal reserve in patients with type 2 diabetes who have microalbuminuria of African and Asian compared with white origin." Curr Hypertens Rep **4**(6): 413; discussion 413-414.
Hotchkiss, R. S., K. W. Tinsley, et al. (2003). "Role of apoptotic cell death in sepsis." Scand J Infect Dis **35**(9): 585-592.
Hsu, H., J. Xiong, et al. (1995). "The TNF receptor 1-associated protein TRADD signals cell death and NF-kappa B activation." Cell **81**(4): 495-504.
Idriss, H. T. and J. H. Naismith (2000). "TNF alpha and the TNF receptor superfamily: structure-function relationship(s)." Microsc Res Tech **50**(3): 184-195.
Katsura, Y. (2002). "Redefinition of lymphoid progenitors." Nat Rev Immunol **2**(2): 127-132.
Kelliher, M. A., S. Grimm, et al. (1998). "The death domain kinase RIP mediates the TNF-induced NF-kappaB signal." Immunity **8**(3): 297-303.
Kim, E. Y., J. J. Priatel, et al. (2006). "TNF receptor type 2 (p75) functions as a costimulator for antigen-driven T cell responses in vivo." J Immunol **176**(2): 1026-1035.
Kirkeboen, K. A., P. A. Naess, et al. (1992). "Importance of nitric oxide in canine femoral circulation: comparison of two NO inhibitors." Cardiovasc Res **26**(4): 357-361.
Kirkeboen, K. A. and O. A. Strand (1999). "The role of nitric oxide in sepsis--an overview." Acta Anaesthesiol Scand **43**(3): 275-288.
Kishimoto, T. (2006). "Interleukin-6: discovery of a pleiotropic cytokine." Arthritis Res Ther **8 Suppl 2**: S2.
Koopman, G., C. P. Reutelingsperger, et al. (1994). "Annexin V for flow cytometric detection of phosphatidylserine expression on B cells undergoing apoptosis." Blood **84**(5): 1415-1420.
Kubista, M., J. M. Andrade, et al. (2006). "The real-time polymerase chain reaction." Mol Aspects Med **27**(2-3): 95-125.
Laemmli, U. K. (1970). "Cleavage of structural proteins during the assembly of the head of bacteriophage T4." Nature **227**(5259): 680-685.
Lanford, P. J., Y. Lan, et al. (1999). "Notch signalling pathway mediates hair cell development in mammalian cochlea." Nat Genet **21**(3): 289-292.
Ledgerwood, E. C., J. S. Pober, et al. (1999). "Recent advances in the molecular basis of TNF signal transduction." Lab Invest **79**(9): 1041-1050.

Lewis, M., L. A. Tartaglia, et al. (1991). "Cloning and expression of cDNAs for two distinct murine tumor necrosis factor receptors demonstrate one receptor is species specific." Proc Natl Acad Sci U S A **88**(7): 2830-2834.

Libermann, T. A. and D. Baltimore (1990). "Activation of interleukin-6 gene expression through the NF-kappa B transcription factor." Mol Cell Biol **10**(5): 2327-2334.

Liu, Z. G., H. Hsu, et al. (1996). "Dissection of TNF receptor 1 effector functions: JNK activation is not linked to apoptosis while NF-kappaB activation prevents cell death." Cell **87**(3): 565-576.

Loetscher, H., Y. C. Pan, et al. (1990). "Molecular cloning and expression of the human 55 kd tumor necrosis factor receptor." Cell **61**(2): 351-359.

Loetscher, H., D. Stueber, et al. (1993). "Human tumor necrosis factor alpha (TNF alpha) mutants with exclusive specificity for the 55-kDa or 75-kDa TNF receptors." J Biol Chem **268**(35): 26350-26357.

Lucas, R., P. Juillard, et al. (1997). "Crucial role of tumor necrosis factor (TNF) receptor 2 and membrane-bound TNF in experimental cerebral malaria." Eur J Immunol **27**(7): 1719-1725.

Lundberg, J. O. and E. Weitzberg (2005). "NO generation from nitrite and its role in vascular control." Arterioscler Thromb Vasc Biol **25**(5): 915-922.

Lutter, D., P. Ugocsai, et al. (2008). "Analyzing M-CSF dependent monocyte/macrophage differentiation: expression modes and meta-modes derived from an independent component analysis." BMC Bioinformatics **9**: 100.

Lutz, M. B., N. Kukutsch, et al. (1999). "An advanced culture method for generating large quantities of highly pure dendritic cells from mouse bone marrow." J Immunol Methods **223**(1): 77-92.

MacMicking, J. D., C. Nathan, et al. (1995). "Altered responses to bacterial infection and endotoxic shock in mice lacking inducible nitric oxide synthase." Cell **81**(4): 641-650.

Mannel, D. N. and B. Echtenacher (2000). "TNF in the inflammatory response." Chem Immunol **74**: 141-161.

Manship, L., R. D. McMillin, et al. (1984). "The influence of sepsis and multisystem and organ failure on mortality in the surgical intensive care unit." Am Surg **50**(2): 94-101.

Mark, K. S., W. J. Trickler, et al. (2001). "Tumor necrosis factor-alpha induces cyclooxygenase-2 expression and prostaglandin release in brain microvessel endothelial cells." J Pharmacol Exp Ther **297**(3): 1051-1058.

Martin, G. S., D. M. Mannino, et al. (2003). "The epidemiology of sepsis in the United States from 1979 through 2000." N Engl J Med **348**(16): 1546-1554.

Mercurio, F. and A. M. Manning (1999). "Multiple signals converging on NF-kappaB." Curr Opin Cell Biol **11**(2): 226-232.

Messadi, D. V., J. S. Pober, et al. (1987). "Induction of an activation antigen on postcapillary venular endothelium in human skin organ culture." J Immunol **139**(5): 1557-1562.

Miyaji, T., X. Hu, et al. (2003). "Ethyl pyruvate decreases sepsis-induced acute renal failure and multiple organ damage in aged mice." Kidney Int **64**(5): 1620-1631.

Morris, S. M., Jr. and T. R. Billiar (1994). "New insights into the regulation of inducible nitric oxide synthesis." Am J Physiol **266**(6 Pt 1): E829-839.

Moss, M. L., S. L. Jin, et al. (1997). "Cloning of a disintegrin metalloproteinase that processes precursor tumour-necrosis factor-alpha." Nature **385**(6618): 733-736.

Mosser, D. M. (2003). "The many faces of macrophage activation." J Leukoc Biol **73**(2): 209-212.
Mosser, D. M. and J. P. Edwards (2008). "Exploring the full spectrum of macrophage activation." Nat Rev Immunol **8**(12): 958-969.
Mosser, D. M. and X. Zhang (2008). "Activation of murine macrophages." Curr Protoc Immunol **Chapter 14**: Unit 14 12.
Movahedi, K., M. Guilliams, et al. (2008). "Identification of discrete tumor-induced myeloid-derived suppressor cell subpopulations with distinct T cell-suppressive activity." Blood **111**(8): 4233-4244.
Munro, J. M., J. S. Pober, et al. (1989). "Tumor necrosis factor and interferon-gamma induce distinct patterns of endothelial activation and associated leukocyte accumulation in skin of Papio anubis." Am J Pathol **135**(1): 121-133.
Nathan, C. (2008). "Metchnikoff's Legacy in 2008." Nat Immunol **9**(7): 695-698.
Nikolic, T., M. F. de Bruijn, et al. (2003). "Developmental stages of myeloid dendritic cells in mouse bone marrow." Int Immunol **15**(4): 515-524.
Nolan, T., R. E. Hands, et al. (2006). "Quantification of mRNA using real-time RT-PCR." Nat Protoc **1**(3): 1559-1582.
Nurden, A. T., C. Bihour, et al. (1993). "Platelet activation in thrombotic disorders." Nouv Rev Fr Hematol **35**(1): 67-71.
Nussler, A. K. and T. R. Billiar (1993). "Inflammation, immunoregulation, and inducible nitric oxide synthase." J Leukoc Biol **54**(2): 171-178.
Park, S. J., T. Nakagawa, et al. (2004). "IL-6 regulates in vivo dendritic cell differentiation through STAT3 activation." J Immunol **173**(6): 3844-3854.
Pennica, D., J. S. Hayflick, et al. (1985). "Cloning and expression in Escherichia coli of the cDNA for murine tumor necrosis factor." Proc Natl Acad Sci U S A **82**(18): 6060-6064.
Peschon, J. J., J. L. Slack, et al. (1998). "An essential role for ectodomain shedding in mammalian development." Science **282**(5392): 1281-1284.
Petzelbauer, P., J. S. Pober, et al. (1994). "Inducibility and expression of microvascular endothelial adhesion molecules in lesional, perilesional, and uninvolved skin of psoriatic patients." J Invest Dermatol **103**(3): 300-305.
Pfaffl, M. W. (2001). "A new mathematical model for relative quantification in real-time RT-PCR." Nucleic Acids Res **29**(9): e45.
Pober, J. S., M. P. Bevilacqua, et al. (1986). "Two distinct monokines, interleukin 1 and tumor necrosis factor, each independently induce biosynthesis and transient expression of the same antigen on the surface of cultured human vascular endothelial cells." J Immunol **136**(5): 1680-1687.
Rauert, H., A. Wicovsky, et al. (2010). "Membrane tumor necrosis factor (TNF) induces p100 processing via TNF receptor-2 (TNFR2)." J Biol Chem **285**(10): 7394-7404.
Rees, D. D. (1995). "Role of nitric oxide in the vascular dysfunction of septic shock." Biochem Soc Trans **23**(4): 1025-1029.
Remick, D. G., G. Bolgos, et al. (2005). "Role of interleukin-6 in mortality from and physiologic response to sepsis." Infect Immun **73**(5): 2751-2757.
Remick, D. G., D. E. Newcomb, et al. (2000). "Comparison of the mortality and inflammatory response of two models of sepsis: lipopolysaccharide vs. cecal ligation and puncture." Shock **13**(2): 110-116.
Ribechini, E., V. Greifenberg, et al. (2010). "Subsets, expansion and activation of myeloid-derived suppressor cells." Med Microbiol Immunol.

Riedemann, N. C., R. F. Guo, et al. (2002). "Increased C5a receptor expression in sepsis." J Clin Invest **110**(1): 101-108.

Ritter, U., A. Meissner, et al. (2003). "Analysis of the maturation process of dendritic cells deficient for TNF and lymphotoxin-alpha reveals an essential role for TNF." J Leukoc Biol **74**(2): 216-222.

Rittirsch, D., L. M. Hoesel, et al. (2007). "The disconnect between animal models of sepsis and human sepsis." J Leukoc Biol **81**(1): 137-143.

Rittirsch, D., M. S. Huber-Lang, et al. (2009). "Immunodesign of experimental sepsis by cecal ligation and puncture." Nat Protoc **4**(1): 31-36.

Rivoltini, L., M. Carrabba, et al. (2002). "Immunity to cancer: attack and escape in T lymphocyte-tumor cell interaction." Immunol Rev **188**: 97-113.

Rodriguez, P. C., D. G. Quiceno, et al. (2007). "L-arginine availability regulates T-lymphocyte cell-cycle progression." Blood **109**(4): 1568-1573.

Rodriguez, P. C., A. H. Zea, et al. (2002). "Regulation of T cell receptor CD3zeta chain expression by L-arginine." J Biol Chem **277**(24): 21123-21129.

Rollins, B. J., T. Yoshimura, et al. (1990). "Cytokine-activated human endothelial cells synthesize and secrete a monocyte chemoattractant, MCP-1/JE." Am J Pathol **136**(6): 1229-1233.

Rosselet, A., F. Feihl, et al. (1998). "Selective iNOS inhibition is superior to norepinephrine in the treatment of rat endotoxic shock." Am J Respir Crit Care Med **157**(1): 162-170.

Rossner, S., C. Voigtlander, et al. (2005). "Myeloid dendritic cell precursors generated from bone marrow suppress T cell responses via cell contact and nitric oxide production in vitro." Eur J Immunol **35**(12): 3533-3544.

Rothe, M., M. G. Pan, et al. (1995). "The TNFR2-TRAF signaling complex contains two novel proteins related to baculoviral inhibitor of apoptosis proteins." Cell **83**(7): 1243-1252.

Rubbo, H., R. Radi, et al. (1994). "Nitric oxide regulation of superoxide and peroxynitrite-dependent lipid peroxidation. Formation of novel nitrogen-containing oxidized lipid derivatives." J Biol Chem **269**(42): 26066-26075.

Sacca, R., C. A. Cuff, et al. (1998). "Differential activities of secreted lymphotoxin-alpha3 and membrane lymphotoxin-alpha1beta2 in lymphotoxin-induced inflammation: critical role of TNF receptor 1 signaling." J Immunol **160**(1): 485-491.

Sauer, H., M. Wartenberg, et al. (2001). "Reactive oxygen species as intracellular messengers during cell growth and differentiation." Cell Physiol Biochem **11**(4): 173-186.

Schmid, I., W. J. Krall, et al. (1992). "Dead cell discrimination with 7-amino-actinomycin D in combination with dual color immunofluorescence in single laser flow cytometry." Cytometry **13**(2): 204-208.

Schneider-Brachert, W., V. Tchikov, et al. (2004). "Compartmentalization of TNF receptor 1 signaling: internalized TNF receptosomes as death signaling vesicles." Immunity **21**(3): 415-428.

Schroder, J., F. Stuber, et al. (1995). "Pattern of soluble TNF receptors I and II in sepsis." Infection **23**(3): 143-148.

Schutze, S., T. Machleidt, et al. (1999). "Inhibition of receptor internalization by monodansylcadaverine selectively blocks p55 tumor necrosis factor receptor death domain signaling." J Biol Chem **274**(15): 10203-10212.

Scott, J. A., S. Mehta, et al. (2002). "Functional inhibition of constitutive nitric oxide synthase in a rat model of sepsis." Am J Respir Crit Care Med **165**(10): 1426-1432.

Shen, F. W., Y. Saga, et al. (1985). "Cloning of Ly-5 cDNA." Proc Natl Acad Sci U S A **82**(21): 7360-7363.

Shulman, M., C. D. Wilde, et al. (1978). "A better cell line for making hybridomas secreting specific antibodies." Nature **276**(5685): 269-270.

Shurety, W., A. Merino-Trigo, et al. (2000). "Localization and post-Golgi trafficking of tumor necrosis factor-alpha in macrophages." J Interferon Cytokine Res **20**(4): 427-438.

Sica, A. and V. Bronte (2007). "Altered macrophage differentiation and immune dysfunction in tumor development." J Clin Invest **117**(5): 1155-1166.

Sinha, P., V. K. Clements, et al. (2007). "Cross-talk between myeloid-derived suppressor cells and macrophages subverts tumor immunity toward a type 2 response." J Immunol **179**(2): 977-983.

Smith, C. A., T. Davis, et al. (1990). "A receptor for tumor necrosis factor defines an unusual family of cellular and viral proteins." Science **248**(4958): 1019-1023.

Smith, C. A., T. Farrah, et al. (1994). "The TNF receptor superfamily of cellular and viral proteins: activation, costimulation, and death." Cell **76**(6): 959-962.

Snyder, S. H. and D. S. Bredt (1991). "Nitric oxide as a neuronal messenger." Trends Pharmacol Sci **12**(4): 125-128.

Speirs, K., L. Lieberman, et al. (2004). "Cutting edge: NF-kappa B2 is a negative regulator of dendritic cell function." J Immunol **172**(2): 752-756.

Sterns, T., N. Pollak, et al. (2005). "Divergence of protection induced by bacterial products and sepsis-induced immune suppression." Infect Immun **73**(8): 4905-4912.

Stillie, R. and A. W. Stadnyk (2009). "Role of TNF receptors, TNFR1 and TNFR2, in dextran sodium sulfate-induced colitis." Inflamm Bowel Dis **15**(10): 1515-1525.

Suvannavejh, G. C., H. O. Lee, et al. (2000). "Divergent roles for p55 and p75 tumor necrosis factor receptors in the pathogenesis of MOG(35-55)-induced experimental autoimmune encephalomyelitis." Cell Immunol **205**(1): 24-33.

Takayama, K., H. Yokozeki, et al. (1999). "IL-4 inhibits the migration of human Langerhans cells through the downregulation of TNF receptor II expression." J Invest Dermatol **113**(4): 541-546.

Tartaglia, L. A., R. F. Weber, et al. (1991). "The two different receptors for tumor necrosis factor mediate distinct cellular responses." Proc Natl Acad Sci U S A **88**(20): 9292-9296.

Theiss, A. L., J. G. Simmons, et al. (2005). "Tumor necrosis factor (TNF) alpha increases collagen accumulation and proliferation in intestinal myofibroblasts via TNF receptor 2." J Biol Chem **280**(43): 36099-36109.

Todd, R. F., 3rd, L. M. Nadler, et al. (1981). "Antigens on human monocytes identified by monoclonal antibodies." J Immunol **126**(4): 1435-1442.

Towbin, H., T. Staehelin, et al. (1979). "Electrophoretic transfer of proteins from polyacrylamide gels to nitrocellulose sheets: procedure and some applications." Proc Natl Acad Sci U S A **76**(9): 4350-4354.

Vermes, I., C. Haanen, et al. (1995). "A novel assay for apoptosis. Flow cytometric detection of phosphatidylserine expression on early apoptotic cells using fluorescein labelled Annexin V." J Immunol Methods **184**(1): 39-51.

Vickers, S. M., L. A. MacMillan-Crow, et al. (1999). "Association of increased immunostaining for inducible nitric oxide synthase and nitrotyrosine with fibroblast growth factor transformation in pancreatic cancer." Arch Surg **134**(3): 245-251.

Victor, F. C., A. B. Gottlieb, et al. (2003). "Changing paradigms in dermatology: tumor necrosis factor alpha (TNF-alpha) blockade in psoriasis and psoriatic arthritis." Clin Dermatol **21**(5): 392-397.

Vielhauer, V., G. Stavrakis, et al. (2005). "Renal cell-expressed TNF receptor 2, not receptor 1, is essential for the development of glomerulonephritis." J Clin Invest **115**(5): 1199-1209.

Villa, P., G. Sartor, et al. (1995). "Pattern of cytokines and pharmacomodulation in sepsis induced by cecal ligation and puncture compared with that induced by endotoxin." Clin Diagn Lab Immunol **2**(5): 549-553.

Vincent, J. L. (2001). "Microvascular endothelial dysfunction: a renewed appreciation of sepsis pathophysiology." Crit Care **5**(2): S1-5.

Volkman, A. and J. L. Gowans (1965). "The Origin of Macrophages from Bone Marrow in the Rat." Br J Exp Pathol **46**: 62-70.

Wallach, D., H. Engelmann, et al. (1991). "Soluble and cell surface receptors for tumor necrosis factor." Agents Actions Suppl **35**: 51-57.

Wang, C. Y., M. W. Mayo, et al. (1998). "NF-kappaB antiapoptosis: induction of TRAF1 and TRAF2 and c-IAP1 and c-IAP2 to suppress caspase-8 activation." Science **281**(5383): 1680-1683.

Wei, X. Q., I. G. Charles, et al. (1995). "Altered immune responses in mice lacking inducible nitric oxide synthase." Nature **375**(6530): 408-411.

Yasuda, H., A. Leelahavanichkul, et al. (2008). "Chloroquine and inhibition of Toll-like receptor 9 protect from sepsis-induced acute kidney injury." Am J Physiol Renal Physiol **294**(5): F1050-1058.

Yasuda, H., P. S. Yuen, et al. (2006). "Simvastatin improves sepsis-induced mortality and acute kidney injury via renal vascular effects." Kidney Int **69**(9): 1535-1542.

Youn, J. I., S. Nagaraj, et al. (2008). "Subsets of myeloid-derived suppressor cells in tumor-bearing mice." J Immunol **181**(8): 5791-5802.

Young, M. R., M. Newby, et al. (1987). "Hematopoiesis and suppressor bone marrow cells in mice bearing large metastatic Lewis lung carcinoma tumors." Cancer Res **47**(1): 100-105.

Zakharova, M. and H. K. Ziegler (2005). "Paradoxical anti-inflammatory actions of TNF-alpha: inhibition of IL-12 and IL-23 via TNF receptor 1 in macrophages and dendritic cells." J Immunol **175**(8): 5024-5033.

Zhang, H., D. Yan, et al. (2008). "Transmembrane TNF-alpha mediates "forward" and "reverse" signaling, inducing cell death or survival via the NF-kappaB pathway in Raji Burkitt lymphoma cells." J Leukoc Biol **84**(3): 789-797.

Zhu, B., Y. Bando, et al. (2007). "CD11b+Ly-6C(hi) suppressive monocytes in experimental autoimmune encephalomyelitis." J Immunol **179**(8): 5228-5237.

Zipper, H., H. Brunner, et al. (2004). "Investigations on DNA intercalation and surface binding by SYBR Green I, its structure determination and methodological implications." Nucleic Acids Res **32**(12): e103.

7 Appendix

Graduate Scool (FOR876):

28/29.11.2008	Workshop: Zandt, Cham (Dr. Anja Lechner, Dr. Anja Wege and Dr. Sven Mostböck)
08/2008-02/2009	Method seminar (Dr. Anja Lechner)
10/2009-03/2010	Seminar: Basics in Immunology - Immune cells: development and function (Dr. Anja Lechner)

International Congress:

09/2008	Joint Annual Meeting of Immunology, Wien
09/2009	European Macrophage and Dendritic Cell Society (EMDS), Regensburg

Presentations:

09/2009	European Macrophage and Dendritic Cell Society (EMDS) ”Mechanisms Dampening Inflammation: Role of TNFR2 in sepsis-induced immune suppression”
17.07.2008	Key note lecture: B.Beutler, Regensburg
08-09.05.2008	Key note lecture: F.Weih, S.Knight, Regensburg

Continuing education:

04/2008	Basic and Advanced Training: Project Leader and Commissary for Biological Safety (BBS), Regensburg

8 Acknowledgments

Mein besonderer Dank gilt Frau Prof. Dr. Daniela N. Männel für die Überlassung dieses interessanten Themas sowie die Unterstützung und Förderung, die mir die letzten drei Jahre entgegen gebracht wurden. Konstruktive Diskussionen begleiteten stets unsere gemeinsamen Besprechungen und waren für das Gelingen dieser Arbeit unabdingbar.

Herrn PD Dr. Thomas Langmann möchte ich für die konstruktiven Besprechungen und die Bereitschaft zur fakultätsinternen Vertretung dieser Dissertation danken.

Herrn Prof. Dr Thomas Hehlgans möchte ich für die Diskussionsbereitschaft während der Mittwochsseminare danken sowie für die Unterstützung bei Klonierungsarbeiten.

Herrn PD Dr. Wulf Schneider möchte ich für diverse Klonierungsarbeiten und retrovirale Transduktionen danken.

Herr Prof. Dr. Harald Wajant stellte mir verschiedenen TNF Mutanten zur Verfügung und ermöglichte dadurch wichtige Experimente. Hierfür einen herzlichen Dank.

Ein großer Dank gilt auch Frau Dr. Anja Lechner und Herrn Dr. Sven Mostböck für Ihre stete Hilfsbereitschaft und fachliche Unterstützung.

Ein besonders herzliches „Danke“ gilt meinen Kollegen Katja, Christian und Tom für die freundliche und angenehme Arbeitsatmosphäre und dafür, dass die Arbeit viel Freude bereitet hat.

Für die praktischen Klonierungsarbeiten möchte ich mich bei Sabine Laberer herzlich bedanken.

Für alle FACS Aria Sort Einsätze möchte ich insbesondere Catherine Botteron danken.

Unserer Sekretärin Luise Eder vielen Dank für die Unterstützung organisatorischer Art.

Liebe Doro, Dir sei an dieser Stelle ein ganz besonderer Dank ausgesprochen für den freundschaftlichen Umgang und die viele Unterstützung Deinerseits, ohne die so manches an Experimenten nicht möglich gewesen wäre.

Allen ehemaligen Kollegen und Mitarbeitern des Instituts für Immunologie vielen Dank für Rat und Tat.

Ein besonderer Dank gilt Eva für ihre seelische und moralische Unterstützung.

Nicht zu vergessen ist ein großer Dank an meine Familie und besonders an meine Eltern: Rosi, Dir vor allem für Deinen uneingeschränkten, positiv-kritischen Beistand und die netten Anekdoten und Weisheiten aus der alten AG Lynen am MPI für Biochemie. Hans, Dir vielen Dank für sämtliche Unterstützung. Ohne Euch wäre so manches nicht möglich gewesen.